Prevention and Treatment of Head and Neck Cancer with Natural Compound Inhibitors of STAT3

by

Rebecca J. Leeman-Neill

B.A., Brandeis University, 2002

Submitted to the Graduate Faculty of

The School of Medicine, Department of Pathology, in partial fulfillment

of the requirements for the degree of

Doctor of Philosophy

University of Pittsburgh

2008

UNIVERSITY OF PITTSBURGH

SCHOOL OF MEDICINE

This dissertation was presented

by

Rebecca J. Leeman-Neill

It was defended on

December 11, 2008

and approved by

Marie DeFrances, MD, PhD, Department of Pathology

Luyuan Li, PhD, Department of Pathology

Shivendra Singh, PhD, Department of Pharmacology

Committee Chair: Alan Wells, MD, DMS, Department of Pathology

Thesis Advisor: Jennifer R. Grandis, MD, Departments of Otolaryngology and Pharmacology

Prevention and Treatment of Head and Neck Cancer

with Natural Compound Inhibitors of STAT3

Rebecca J. Leeman-Neill, BA

University of Pittsburgh, 2008

Head and neck squamous cell carcinoma (HNSCC) is a commonly occurring malignancy associated with severe morbidity, persistently high mortality rates, frequent recurrence, and the appearance of second primary tumors (SPTs). A great need exists, therefore, for new therapies, including complementary and preventive approaches to treating HNSCC. Signal transducer and activator of transcription (STAT)-3, an oncogenic transcription factor, shows promise as an important therapeutic target in the treatment of HNSCC. The current study focuses on the STAT3-targeting activities of two natural compounds, guggulsterone and honokiol, and investigation of their antitumor activity in HNSCC. Guggulsterone, a compound contained in the resin of the *Commiphora mukul* plant, used in Indian Ayurvedic medicine, is widely available as a dietary supplement and associated with few side effects. Honokiol is a naturally-occurring compound that has been used in traditional Chinese medicine and is derived from the plant, *Magnolia officinalis*. Both compounds have been shown to have anticancer activity in various models and to inhibit nuclear factor kappa B (NFκB), an oncogenic transcription factor. NFκB and STAT3 interact with one another in various ways. Therefore, we hypothesized that guggulsterone and/or honokiol might be useful in targeting STAT3. Both compounds inhibited growth and invasiveness and induced apoptosis in HNSCC cell lines, in addition to decreasing levels of phosphotyrosine STAT3, and, for guggulsterone, total STAT3. Guggulsterone was also

found to cause cell cycle arrest and to target hypoxia-inducible factor (HIF)-1α, a potential therapeutic target whose expression is correlated with poor clinical outcome in HNSCC. Guggulsterone-induced growth inhibition relied partly on its ability to inhibit STAT3. Both compounds enhanced the activities of current HNSCC therapies and modestly inhibited tumor growth in the xenograft model of HNSCC. To test the chemopreventive potential of STAT3 and epidermal growth factor receptor (EGFR) inhibition, a study administering *Guggulipid*, a guggulsterone-containing nutraceutical, or erlotinib, an EGFR-targeting tyrosine kinase inhibitor (TKI) to mice treated orally with a carcinogen is currently underway. Our results so far suggest that guggulsterone and honokiol-mediated inhibition of STAT3 and guggulsterone-mediated inhibition of HIF-1α provide a biologic rationale for further clinical investigation of these compounds as complementary and preventive treatments for HNSCC.

TABLE OF CONTENTS

LIST OF TABLES

LIST OF FIGURES

FORWARD

First and foremost, a gigantic thank you to Dr. Jennifer Grandis. She has been an amazing role model and inspiration, an outstanding mentor, so generous with her time, wisdom and resources, and a friend. I consider myself extremely lucky to have had the opportunity to work with her.

I also want to thank the Grandis lab, a group of wonderful people who have been helpful to me, as friends, collaborators and mentors, in too many ways to list. Though many have helped with my project, a few deserve special mention: Sarah Wheeler, who, as a rotation student, performed several important experiments for the guggulsterone project, Dr. Quan Cai, for all of his work on the honokiol project, and Maria Freilino for her many hours spent weighing, feeding and making slides from our hundreds of mice.

Thank you to my committee, Dr. Marie DeFrances, Dr. Alan Wells, Dr. Luyuan Li, and Dr. Shivendra Singh for taking the time to help me with my plans and collectively mentor me throughout graduate school. I am particularly grateful to Dr. Singh for, in his expertise in the field of cancer chemoprevention, being a co-advisor to me on this project, collaborating with us, and providing important advice and resources. Thank you also to Dr. Barry London, my career advisor, whose sage advice continues to help me through my MD-PhD training. I would also

like to thank University of Pittsburgh's MSTP for supporting me and giving me the opportunity to be trained by such fantastic mentors.

Thank you also to the people who have collaborated with me on this project: Dr. Mark Lingen, Dr. Jack Arbiser, Bill Gooding and especially Dr. Raja Seethala, a fantastic teacher who has spent countless hours turning me into a mouse pathologist.

Finally, thank you to my friends and family for being so supportive throughout my training. Thank you, especially, to my wonderful husband, Daniel, for all of his love and support and for his important help with my science and statistics.

LIST OF ABBREVIATIONS

CDK	Cyclin dependent kinase
CHX	Cyclohexamide
DMEM	Dulbecco's modification of Eagle's medium
DMSO	Dimethyl sulfoxide
DNA	Deoxyribonucleic acid
EC_{50}	Half maximal effective concentration
EGF	Epidermal growth factor
EGFR	Epidermal growth factor receptor
ELISA	Enzyme linked immunosorbent assay
ER	Estrogen receptor
FBS	Fetal bovine serum
FXR	Farnesoid x receptor
GAPDH	Glyceraldehyde 3-phosphate dehydrogenase
GFP	Green fluorescent protein
H & E	Hematoxylin and eosin
HIF	Hypoxia inducible factor

HNSCC	Head and neck squamous cell carcinoma
IKK	Inhibitor of NFκB kinase
ITC	Isothiocyanate
IκB	Inhibitor of NFκB
Jak	Janus kinase
MMP	Matrix metalloproteinase
MTT	3-(4, 5-dimethylthiazol-2-yl)-2,5-diphenyltetrazolium bromide)
NFκB	Nuclear factor kappa B
NRTK	Non-receptor tyrosine kinase
OD	Optical density
PBS	Phosphate buffered saline
PIAS	Protein inhibitor of activated STAT
PR	Progesterone receptor
PSTAT	Phosphorylated STAT
PXR	Pregnane x receptor
Rb	Retinoblastoma
RLU	Relative light units
RNA	Ribonucleic acid
ROS	Reactive oxygen species
RTK	Receptor tyrosine kinase
SCC	Squamous cell carcinoma
SH2	Src homology domain 2
SHP	SH2 containing tyrosine phosphatase

siRNA	Small interfering RNA
SOCS	Suppressor of cytokine signaling
SPT	Second primary tumor
STAT	Signal transducer and activator of transcription
TGF	Transforming growth factor
TKI	Tyrosine kinase inhibitor
TUNEL	TdT-mediated dUTP-biotin nick end labeling
Tyr	Tyrosine
VEGF	Vascular endothelial growth factor

PREFACE

One chapter of this dissertation contains a published manuscript:

Leeman R.J., Lui V.W., Grandis J.R. "STAT3 as a therapeutic target in head and neck cancer." Expert Opin Biol Ther. 2006 Mar; 6(3):231-41.

My training has been funded by the following NIH grants:

University of Pittsburgh's Medical Scientist Training Program (T32 GM08208-16)

Research Training in Otolaryngology (T32 DC000066)

NRSA F-30 Research Training Grant ("Prevention of Head and Neck Carcinogenesis with a Plant-Derived Compound" F30ES015669-01)

1.0 INTRODUCTION

1.1 THE GOAL OF HEAD AND NECK CANCER CHEMOPREVENTION

1.1.1 Head and neck squamous cell carcinoma

Head and neck squamous cell carcinoma (HNSCC) carries a mortality rate of over 50%, which has not changed in decades. It is the sixth most common cancer in the United States (1) and the single most common cancer in many developing countries, where two-thirds of new cases arise (2, 3). HNSCC is thought to be caused by the molecular effects of environmental carcinogens. Many studies have conclusively identified links between exposures to tobacco, alcohol and betel quid and HNSCC (4). Additionally, several epidemiological studies have identified occupational exposures that are associated with an increased risk of HNSCC, including asbestos (5)**,** coal dust (6), organic solvents (6, 7), welding fumes (8), polycyclic aromatic hydrocarbons (8), and formaldehyde (9), among others. Predispositions to HNSCC include genetic phenomena that affect the cell's ability to respond to carcinogen exposures (4, 10). Slaughter *et al.* define the concept of "field cancerization" to describe molecular changes that arise throughout the upper aerodigestive tract in response to carcinogen exposure and to explain observations that histologically normal epithelium in the oral cavities of HNSCC patients contain cancer-like molecular alterations (11). This results in frequent second primary tumors (SPTs), which occur at

a rate of 3-6% per year, among the highest for any neoplasm (12, 13, 14). HNSCC therapies include surgical intervention, radiation, conventional chemotherapy (e.g. cisplatin), and strategies to inhibit the epidermal growth factor receptor (EGFR) (e.g. cetuximab). Those patients who survive their initial treatment often suffer severe morbidity resulting from damage to the upper aerodigestive tract secondary to treatment or from tumor invasion. A great need exists, therefore, for new therapies, including complementary and preventive approaches to treating HNSCC.

1.1.2 Cancer prevention studies

As cancer is a devastating and frequently fatal disease, studies identifying methods for preventing cancer are very important. Cancer is thought to develop in various stages termed, *initiation*, which refers to changes in DNA, often caused by exposure to a carcinogen or virus, *promotion*, which includes other molecular, tissue-specific changes, such as alterations in growth factors, that encourage the affected cells to grow abnormally, and *progression*, during which the affected cells acquire new phenotypes that make them cancer cells (Figure 1). Upon histologic examination of tissue, carcinogenesis can, to some extent, be visualized, beginning with mild dysplasia, as initiation and promotion cause cells to grow abnormally, and ultimately leading to invasive cancer. The goal of cancer prevention is to inhibit the process of carcinogenesis. Primary prevention strategies, such as smoking cessation, aim to decrease the risk of cancer initiation. Secondary prevention strategies, such as surgical removal of pre-neoplastic lesions, is directed at preventing cancer promotion and progression.

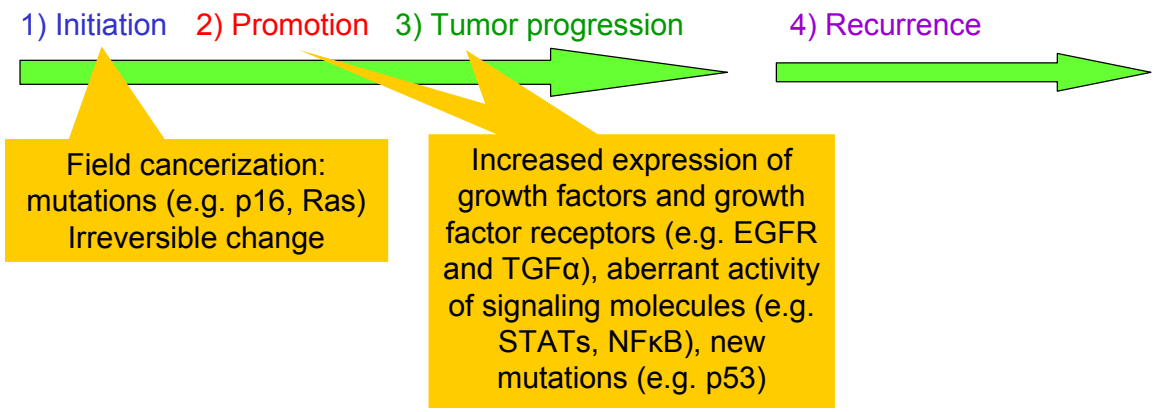

Figure 1. Steps in carcinogenesis, highlighting changes that occur in head and neck carcinogenesis

Chemopreventive agents, drugs used for cancer prevention, can be applied to secondary prevention of HNSCC, for example in patients with a pre-malignant lesion or in patients who have had HNSCC and are at high risk for recurrence and/or SPTs, or even in patients whose epithelium displays molecular changes associated with high risk. If the agent is very safe and devoid of major side effects, it may also be used in primary prevention to prevent risk of cancer initiation, from carcinogen exposure, for example.

Both preclinical and clinical studies of potential chemopreventive agents present unique challenges. Clinical prevention studies require administration of interventions to patients who do not, at the time, have disease. Furthermore, following completely healthy individuals for years, in order to determine whether or not they eventually develop cancer, is a difficult and expensive study design. More realistic trial endpoints, which may include effects of the chemopreventive agent on biomarkers or rates of recurrence in patients who have had cancer, reveal valuable but more limited information about the efficacy of a chemopreventive agent.

The challenges posed by clinical trials of preventive agents underscore the importance of preclinical trials in first determining a biologic rationale for use of the agent in chemoprevention. *In vitro* studies, which are limited, due to a general lack of cellular models that truly mimic carcinogenesis, are nonetheless important in identifying molecular alterations that can be targeted by a specific agent. Additionally, if an agent inhibits the mechanisms that cause cancer cells to grow, for example, this may sometimes be reflective of the agent's ability to halt cancer promotion and progression. True preclinical evidence of cancer prevention, however, requires *in vivo* investigation, employing carcinogen-induced and transgenic animal models of cancer.

1.1.3 HNSCC chemoprevention to date

Because HNSCC is a common and devastating cancer that: a) has a limited response to currently available treatments b) results from carcinogen exposure and c) commonly recurs and has a high rate of SPT development, primary and secondary prevention strategies represent an important approach to this neoplasm. Based on early observations that tumors of the upper aerodigestive tract and lungs occurred more frequently in cattle who were deficient in vitamin A (15), studies investigating high-dose retinoids as chemoprevention for HNSCC demonstrated efficacy in delaying carcinogenesis in humans but were associated with considerable toxicity (16, 17)**.** Since then, trials involving administration of tolerable doses of retinoids have not demonstrated chemoprevention of HNSCC (18, 19)**.** The need for identification of new approaches to prevent HNSCC became apparent. Recent clinical trials demonstrating chemoprevention of HNSCC have employed green tea (20, 21) and Bowman-Birk inhibitor derived from soybeans (22). Studies investigating potential roles for cyclooxygenase (COX)-2 and epidermal growth factor

receptor (EGFR) inhibition in HNSCC chemoprevention are also currently underway (23). Preclinical and clinical studies have arrived at various potential molecular targets for chemoprevention of HNSCC. In the current study, we focus on one plausible target of HNSCC chemoprevention: signal transducer and activator of transcription (STAT)-3.

1.2 ONE TARGET OF HNSCC CHEMOPREVENTION: STAT3

1.2.1 Introduction to STATs

The signal transducer and activator of transcription (STAT) proteins are so named due to the role they play in relaying signals received by specific cell surface receptors to induce transcriptional changes within the cell (Figure 2). So far, seven distinct STAT molecules have been identified. These include STATs 1, 2, 3, 4, 5a, 5b and 6. STATs were originally discovered in the context of cytokine signaling (24-26). Many cytokine receptor proteins, including those for most of the interleukins, the interferons and colony-stimulating factors, have a receptor component, but not an enzymatic component (27). Instead, Janus kinase (Jak) proteins are constitutively non-covalently associated with cytokine receptors (26, 27). Following ligand binding and aggregation of the receptor subunits, two associated Jaks transphosphorylate at tyrosine residues, thereby undergoing reciprocal activation (28, 29). These activated Jaks transmit the cytokine signal via recruitment and activation of STATs through Src homology 2 (SH2) domains on STATs (26, 29-

32). Signaling through receptor tyrosine kinases, including growth factor receptors such as epidermal growth factor receptor (EGFR) and platelet-derived growth factor receptor, also leads to STAT activation via direct recruitment of the STAT SH2 domains by the receptor itself (24, 33-35). Specific tyrosine residues on the EGFR, Y1068 and Y1086, have been found to recruit STAT3 proteins in head and neck squamous cell carcinoma (HNSCC) (36). Non-receptor tyrosine kinases, in addition to Jaks, such as Src and Abl, have also been found to activate STATs (29, 37, 38). It was previously assumed that tyrosine phosphorylation was required for STAT activation, as is the case with STAT1 (39). Recent studies have shown that STAT3 can be activated and imported into the nucleus independently of tyrosine phosphorylation (40). There is conflicting evidence regarding whether or not STAT activation may also be regulated by arginine methylation (41, 42).

Following activation, STATs dimerize, forming either homodimers, such as serum-inducible factor (SIF)-A, a STAT3 dimer, or heterodimers, such as SIF-B, a STAT1–STAT3 dimer. Acetylation of a single lysine residue on STAT3 is required for formation of these dimers (43). STAT dimers translocate to the nucleus, where they bind gene-regulatory elements, such as the serum/sis-inducible element (SIE) in the promoter of the c-fos gene (26, 35, 44) or the IFN-γ-activated sequence (GAS) in the promoter of the guanylate-binding protein gene, and alter transcription of specific genes (45, 46). Within the nucleus, STATs can associate with other transcription-regulatory proteins. For example, STAT3 has the ability to bind c-Jun as well as a gene regulatory element next to an activator protein (AP)-1 site on DNA, and the ability to work synergistically with AP-1 in transcriptional regulation (47, 48). The various STAT target genes (Table 1) play diverse roles in normal cellular functions, including growth, apoptosis and

differentiation. Each receptor that transduces its signal via STATs activates a specific STAT or set of STAT molecules. Some of the activated STATs have been identified as potential oncogenes (STAT3 and STAT5) or tumor suppressors (STAT1) (49).

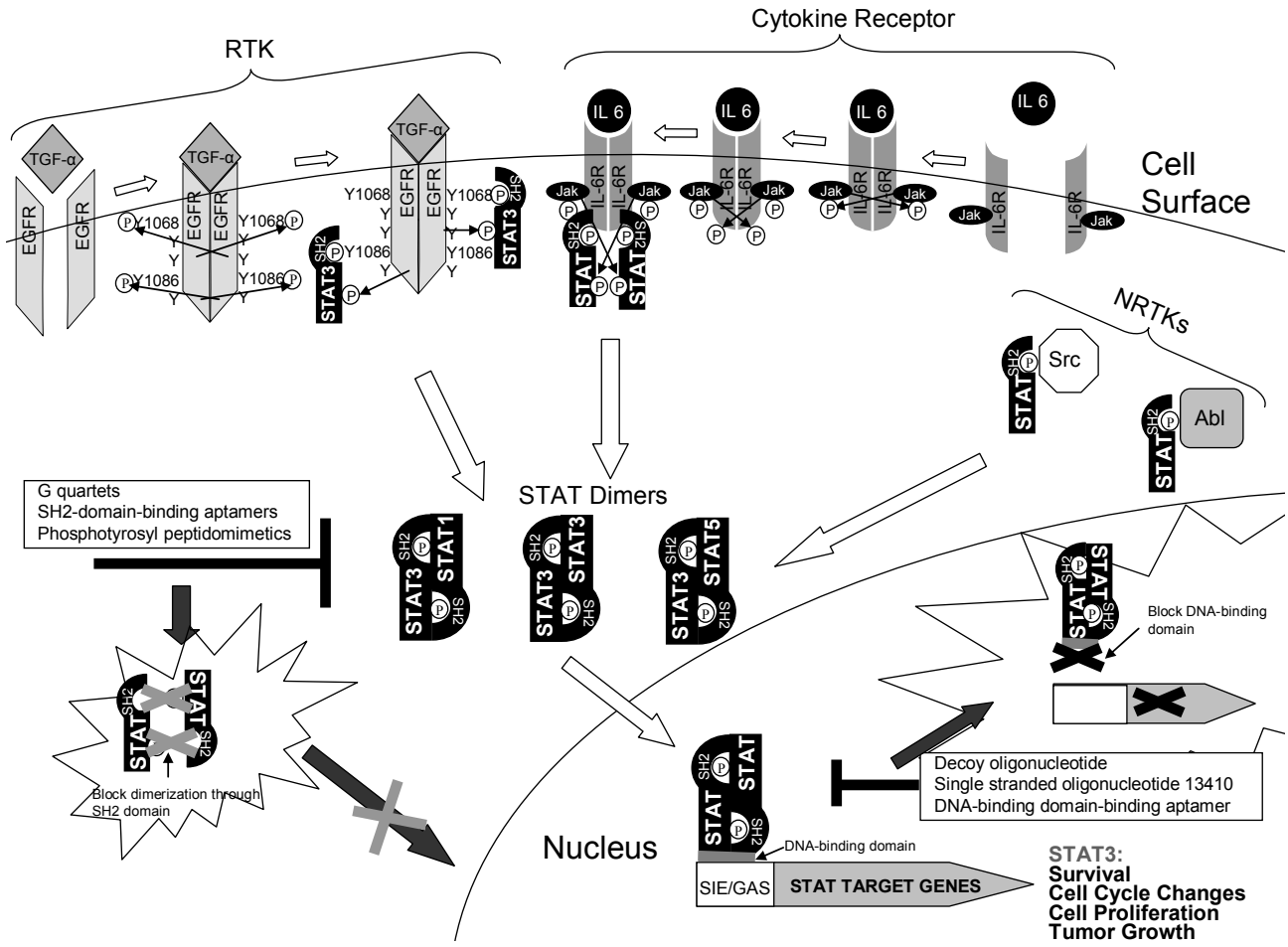

Figure 2. STAT signaling and molecular inhibitors of STATs. Receptor tyrosine kinases such as EGFR bind growth factors (e.g. TGF-α), and cytokine receptors such as IL-6R dimerize following binding of their ligand. Cytokine receptors are constitutively associated with Jaks. Following dimerization, transphosphorylation occurs. STAT proteins are then recruited to phosphotyrosine residues, specifically Y1068 and Y1086 on the EGFR in HNSCC, through their SH2 domains. Activated NRTKs, such as Src and Abl, can also recruit STATs to phosphotyrosine residues. Activated STATs form homo- or heterodimers through their SH2 domains and translocate to the nucleus where they bind gene regulatory elements, including the SIE or the GAS, resulting in the transcription of specific STAT target genes. Small molecule inhibitors of STAT3 have been developed to interfere with dimerization of STAT3 by interacting with the SH2 domain and surrounding regions. Inhibition of dimerization prevents STAT3 from translocating to the nucleus. Other small molecule inhibitors of STAT3 have been developed to inhibit DNA binding by STAT3 by interacting with the DNA-binding site of STAT3.

1.2.2 Role of STAT3 in oncogenesis

The role of STAT3 in oncogenesis first became evident with the discovery that activated STAT3 was required for cellular transformation by the viral oncogene *v-src,* as well as observations that inhibition of STAT3 with a dominant-negative mutant prevented *v-src*-mediated transformation (37, 50). Subsequently, using a constitutively active form of STAT3 (STAT3C), it was shown that activated STAT3 alone has the capacity to transform immortalized fibroblasts (51). In addition to its role in transformation, STAT3 levels are elevated in numerous human malignancies, including leukemias, lymphomas, multiple myeloma, breast cancer, prostate carcinoma, renal cell carcinoma, lung cancer, ovarian carcinoma, pancreatic adenocarcinoma, melanoma, and head and neck squamous cell carcinoma (HNSCC) (52). Further evidence of the importance of STAT3 in oncogenesis is supported by studies demonstrating growth inhibition of myeloma, breast cancer, melanoma and HNSCC cells using a dominant-negative STAT3 mutant construct (STAT3β) (53-56). The growth and survival of normal fibroblasts, however, were not affected by the dominant-negative STAT3 construct, suggesting that only the proliferation of neoplastic cells depends on STAT3 (57).

1.2.3 STAT3 target genes

The oncogenic effects of STAT3 are mediated, at least in part, through the expression of STAT3 target genes. STAT3 target genes have been identified in a number of tumor and non-tumor systems via the expression of dominant-negative STAT3, constitutively activated STAT3 (STAT3C), or specific targeting of STAT3 by siRNA or the STAT3 decoy described below. The

number of reported STAT3 target genes is increasing (Table 1). Among the known STAT3 target genes are cell cycle regulators, antiapoptotic genes and pro-angiogenic factors. B cells lacking c-Rel, a transcription factor that modulates Bcl-x_L, which is also a STAT3 target gene, can be partially rescued from a hypoproliferative phenotype by IL-6, but not through STAT3-activated transcription of Bcl-x_L (58). This suggests that multiple pathways are involved in proliferation and survival of B cells, at least. Interestingly, STAT3 regulates its own expression and induces expression of negative regulators of STAT3, such as the suppressor of cytokine signaling (SOCS)3. A recent study by Dauer et al. demonstrated that STAT3 regulates genes that are common both to cancer and wound healing (59). It is worth noting that some STAT3 target genes are also shared by other members of the STAT family, such as STAT5 (e.g., cyclin D1, pim-1 and p21/waf1). The exact mechanisms underlying such a redundancy are unknown. The structural homology shared among the STAT family members, as well as the existence of heterodimers between STAT3 and other members of the STAT family, may play a potential role. Although constitutive activation of STAT3 is believed to be crucial for oncogenic transcriptional control, the function of unphosphorylated STAT3 has also been investigated. Stark *et al.* showed that overexpression of an unphosphorylable STAT3 (Y705F mutation) could induce the expression of some genes that are regulated by activated STAT3 (e.g., c-fos, c-jun, bcl-x_L, c-myc, dp1) (60). Interestingly, they also identified a set of genes that were only induced by the expression of unphosphorylable STAT3 (Y705F), such as meiosis-specific nuclear structural protein 1 (mns1), p21-activated kinase-3 (mpak-3) and transcription factor IIH. These results suggest that unphosphorylated STAT3 may contribute to carcinogenesis.

Table 1. STAT3 Target Genes

Class	Gene	Regulated by STAT3 and/or other STATs
Cell cycle regulator	Cyclin D1	STAT3 (129); STAT5 (152)
	Cyclin D3	STAT3 (153)
	c-Myc	STAT3 (154); STAT5 (155)
	p19INK4D	STAT3 (156)
	p21 waf1	STAT3 (157); STAT5 (158)
	Pim-1	STAT3 (159); STAT5 (160)
	p27	STAT3 (161); STAT5 (162)
Anti-apoptotic	Survivin	STAT3 (163)
	Mcl-1	STAT3 (164)
	TIMP1	STAT3 (176)
	Bcl-2	STAT3 (165); STAT5 (155)
	Bcl-x_L	STAT3 (54); STAT5 (166)
Angiogenesis	VEGF	STAT3 (167)
Metastasis	HIF-1α	STAT3 (168)
	MMP-2	STAT3 (169)
	MMP-9	STAT3 (170)
Negative regulator of STAT3	SOCS-3	STAT3 (171)
	TEL/ETV6	STAT3 (172)
Others	α_2-macroglobulin	STAT3 (173)
	α-antichymotrypsin (Serpin A3)	STAT3 (174)
	Jun B	STAT3 (175)

1.2.4 Proteins regulating STAT3 activity in cancer

As of yet, no naturally occurring constitutively active mutant of STAT3 has been detected in cancer cells or human tumors. In general, elevated levels of activated STAT3 are due to aberrations in other proteins involved in STAT3 signaling, including proteins upstream in the STAT3 signaling pathway and physiological regulators of STAT3. Approaches that block

molecules upstream from STAT3 (e.g., EGFR, Src, Jak2) have been developed and have been approved for use in cancer patients (e.g., cetuximab, erlotinib) or are being tested in clinical trials (61). Another possible approach would enhance the proteins that negatively regulate activation of STAT3, such as SOCS-1, SOCS-3 (62), protein inhibitor of activated STAT (PIAS)3 (63) and GRIM-19 (64).

1.2.4.1 The role of proteins upstream of STAT3 in cancer

Among the proteins upstream of STAT3 in the STAT3 signaling pathway, several, including TGF-α, EGFR, Jaks, Src and p38, have been shown to play a role in STAT3-mediated oncogenesis. Some of these upstream proteins have been targeted in efforts to develop cancer therapeutics. EGFR inhibitors have been reported to abrogate STAT3 activation and are currently approved for use in several cancers (61, 65). A mutation causing constitutive tyrosine phosphorylation and, therefore, activation of Jak2, a tyrosine kinase upstream of STATs, has been found in subsets of patients with several different myeloproliferative disorders (66, 67). c-Src, an oncoprotein, requires STAT3 activation for cell transformation (68). Src-specific small molecule inhibitors cause inhibition of STAT3 activation in the platelet-derived growth factor receptor pathway (68) and in cells with otherwise constitutively active STAT3 (56). Treatment of human melanoma cells with Src inhibitors PD180970 and PD166285 blocks STAT3 DNA binding and expression of STAT3 target genes, and results in decreased cell growth and increased apoptosis (57). Src inhibitors are now being tested in Phase I/II trials in cancer patients, including HNSCC.

1.2.4.2 The role of physiological regulators of STAT3 in cancer

Although mechanisms of STAT3 activation, deactivation, expression and degradation are incompletely understood, several proteins have been found to regulate STAT3 activity in the cell (69, 70). Mutations resulting in aberrant functioning of some of these STAT3 regulatory proteins have been found in various human malignancies (71-78). Some of the SH2-domain containing SOCS molecules associate with phosphorylated Jaks to block STAT3 activation (71-78). SOCS-1, whose transcription is regulated by STAT3, and possibly by other STATs as well, inhibits STAT3 activation (79-81). Hypermethylation-associated transcriptionally silent mutants of SOCS-1 have been found in several human cancers (71-74). A peptide mimetic of SOCS-1, Tkip, has been shown to inhibit both constitutive activation of STAT3 and IL-6-induced STAT3 activation in prostate cancer cells (82). A hypermethylation associated silent mutant form of SOCS-3, a protein that can also inhibit Jak activation (83), was found in human lung cancer (75). The PIAS proteins specifically associate with and negatively regulate the transcription factor activity of STATs. PIAS3 blocks DNA binding by STAT3 by interrupting dimerization or causing dissociation of dimers (63, 69, 84). An absence of PIAS3 expression has been observed in anaplastic lymphoma kinase-positive T/null cell lymphoma (76). SH2-containing phosphatase (SHP)-1 has been found to regulate STAT signaling by dephosphorylating Jak1 (85) and Jak2 (69, 70, 86, 87). Hypermethylation-associated transcriptionally silent mutants of SHP-1 have been detected in leukemias, lymphomas and multiple myeloma (77, 78). The STAT3-interacting protein (StIp1) regulates STAT3 activation and transcription factor activity. StIp1 interacts with both Jaks and STAT3, and may promote Jak/STAT3 interactions (88). A gene associated with retinoid-IFN-induced mortality (GRIM-19) has been identified and found to associate with STAT3 and inhibit STAT3-mediated gene expression and proliferation of v-Src-transformed

cells (64). Strategies to enhance negative regulators of STAT3 have not been developed to date, but may contribute to STAT3 targeting for cancer therapy.

1.2.5 STAT3 in head and neck squamous cell carcinoma

1.2.5.1 Constitutive activation of STAT3 in HNSCC

HNSCC cell lines and tumors have been found to contain constitutively active SIF-A (STAT3) homodimers and SIF-B (STAT3 and STAT1) heterodimers. Levels of expression and phosphorylation of STAT3, but not STAT1, were elevated in HNSCC cells as compared with levels in normal epithelial cells (53), and in HNSCC tumor samples compared with normal epithelium (89). Both tumor and normal epithelium from HNSCC patients were found to have higher levels of STAT3 expression and activation than did epithelium from non-cancer patients (89). The increased expression and activation of STAT3 in HNSCC has been found to be associated with elevated transforming growth factor (TGF)-α/EGFR signaling. TGF-α treatment of HNSCC cells led to an increase in expression and phosphorylation of STAT3. Both activated STAT3 complexes (SIF-A and SIF-B) were found to increase in a dose-dependent manner with TGF- α treatment of HNSCC cells, and to decrease with TGF-α-neutralizing antibody treatment (53). In HNSCC cell lines, levels of activated STAT3 closely paralleled levels of EGFR mRNA and protein, but not TGF-α mRNA, implying that levels of STAT3 activation are limited primarily by amounts of EGFR and not by EGFR ligand levels (90). STAT3 is also activated by an interleukin (IL)-6/gp130 interaction in an EGFR-independent fashion in HNSCC. Immunodepletion of IL-6 secreted by HNSCC cells *in vitro* resulted in abrogation of STAT3 phosphorylation. Thus, IL-6 autocrine/paracrine stimulation of STAT3 may contribute to HNSCC tumorigenesis (91).

1.2.5.2 STAT3 mediates proliferation and survival in HNSCC

Activated STAT3 is necessary for the growth of HNSCC lines. Transfection of HNSCC cells with dominant-negative STAT3 mutant constructs or treatment with antisense oligonucleotides specific for STAT3 resulted in growth inhibition, apoptosis and decreased STAT3 target gene expression (53, 90, 92). Cells containing a dominant-active STAT3 mutant construct proliferated independently of EGFR ligand and EGFR activity, indicating that STAT3 activation can lead to HNSCC growth without EGFR activation (90). Bcl-x_L, an antiapoptotic protein and STAT3 target gene, may contribute to the survival of HNSCC cells containing activated STAT3. Decreased expression of Bcl-x_L was observed in HNSCC xenografts treated with STAT3 antisense gene therapy (89). STAT3 alters cell cycle regulation in HNSCC. HNSCC cells transfected with a dominant-active STAT3 mutant construct contained fewer cells in G1-G0 and more cells in G2-M than did samples of HNSCC cells transfected with the vector control. The cells expressing a dominant-active STAT3 construct also continued cycling during serum starvation, unlike cells containing the vector control. However, little, if any, change in expression levels of cell cycle regulatory proteins was observed by immunoblot (90).

1.2.5.3 Src kinases and STAT3 activation in HNSCC

Src family kinases have been implicated in the control of STAT3- and STAT5-mediated HNSCC cell growth. TGF-α treatment of HNSCC cells resulted in increased activation of several Src family kinases, including lyn, fyn, yes and c-Src. Activation of these Src family kinases was found to be dependent on activation of EGFR, which forms a complex with both STAT3 and STAT5. Activated STAT5 and STAT3 levels paralleled levels of activated Src. Inhibition of c-Src or transfection of HNSCC with a dominant-negative c-Src mutant construct resulted in

decreased levels of STAT3 and STAT5 activation, suggesting that both STAT3 and STAT5 activation-mediated growth in HNSCC are also dependent on c-Src activation (93).

1.2.5.4 STAT3 in human HNSCC tumors

Immunohistochemistry studies using an antibody specific for phosphotyrosine STAT3 found that activated STAT3 was detected only in the basal epithelium in non-cancer patients. In HNSCC patients, however, STAT3 was found throughout both normal epithelium and, at higher levels, in HNSCC tumors. These results suggest that STAT3 activation may be an early step in oncogenesis (89). The finding of increased STAT3 activation in the adjacent histologically normal mucosa suggests that STAT3 activation may result from 'field cancerization', a phenomenon described by Slaughter to indicate early changes in tissue, following exposure to carcinogens, that predate histological evidence of neoplasia. Investigations of tumor samples from HNSCC patients who had chewed tobacco for > 10 years support this hypothesis. In these studies, STAT3 protein levels were shown to be high in early-stage tumors compared with late-stage tumors (94). Differentiation of head and neck cancer cells may also depend on STAT3 activation. In tumor samples from head and neck cancer patients, STAT3 expression levels were found to be highest in poorly differentiated tumors, whereas STAT1 levels were highest in well-differentiated tumors (95). It has been suggested that differentiation of HNSCC may depend on a STAT1/STAT3 balance within the cell (95). These cumulative observations have led to the development of strategies to target STAT3 for cancer therapy.

1.2.6 Therapies targeting STAT3

In addition to the aforementioned therapies targeting proteins upstream of STAT3, several strategies to directly target STAT3 signaling have been proposed as cancer therapies and tested in preclinical studies (Table 2). These include molecular therapies that directly inhibit STAT3 dimerization, the interaction of STAT3 with gene-regulatory elements, or expression of STAT3. In addition, chemical compound screens have identified several molecules, such as cucurbitacin, that appear to specifically alter the STAT3 pathway (96).

Table 2. Strategies to Target STAT3

Mechanism of Inhibition	Method
Blocks STAT3 DNA-binding site	Duplex decoy oligonucleotide (113)
	Single stranded oligonucleotide 13410 (117)
	Peptide aptamer that binds STAT3 DNA-binding site (103)
Interrupts STAT3 dimerization through SH2 domain	Phosophotyrosyl peptidomimetics (99)
	Peptide aptamer that binds SH2 domain and surrounding region (103)
	G quartets (105)
Inhibits translation of STAT3 mRNA	siRNA (111)
	Antisense therapy (53, 90)

1.2.6.1 STAT3-specific molecular therapies

Peptidomimetic inhibitors of STAT3 dimerization

Fusion peptides consisting of specific protein domains have been used to interrupt the dimerization of Myc, a transcription factor associated with oncogenesis, with another protein necessary for its transcriptional activity, Max. These small-molecule inhibitors of dimerization have been shown to prevent Myc-induced transformation of fibroblasts (97). A similar approach has been taken to inhibiting STAT3 dimerization. Phosphotyrosyl peptides have been designed based on the SH2-binding domain of phosphorylated STAT3 and modified to improve potency (98-100). As STATs possess transcription factor activity only once they have dimerized via their SH2 domain (51), blocking the SH2 domain with phosphotyrosyl peptides should theoretically prevent STAT3-mediated transcription of STAT3 target genes. Treatment with peptidomimetic STAT3 inhibitors has resulted in inhibition of STAT3 transcriptional activity, growth inhibition and apoptosis in Src-transformed mouse fibroblasts and human breast carcinoma cells (98, 99).

Peptide aptamers

A modified yeast two-hybrid screen has been developed to select peptides that bind specific known regions of proteins. These peptides are known as aptamers and are being developed as agents to disrupt interactions between proteins (101). For example, peptide aptamers specific for EGFR have been shown to inhibit tyrosine phosphorylation of both p46 Shc and STAT3 by EGFR, and inhibited proliferation of vulval carcinoma cells (102). Aptamers that bind to the dimerization domain (SH2 and surrounding region) or the DNA-binding domain of STAT3 were identified using a modified yeast two-hybrid screen. The aptamer that bound to the DNA-binding

domain of STAT3 proved to effectively prevent DNA binding by STAT3 and transcription of the STAT3 target gene, Bcl-x_L, and to cause caspase-dependent apoptosis in murine melanoma and human myeloma cells (103).

G quartets

The correct ionic environment, particularly K+, can induce G-rich lengths of DNA to form a G quartet structure that may then bind specific sites on target proteins to inhibit the function of the protein. For example, G-rich oligonucleotides that form G quartets have been found to bind a cellular protein, most likely nucleolin, which is associated with cell proliferation, to inhibit proliferation of prostate, breast and cervical carcinoma cells (104). STAT3-specific G quartets, which form hydrogen bonds with the SH2 region of the STAT3 protein, thus destabilizing the STAT3 dimer, have been reported (105). When used to treat hepatocellular carcinoma cells and breast and prostate cancer xenografts, G quartets were shown to inhibit STAT3 activation, expression of antiapoptotic STAT3 target genes Bcl-X_L and Bcl-2, and the growth of tumor xenografts, in addition to inducing apoptosis within the tumor xenografts (105-108). The G quartets used to target STAT3 were relatively specific, showing fourfold greater inhibition of STAT3 over STAT1 *in vitro* and even greater inhibition of STAT3 compared with STAT1 in IL-6-stimulated hepatocellular carcinoma cells (105, 108).

Inhibition of STAT3 expression

Oligonucleotide therapies targeting the expression of several oncogenic proteins have been tested in clinical trials (109). Treatment with an antisense oligonucleotide or plasmid directed against the STAT3 translation start site resulted in growth inhibition, apoptosis and decreased STAT3

target gene expression in HNSCC cells and tumor xenografts (53, 92). STAT3-specific siRNA has been used to specifically knockdown STAT3 expression in a laryngeal cell line, which resulted in growth inhibition (110). Treatment of an astrocytoma cell line with STAT3-specific siRNA also caused knockdown of STAT3 expression, increased caspase-dependent apoptosis and decreased expression of STAT3 target genes, survivin and Bcl-X_L (111). These results indicate that specific targeting of STAT3 gene expression can be therapeutic. However, the delivery of such a gene to the tumor is still the major obstacle for clinical use.

STAT3 transcription factor decoy

One approach to directly targeting a transcription factor is a double-stranded transcription factor decoy oligonucleotide, which interacts with the DNA-binding domain of a transcription factor to prevent its actions. A transcription factor decoy specific for nuclear factor-κB has been shown to prevent hepatic metastases of murine reticulosarcoma *in vivo* (112). To target STAT3, a 15-mer double-stranded oligonucleotide with phosphorothioate modifications has been designed based on the SIE sequence within the promoter region of the c-fos gene and modified to have higher affinity (113). Theoretically, the STAT3 decoy should bind to the DNA-binding region of the activated STAT3 dimer, preventing it from interacting with gene regulatory elements in the promoter regions of STAT3 target genes and abrogating STAT3-mediated transcription of STAT3 target genes. Treatment of HNSCC cells with the STAT3 decoy resulted in specific killing of three different HNSCC cell lines and inhibited transcription of Bcl-X_L within these cells (113). In *in vivo* studies of HNSCC xenografts, intratumoral injection with the STAT3 decoy decreased STAT3 activation in the tumors, tumor size and expression of Bcl-X_L, cyclin D1 and VEGF (114). A Phase 0 clinical trial with the STAT3 decoy in HNSCC patients has

opened in September, 2008. The therapeutic effects of the STAT3 decoy have also been shown in tumor models other than HNSCC. In a study investigating the role of STAT3 in skin tumor development using a two-stage chemical carcinogenesis model, the STAT3 decoy demonstrated antitumor effects on initiated keratinocytes possessing an activated Ha-ras gene, both *in vitro* and *in vivo* (115). Therefore, the STAT3 decoy may prove useful as an anticancer strategy in malignancies where STAT3 activation contributes to tumor development.

Single-stranded oligonucleotide inhibitor

In most efforts to use a nucleic acid sequence to block a transcription factor, a double-stranded oligonucleotide, such as the aforementioned STAT3 decoy oligonucleotide, is used. A palindromic, single-stranded oligonucleotide, which forms a hairpin loop, has been employed to block the cyclic AMP response element (CRE) and block transcription activated by CRE and AP-1, and has been shown to abrogate the proliferation of MCF-7 breast cancer cells (116). In targeting STAT3, however, one study found that a single-stranded oligonucleotide, 13410, representing the sequence of the consensus STAT3 DNA-binding site, was more efficient at inducing apoptosis in human prostate cancer cells than double-stranded transcription factor decoys. This single-stranded oligonucleotide induced apoptosis in a caspase-dependent manner and prevented binding of STAT3 to the promoter of survivin, a STAT3 target gene. *In vivo* studies with 13410 demonstrated a decrease in prostate cancer xenograft tumor volume and an increase in cell death within the tumors (117). Barton *et al.* present a model suggesting that, similar to the STAT3 decoy oligonucleotide, 13410 may inhibit STAT3 target gene transcription by preventing binding of the STAT3 dimer to DNA. Future studies are necessary to determine the mechanism of action of this single-stranded oligonucleotide (117).

1.2.6.2 Compounds that alter the STAT3 pathway

STAT3 inhibition by various natural compounds has been demonstrated. Resveratrol, auranofin, magnolol, curcumin, epigallocatechin-3-gallate, curcurbitacin I, indirubin, flavipiridol, piceatannol, and parthelonide have all been shown to inhibit STAT3 tyrosine phosphorylation (96, 118-125). With each of these compounds, inhibition of STAT3 tyrosine phosphorylation has been shown to be mediated through effects on signaling mediators upstream of STAT3, including IL-6, Jak1, Jak2, Src, EGFR and SHP-2, a physiological STAT3 inhibitor (96, 118-125).

Treatment of HNSCC cells with retinoids, both LGD1069, specific for the RXR receptor, and LGD1550, specific for the RAR receptor, alters the TGF-α/EGFR signaling pathway, resulting in growth inhibition and a decrease in levels of activated STAT3 (126, 127). When human oral squamous cell carcinoma (OSCC) cells were treated with the non-steroidal anti-inflammatory drug sulindac, decreased expression and activation of STAT3, accompanied by growth inhibition, resulted (128). The same effects were observed following treatment with a peroxisome proliferator-activated receptor-γ agonist, 15-PGJ2 (129).

1.2.7 Interactions between STAT3 and NFκB

The two natural compounds investigated in the present study, guggulsterone and honokiol, both of which are discussed below, have been found to inhibit a different oncogenic transcription

factor, nuclear factor kappa B (NFκB). Based on information regarding interactions between NFκB and STAT3, we hypothesized that these two NFκB-inhibiting natural compounds might also target STAT3.

1.2.7.1 NFκB activity

NFκB is a family of transcription factors including NFκB1, NFκB2, RelA, c-Rel and RelB. These transcription factors form dimers that are sequestered in the cytoplasm by the inhibitors of NFκB (IκBs). Upon signaling through inflammatory cytokines or carcinogen exposure, for example, the IκBs are proteolyzed, releasing the NFκB dimer and allowing it to enter the nucleus and bind a gene regulatory element (130). NFκB target genes include antiapoptotic genes, such as the inhibitors of apoptosis (IAPs), Bcl-x_L and Bcl-2 family genes, cell cycle regulatory genes, such as c-myc, c-myc-b, cyclins D1, D2, D3, and E, and molecules that mediate tumor invasion such as adhesion molecules and matrix metalloproteinases (130-132). In HNSCC, NFκB promotes survival, growth, invasion, pro-inflammatory cytokine expression, and expression of other genes that promote malignancy (133-136). Several cellular proteins are believed to regulate NFκB. A recent study implicated protein kinase casein kinase 2 activity in HNSCC's aberrant activation of NFκB through activation of an NFκB activator, IκB kinase (137).

1.2.7.2 Pathways Converging to Promote HNSCC

Signal Transducer and Activator of Transcription (STAT)-3 and Nuclear Factor Kappa B (NFκB) are both oncogenic transcription factors that have been found to be constitutively active in HNSCC (133). Both bind gene regulatory elements and activate transcription of target genes involved in the control of critical cellular processes such as the cell cycle, apoptosis, and

invasion. HNSCC therapeutics under investigation have been shown to inhibit growth through downregulation of STAT3 or NFκB activity (138, 139). The molecular pathways involving each of these transcription factors converge in HNSCC to promote transcription of some of the same oncogenes, including cyclin D1, which is often overexpressed in HNSCC (140). Molecular crosstalk between STAT3 and NFκB has been observed in HNSCC cell lines (141). Interleukin-6 (IL-6) secretion, which stimulates STAT3 signaling in HNSCC, was found to be dependent on IL-6 promoter binding by NFκB (141). Furthermore, STAT3 and NFκB have been found to affect one another's binding to other gene regulatory elements (142, 143) and even to form a complex in certain systems (144-146). Figure 3 outlines the interactions between STAT3 and NFκB.

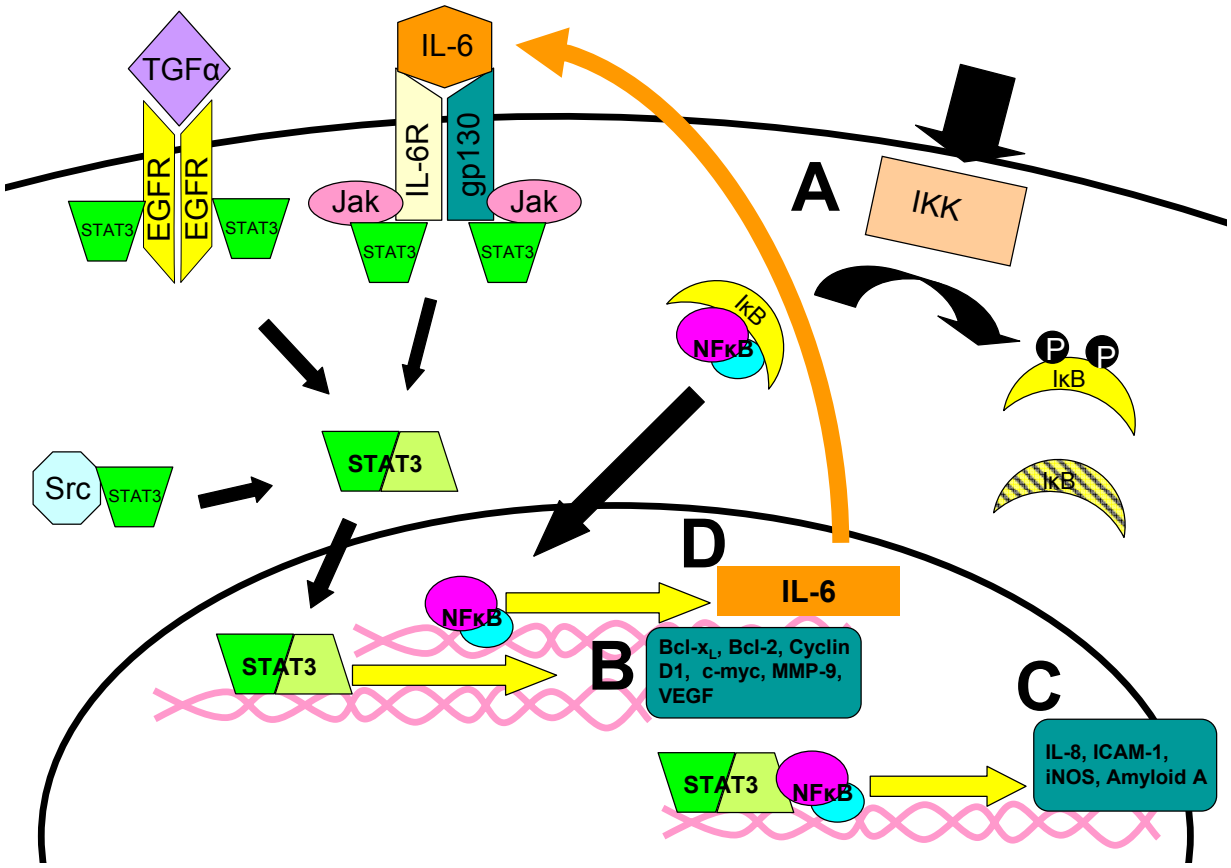

Figure 3. Interactions between NFκB and STAT3 (A) IKK phosphorylates IκB, signaling it for proteolysis and releasing NFκB, which translocates to the nucleus and binds DNA as a transcription factor. (B) NFκB and STAT3 have various target genes, which are involved in tumorigenesis, in common. (C) NFκB and STAT3 interact directly in regulating certain target genes. (D) Crosstalk between NFκB and STAT3 in HNSCC cells: NFκB regulates the expression of IL-6, which stimulates STAT3 activation (141).

1.3 THE ROLE OF NATURAL COMPOUNDS IN CANCER PREVENTION AND THERAPY

Human health is greatly impacted by our diet. One example of this is evidenced by observational and case controlled studies about the effects of dietary plants on cancer risk, which have shown that the risks of developing various types of cancer, including HNSCC, decrease with an increased consumption of plants (147-149). Studies indicating the molecular factors and cellular processes targeted by plant-derived compounds have led to several clinical trials to test their anti-tumor properties (150, 151). Plant extracts often contain complex mixtures of compounds that have diverse effects on cell signaling, an advantage over single agent therapies. Additionally, as opposed to engineered molecular inhibitors, these compounds are often more available and less expensive. Many plants, including those that contain the compounds investigated in the current study, have been used, over generations, for therapeutic purposes in Eastern and alternative medicine, resulting in informal testing for toxicity, bioavailability and efficacy long before the advent of the modern day clinical trial.

1.4 RATIONALE FOR THE CURRENT STUDY

Various studies have demonstrated the important role that STAT3 plays in HNSCC and have focused on devising therapies that target STAT3 (138). Clinical trials of chemopreventive agents for HNSCC have not focused on directly targeting STAT3, however, despite evidence that aberrant activation of STAT3 may be an early step in HNSCC carcinogenesis (89, 94). The

current study aims to identify and characterize natural compounds that target STAT3 to investigate their potential for use in the treatment and prevention of HNSCC.

2.0 ROTATION REPORT: SCREENING NATURAL COMPOUNDS FOR ANTICANCER ACTIVITY IN HNSCC

2.1 INTRODUCTION

In order to identify candidate agents for HNSCC chemoprevention and treatment, various natural compounds and analogues of natural compounds were screened for efficacy in HNSCC cell lines. The compounds investigated included ginsenosides, isothiocyantes and guggulsterone. *In vitro* growth inhibition of two human HNSCC cell lines and STAT3 inhibition were parameters used to investigate candidate compounds.

2.1.1 Ginseng

Panax ginseng, a plant used for treatment of various ailments in Eastern medicine, contains several compounds, referred to as "ginsenosides," some of which have been shown to have anticancer properties. These compounds have been found to induce differentiation, cause apoptosis and inhibit growth in various cancer cell lines. Possible mechanisms of ginsenosides' activity include their ability to inhibit the effects of carcinogens and their antioxidant activities (177, 178).

2.1.2 Isothiocyanates

Certain cruciferous vegetables like cabbage, broccoli and cauliflower contain high concentrations of isothiocyanates (ITCs). Epidemiological studies have shown decreased risk of developing prostate cancer, breast cancer, non-Hodgkin's lymphoma, and bladder cancer in humans with increased consumption of cruciferous vegetables (149). Upon chewing of these vegetables, ITCs are released by the hydrolytic action of myrosinase, an enzyme present in plants but separated cellularly from their substrates, glucosinolates, of which over 120 have been identified (149, 179). ITC's actions include induction of phase I and phase II enzymes of drug and carcinogen metabolism, induction of growth arrest and apoptosis in cancer cells, and changes in certain signaling pathways, including MAP kinase signaling pathways (149, 180, 181). In a study by Lui *et al.*, benzyl ITC (BITC) was shown to cause apoptosis in HNSCC cells and to activate the p38 MAPK and MEK/MAPK pathways (182). In this study, we examine both aromatic ITCs and aliphatic ITCs, including sulforaphane, an ITC found in broccoli and other cruciferous vegetables, and its analogues, in HNSCC.

2.1.3 Guggulsterone

Guggulsterone, a compound derived from the plant, *Commiphora mukul,* has been used in Indian Ayurvedic medicine for thousands of years and has anticancer activity in various cancer models (183)**.** This compound, which has two stereoisomers, has been shown to have complex effects on cell signaling in cancer. Guggulsterone will be discussed in greater detail in Chapter 3.

2.2 MATERIALS AND METHODS

2.2.1 Cell culture

1483 and UM-22b human HNSCC cells were grown and maintained in DMEM containing 10% FBS. These two cell lines were chosen in order to lend diversity to the study and to provide for easy translation into the xenograft model of HNSCC.

2.2.2 Trypan blue survival assay

1483 and UM-22b cells were plated and, the following day, were treated with DMEM/10% FBS containing a ginsenoside, isothiocyanate or isomer of guggulsterone (1, 2.5, and 5 μM) or DMSO, the vehicle for each drug. Each sample contained 0.5 μl/ml DMSO. All experiments were performed with triplicate samples. On the day of cell collection, either 24 hours or 72 hours post treatment, both floating and attached cells were collected and resuspended in trypan blue dye Invitrogen, Carlsbad, CA). Live cells were counted under an inverted microscope using a hemocytometer.

2.2.3 Western blot

1483 and UM-22b cells were plated and, the following day, were treated with DMEM/10% FBS containing a ginsenoside, isothiocyanate or isomer of guggulsterone (1, 2.5, and 5 μM) or DMSO, the vehicle for each drug. Each sample contained 0.5 μl DMSO per ml of medium. On

the day of collection, either 24 or 72 hours post-treatment, medium was removed, cells were washed in cold phosphate buffered saline (PBS), were scraped from the plate into lysis buffer (Tris-HCl, pH 7.6(10mM), 0.5M EDTA (5mM), NaCl (50mM), $Na_4P_2O_7$ (30mM), NaF (50mM), Na_3VO_4 (1mM), 1% Triton X-100), sonicated and lysates collected. Lysates were separated by SDS-PAGE and transferred to a Trans-blot nitrocellulose membrane (Bio-Rad Laboratories, Hercules, CA). The membrane was rinsed in Tris-buffered Saline – Tween (TBST) and then blocked with 5% milk in TBST. Primary antibodies against P-tyr705-STAT3 (Cell Signaling Technology, Beverly, MA), total STAT3 (Cell Signaling Technology, Beverly, MA) and β-actin was diluted in 5% milk/TBST. The appropriate hrp-linked secondary antibodies (Bio-Rad Laboratories, Hercules, CA) were diluted in 5% milk/TBST. The membrane was finally developed using luminol solutions (Santa Cruz, Santa Cruz, CA) and visualized by autoradiography.

2.3 RESULTS

2.3.1 Screening compounds for cytotoxicity against HNSCC cells

Trypan blue dye exclusion assays were used to compare the effects of various compounds on growth of 1483 and UM-22b cells. In addition to their ability to grow *in vivo*, thus having potential for use in continuation of this study in the xenograft model of HNSCC, they were also chosen because the anticancer properties of aromatic isothiocyanates had been tested in these two cell lines (182). Figures 4a, 4b, and 4c show graphs of the results of trypan blue dye

exclusion assays with 1483 and UM-22b cells treated with up to 5 μM concentrations of non-isothiocyanate compounds, aromatic isothiocyanates, and aliphatic isothiocyanates, respectively. Figure 4d shows the cumulative data for screening of all compounds in 1483 and UM-22b cells. Our observations indicate that, of all of the compounds screened, 1-Isothiocyanato-9-methyl-sulfinyl nonane was the most effective at inhibiting growth of HNSCC cells. In general, the longer-chain aliphatic sulforaphane analogues, including 1-Isothiocyanato-9-methyl-sulfinyl nonane, 1-Isothiocyanato-6-methyl-sulfinyl hexane, Alyssin and Alyssin sulfone, inhibited growth more effectively than the non-isothiocyanate compounds and the aromatic isothiocyanates.

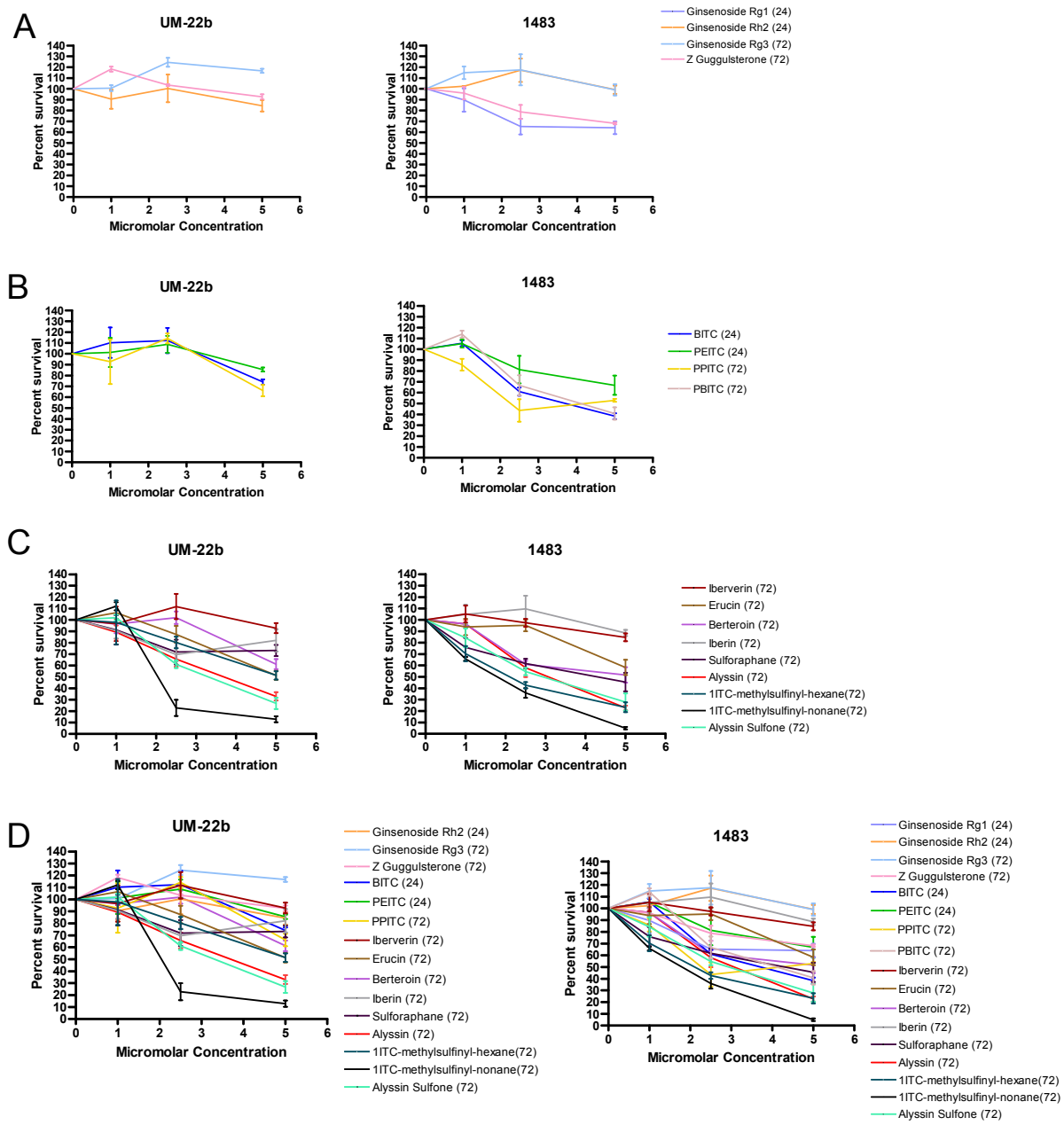

Figure 4. Screening natural compounds and their analogues for growth inhibition of HNSCC cell lines. 1483 and UM-22b cells were treated with (A) non-isothiocyanates, including Z-guggulsterone and three different ginsenosides (Rg1, Rg2, Rg3) (B) aromatic isothiocyanates, including Benzyl-ITC (BITC), 2-Phenylethyl-ITC (PEITC), 3-Phenylpropyl-ITC (PPITC), and 4-Phenylbutyl-ITC (PBITC) and (C) aliphatic isothiocyanates, including sulforaphane and its analogues. Duration of treatment, in hours, is shown in parentheses. Cells were stained with trypan blue dye and counted. (D) Consolidated data for all compounds screened in each cell line. Each experiment was performed once.

Table 3. Structures of and Growth Inhibition by Compounds Screened

Class	*Compound*	*Structure*	*%growth inhibition at 5μM (1483)*	*%growth inhibition at 5μM (UM-22b)*
Non-Isothiocyanate	**Guggulsterone**	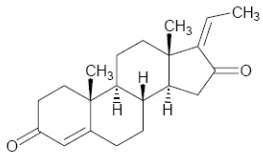	31.9 (72h)	7.42 (72h)
	Ginsenoside Rg1	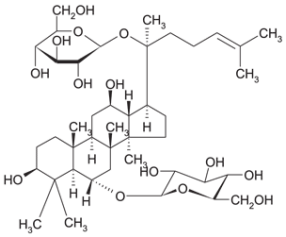	37.0 (24h)	
	Ginsenoside Rh2	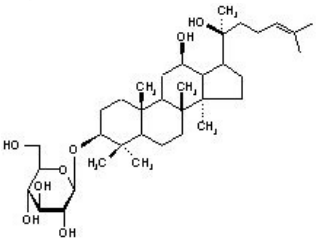	0.81 (24h)	15.75(24h)
	Ginsenoside Rg3	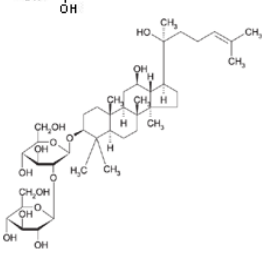	1.04 (72h)	0 (72h)
Aromatic Isothiocyanate	**Benzyl-ITC** (BITC)	Ph-CH_2-N=C=S	61.70 (24h)	26.02(24h)
	2-Phenylethyl-ITC (PEITC)	Ph-$(CH_2)_2$-N=C=S	33.15 (24h)	14.50(24h)
	3-Phenylpropyl-ITC (PPITC)	Ph-$(CH_2)_3$-N=C=S	47.10 (72h)	33.94(72h)
	4-Phenylbutyl-ITC (PBITC)	Ph-$(CH_2)_4$-N=C=S	59.24 (72h)	
Methylsulfenyl Isothiocyanate	**Iberverin** (3-(Methylthio)propyl-ITC)	CH_3-S-$(CH_2)_3$-N=C=S	15.38 (72h)	7.19 (72h)
	Erucin (4-(Methylthio)butyl-ITC)	CH_3-S-$(CH_2)_4$-N=C=S	41.77 (72h)	48.68(72h)
	Berteroin (5-(Methylthio)pentyl-ITC)	CH_3-S-$(CH_2)_5$-N=C=S	48.36 (72h)	38.83(72h)
Methylsulfinyl Isothiocyanate	**Iberin** (3-(Methylsulfinyl)propyl-ITC)	CH_3-SO-$(CH_2)_3$-N=C=S	11.53 (72h)	17.89(72h)
	Sulforaphane (4-(Methylsulfinyl)butyl-ITC)	CH_3-SO-$(CH_2)_4$-N=C=S	54.52 (72h)	26.85(72h)
	Allysin (5-(Methylsulfinyl)pentyl-ITC)	CH_3-SO-$(CH_2)_5$-N=C=S	77.33 (72h)	66.99(72h)
	1-Isothiocyanato-6-methyl-sulfinyl hexane	CH_3-SO-$(CH_2)_6$-N=C=S	76.72 (72h)	48.66(72h)
	1-Isothiocyanato-9-methyl-sulfinyl nonane	CH_3-SO-$(CH_2)_9$-N=C=S	94.99 (72h)	87.1 (72h)
Methylsulfonyl Isothiocyanate	**Alyssin Sulfone** (5-(Methylsulfonyl)pentyl-ITC)	CH_3-SO_2-$(CH_2)_5$-N=C=S	72.12 (72h)	73.19(72h)

2.3.2 Effects of tested compounds on STAT3 activity in HNSCC cells

Compounds were screened for their ability to alter the activity of STAT3 in 1483 and UM-22b cells. Western blots probing lysates from cells treated with some of the isothiocyanates screened are shown in Figure 5. Not all compounds tested for their growth inhibitory activity were screened for STAT3 targeting. In this preliminary study, the ginsenosides Rg1 and Rh2, and the isothiocyanate PPITC, did not inhibit STAT3 in HNSCC cells. On the other hand, the isothiocyanates, PBITC, sulforaphane and alyssin all induced modest decreases in phosphotyrosine STAT3 in individual experiments. Chapter 4 will discuss the STAT3 inhibitory activity of guggulsterone, which was later determined.

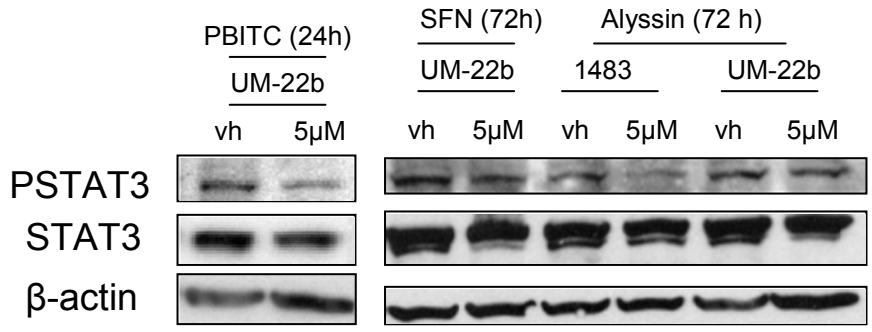

Figure 5. STAT3 inhibition by isothiocyanates. **1483 or UM-22b cells were treated with PBITC (5 μM, 24 h), alyssin (5 μM, 72 h) or sulforaphane (5 μM, 72 h) or with DMSO as a vehicle control. Whole cell lysates were probed for phosphotyrosine STAT3, total STAT3 and β-actin, as a loading control.**

2.4 DISCUSSION

The current study was performed to screen naturally occurring compounds and their analogues for their anticancer and STAT3-targeting activity in HNSCC cells, in hopes of identifying a candidate chemopreventive agent for HNSCC. Although growth inhibition and STAT3 targeting, on their own, are not indicative of a compound's chemopreventive activity, these parameters were chosen in consideration of the important role that STAT3 plays in HNSCC and the assumption that growth inhibition of HNSCC cell lines might reflect a compound's ability to inhibit head and neck carcinogenesis.

Definite conclusions about which class of aliphatic isothiocyanates, defined by the oxidation state of sulfur, is most cytotoxic to HNSCC cells cannot be drawn from these data. These data do suggest a general trend within each class of aliphatic isothiocyanates, however. Compounds with longer hydrocarbon chains more effectively inhibit growth of 1483 and UM-22b cells. Also, other studies have found that aromatic hydrocarbons with longer chain spacers beyond the aromatic ring have greater anticancer activity (182, 184). In general, however, longer chain length does not necessarily indicate optimal activity in all malignancies (184). It seems that there is more complexity to the structural basis of a compound's activity against cancer. Future experiments with require examination of the specificity of each compound's growth inhibitory effect in cancer cells as compared to normal cell lines.

STAT3 activity may be an early event in HNSCC carcinogenesis, suggesting that STAT3 targeting may potentially prevent HNSCC. To our knowledge, alterations in STAT3 activity after treatment with ginsenosides and isothiocyanates have not been previously examined. In the

current study, the isothiocyanates PBITC, alyssin, and sulforaphane were found to induce modest decreases in phosphotyrosine STAT3 (Figure 5). These experiments have not been repeated.

After conducting this screen for candidate chemopreventive agents, our strategy for choosing a compound to investigate changed. We realized that *in vivo* growth inhibition is an imperfect parameter for measuring the chemopreventive activity of a compound and that almost all of the compounds screened are unavailable as clinical formulations. This would pose significant barriers to their translation into the clinic, were they found to have chemopreventive activity. Upon determining the STAT3-inhibitory effects of guggulsterone (Chapter 3), we decided to focus our study on guggulsterone, despite our observations that HNSCC cell lines were much more sensitive to some of the other compounds screened. Guggulsterone is widely available as a dietary supplement and has been used in clinical trials, demonstrating few and mild side effects (183, 185). These characteristics make guggulsterone a very good candidate chemopreventive drug, at least in terms of practical considerations.

3.0 GUGGULSTERONE INHIBITS GROWTH OF HEAD AND NECK SQUAMOUS CELL CARCINOMA VIA TARGETING OF SIGNAL TRANSDUCER AND ACTIVATOR OF TRANSCRIPTION-3 SIGNALING

3.1 INTRODUCTION

3.1.1 Guggulsterone

For over 2000 years, the extract of the plant *Commiphora mukul* has been used in Indian Ayurvedic medicine as a treatment for numerous ailments. Guggulsterone, a compound contained in this plant resin, is widely available as a dietary supplement and has been used in many clinical trials that have focused on its cholesterol-lowering potential. The steroid-like structure of guggulsterone contains four hydrocarbon rings and has two isomers, Z and E. In clinical studies with guggulsterone, human subjects experienced decreased cholesterol and triglyceride levels and mild side effects, including rash, headache and diarrhea (183, 185). The relative safety of this drug makes it a good candidate for complementary and preventive therapy.

3.1.2 Guggulsterone's NFκB inhibiting activity

Guggulsterone's anticancer activity was first demonstrated by Shishodia et al. who, based on an earlier study demonstrating guggulsterone's anti-inflammatory activity (186), hypothesized that

guggulsterone may affect nuclear factor kappa B (NFκB), a transcription factor that plays a role in both inflammation and cancer (187). Guggulsterone treatment of lung cancer cells was then shown to inhibit both nuclear factor kappa B (NFκB) and its activator, IκB (inhibitor of NFκB) kinase, promoting apoptosis and decreasing the expression of antiapoptotic genes, cell cycle promoting genes, and genes that control metastasis (187). NFκB DNA binding was shown to decrease with guggulsterone treatment of various cell lines, including the HNSCC cell line MDA1986 (187).

3.1.3 Guggulsterone's anticancer activity

Subsequent studies demonstrated guggulsterone-induced apoptosis that was mediated by caspases and changes in expression of Bax and Bak in prostate cancer cells (188). In acute myeloid leukemia cells, apoptosis was induced through mitochondrial dysfunction, differentiation and the generation of reactive oxygen species (189). Two studies have implicated c-Jun N-terminal kinase (JNK) as a mediator of guggulsterone's anticancer effects on human monocytic leukemia cells (190) and prostate cancer cells (191). One study reported inhibition of tumor angiogenesis in both *in vitro* assays and, using an animal model of prostate cancer, in the first reported *in vivo* demonstration of guggulsterone's anticancer activity (192). Finally, a very recent study has demonstrated inhibition of NFκB signaling and inhibition of skin tumorigenesis *in vivo* by topical guggulsterone administration (193).

3.1.4 Rationale for investigating guggulsterone's STAT3-targeting activity

Based on previous reports of interactions between NFκB and STAT3 (Figure 3), we hypothesized that guggulsterone may target STAT3 in HNSCC. Attempts to target STAT3, a putative therapeutic target in HNSCC, have been the focus of various preclinical studies using, nucleic acids, like the STAT3 transcription factor decoy, and proteins, such as peptidomimetics, for example. For the most part, several obstacles need to be overcome before molecules like these can be successful in the clinic, much more so than a safe and widely available nutraceutical like guggulsterone. In a very recent study, Ahn et al. demonstrated guggulsterone-induced decreases in levels of phosphotyrosine STAT3 in both multiple myeloma and HNSCC cell lines (194). In the same study, guggulsterone's effect on phosphotyrosine STAT3 was shown to be mediated through activity of the protein tyrosine phosphatase and physiological regulator of STAT3, SHP-1 (194).

In the current study, we investigated guggulsterone's effects in HNSCC preclinical models and the role of STAT3 signaling in mediating these effects. Our results demonstrate that guggulsterone induces apoptosis, cell cycle arrest and decreases in invasiveness of HNSCC cells. Further investigation suggested that guggulsterone enhances the effects of currently available HNSCC therapies. Furthermore, the expression of HIF-1α, an important therapeutic target and marker of poor prognosis, which is downstream of both NFκB and STAT3, was found to decrease dramatically with guggulsterone treatment. Guggulsterone's growth inhibitory effects were mediated, at least in part, by modulation of STAT3 signaling, notably characterized by decreases in both total STAT3 as well as phosphotyrosine STAT3 expression. Guggulsterone

inhibited HNSCC tumor growth *in vivo,* thereby supporting the future clinical development of this compound in HNSCC.

3.2 MATERIALS AND METHODS

3.2.1 Cell lines and reagents

The HNSCC cell lines used in this study were derived from human HNSCC tumors (195). The PCI-37a cell line was created at University of Pittsburgh (196). UM-22b cells were provided Dr. Thomas Carey (University of Michigan, Ann Arbor, MI) (197) and 1483 cells by Dr. Gary Clayman (MD Anderson Cancer Center, Houston TX) (198). All HNSCC cell lines were cultured in Dulbecco's modification of eagle's medium (Mediatech, Manassas, VA) with 10% heat-inactivated FBS (Invitrogen, Carlsbad, CA). E and Z guggulsterone (Steraloids, Inc, Newport, RI) were both dissolved in 100% dimethylsulfoxide (DMSO) when used to treat cell cultures and suspended in saline for animal treatments. *Guggulipid* (Sabinsa Corporation, Piscataway, NJ) was suspended in 5% ethanol/corn oil for animal treatments. Cisplatin (Bedford Laboratories, Bedford, OH) and cetuximab (ImClone, New York, NY), both diluted in saline, and erlotinib (OSI Pharmaceuticals, Melville, NY), dissolved in DMSO, were also used in the described studies. The characteristics of HNSCC cell lines used in this study are shown in Table 4.

Table 4. Characteristics of HNSCC Cell Lines

	1483	UM-22b	PCI-37a
TNM stage	T2N1M0	T2N1M0	T3N2M0
Gender	male	female	male
p53 mutation	unknown	yes	unknown
Tumor site	oral cavity	lymph node metastasis from hypopharynx	larynx
Doubling time	~36h	~24h	~80h
Tumors in nude mice	yes	yes	no

3.2.2 Guggulsterone treatment of cell cultures

Unless otherwise specified, HNSCC cell lines were treated with DMEM containing an even mixture of guggulsterone's E and Z stereoisomers (Steraloids, Inc, Newport, RI) dissolved in 100% dimethylsulfoxide (DMSO). Each given concentration of the even mixture represents E-guggulsterone as one half the concentration and Z-guggulsterone as the other half. Vehicle control cells were treated with an equal volume of DMSO.

3.2.3 Trypan blue dye exclusion assay

Following 72-hour treatments with guggulsterone or vehicle, floating cells were collected as well as adherent cells, which were harvested by trypsinization. Cells were resuspended in trypan blue dye (Invitrogen, Carlsbad, CA). Live cells, as judged by exclusion of trypan blue dye, were counted under an inverted microscope, using a hemocytometer. Percent survival was calculated relative to the number of surviving cells from cultures treated with vehicle. Data from cell-counting experiments represent averages from triplicate wells in multiple separate experiments. EC_{50}s were calculated using Graphpad Prism software version 4.03 (GraphPad Software Inc.).

3.2.4 MTT assays

HNSCC cells were plated and treated with guggulsterone for 72 hours. Medium was removed and replaced with thiazolyl blue tetrazolium (Sigma Chemical) solution in PBS. Cells were incubated at 37˚C until appearance of blue color. Thiazolyl blue tetrazolium was removed and replaced with 100% DMSO. Optical density of each sample was measured using a plate reader (μQuant, Bio-tek Instruments, Inc). Blanked readings of guggulsterone-treated cells were compared to those for vehicle-treated cells.

3.2.5 Cell death detection ELISA

HNSCC cells were treated with guggulsterone for up to 12 hours. Floating cells were collected as well as adherent cells, which were harvested by trypsinization. Apoptosis was assayed through detection of histone-associated DNA fragments present in cell lysates using a Cell Death Detection ELISA (Roche Diagnostics, Indianapolis, IN) according to the manufacturer's instructions. The enrichment factor represents the ratio of histone-associated DNA fragments, represented by duplicate, blanked OD readings from multiple experiments, such that enrichment factor=(average blanked OD of guggulsterone-treated cells)/(average blanked OD of vehicle-treated cells).

3.2.6 Cell cycle analysis

HNSCC cell lines were treated with guggulsterone or vehicle for 24 hours (triplicate cultures in each of multiple experiments). Floating cells were collected as well as adherent cells, which were harvested by trypsinization. Cells were fixed in 70% ethanol/PBS for at least one hour at 4°C and stained with propidium iodide/RNase A reagent (BD Biosciences, San Diego, CA) for one hour at room temperature in the dark. Cells underwent flow cytometric analysis with a BD FACSCalibur flow cytometer. BD CellQuest software was used for acquisition of data and BD Modfit software for data analysis.

3.2.7 Matrigel invasion assays

UM-22b cells were plated, in serum free DMEM in matrigel-coated modified Boyden inserts with a pore size of 8 μm (BD Biosciences, San Diego, CA), the lower well containing DMEM/10% FBS. Both the insert and outer well also contained 10 ng/ml epidermal growth factor (EGF) and either one or a combination of the following treatments: an even mixture of guggulsterone's stereoisomers (8.3 μM), erlotinib (5 μM), cetuximab (4 μg/ml), or vehicle. Matrigel inserts were fixed, stained with Hema 3 (Fisher Scientific), and counted (at least 4 fields per insert) as previously described (199).

3.2.8 Immunoblotting

HNSCC cells were treated with guggulsterone or vehicle for 72 hours. Cells were harvested by scraping in lysis buffer (Tris-HCl, pH 7.6 (10mM), EDTA (5mM), NaCl (50mM), $Na_4P_2O_7$ (30mM), NaF (50mM), Na_3VO_4 (1mM), Triton X-100 (1%) (200), and briefly sonicated. Protein concentration in lysates was quantified using protein assay solution (Bio-Rad Laboratories, Hercules, CA) and comparing lysates to a standard curve of bovine serum albumin solutions. Approximately 40 μg of protein were loaded onto an 8% polyacrylamide gel. After SDS-PAGE, lysates were transferred onto a Trans-blot nitrocellulose membrane (Bio-Rad Laboratories, Hercules, CA). The membrane was blocked in blocking solution of 5% nonfat dry milk in TBST (0.2% Tween 20 in PBS) for one hour at room temperature. A primary antibody for phosphotyrosine (Y705) STAT3, total STAT3 (Cell Signaling Technology, Beverly, MA) or HIF-1α (BD Biosciences, San Diego, CA), at a 1:1000 dilution in blocking solution, was used to probe the membrane overnight at 4°C. The primary antibody for β-actin (Calbiochem, San Diego, California) was diluted at 1:5000 in blocking solution and used to probe membranes for 45 minutes at room temperature. Membranes were then incubated with secondary antibodies (1:3000 in blocking solution) for 15 minutes in the case of blots probed for β-actin (secondary is goat anti mouse IgM-horseradish peroxidase conjugate; Bio-Rad Laboratories, Hercules, CA) and for 1 hour in the case of blots probed for phosphotyrosine STAT3, STAT3 (secondary is goat anti rabbit IgG- horseradish peroxidase conjugate; Bio-Rad Laboratories, Hercules, CA) or HIF-1α (secondary is goat anti mouse IgG- horseradish peroxidase conjugate; Bio-Rad Laboratories, Hercules, CA). Membranes were washed in TBST three times after incubation with each antibody. Membranes were developed using luminol reagents (Santa Cruz, Santa Cruz, CA) and visualized by autoradiography. Densitometric analyses were performed using DigiDoc1000

software (Alpha Innatech Corporation, San Leandro, CA). Densitometric values for bands representing STAT3 or PSTAT3 were normalized to β-actin such that relative units=densitometric value for protein of interest/densitometric value for corresponding β-actin band. Displayed values represent the relative units for each sample divided by the relative units for vehicle control.

3.2.9 STAT3 siRNA transfection

1483 and UM-22b cells were transfected with STAT3 siRNA (siGenome Duplex STAT3) or GFP siRNA (GFP duplex 1), (Dharmacon, Lafayette, CO) plus 6 µl Lipofectamine 2000 (Invitrogen, Carlsbad, CA), per well of a 6 well plate, in 1.5 ml OPTIMEM 1 medium (Invitrogen, Carlsbad, CA) for 4 hours. DMEM/10% FBS was then replaced.

3.2.10 Realtime RT-PCR for STAT3

1483 and UM-22b cells were treated with vehicle or guggulsterone for 1, 4, 6, 8, 12, 16 and 24 hours or transfected with STAT3 siRNA, as described above. Other controls were untreated wildtype and STAT3-knockout mouse embryonic fibroblasts. RNA was extracted using the Versagene RNA-Cell Kit with on-column DNase treatment according to the manufacturer's instructions (Gentra Systems, Minneapolis, MN). Reverse transcription of the isolated RNA was then performed using SuperScript First-Strand Synthesis System for RT-PCR (Invitrogen, Carlsbad, CA) according to the manufacturer's instructions. Real time PCR employed the

Applied Biosystems ABI Prism 7000 Sequence Determination System (Applied Biosystems, Foster City, CA). Samples were prepared using TaqMan Universal PCR Master Mix and 312.5 ng of cDNA (Applied Biosystems, Foster City, CA). The thermocycler conditions were as follows: 1x 95 °C for 5 min; 40x (30sec 95 °C denaturation, 1 min 60 °C annealing, 45 sec 72 °C extension); 1x 72 °C for 5 min. Primer and probe sequences: STAT3F 5'-ATCCTGAAGCTGACCCAGGTA-3'; STAT3R 5'-AGGTCGTTGGTGTCACACAGA-3'; STAT3 Probe 5'-CGCTGCCCCATACCTGAAGACCAAGTTT-3'; β-ActinF 5'-GCAAAGACCTGTACGCCAACA-3'; β-ActinR 5'-TGCATCCTGTCGGCAATG-3'; β-Actin Probe 5'-TGGCGGCACCACCATGTACC-3' (39).

3.2.11 RT-PCR

Cell homogenization was completed using the QIAshredder kit (Invitrogen, Carlsbad, CA) and subsequent RNA isolation was performed with the RNeasy Mini Kit (Invitrogen, Carlsbad, CA) with the optional on column DNase treatment. Reverse transcription of the isolated RNA was performed using SuperScript First-Strand Synthesis System for RT-PCR (Invitrogen, Carlsbad, CA). PCR was performed using PCR Master Mix (Promega, Madison, WI) and 125 ng of cDNA. Primer sequences for amplification of FXR: FXRsense 5'-TGCTGAAAGGGTCTGCGGTTG-3'; FXRantisense 5'-CACGTCCCAGATTTCACAGAG-3'. Primer sequences for amplification of Bcl-X_L: Bcl-$X_L$sense 5'-CCCAGAAAGGATACAGCTCG-3', Bcl-$X_L$antisense 5'-AAAGTATCCCAGCCGCCGTTCT-3'. Primer sequences for amplification of Cyclin D1: cyclinD1sense 5'-CTGTGCTGCGAAGTGGAAACC-3', cyclinD1antisense 5'-CAGGAAGCGGTCCAGGTAGTT-3'. Primer sequences for amplification of house-keeping

gene, GAPDH: GAPDH Fwd 5'- TGGAATTTGCCATGG GTG -3'; GAPDH Rev 5'- GTGAAGGTCGGAGTCAAC -3', The thermocycler conditions were as follows: 1x 94 °C for 5 min; 35x (1 min 94 °C denaturation, 30 sec 56 °C annealing, 30 sec 72 °C elongation); 1x 72 °C for 7 min. RT-PCR products were resolved on a 1.5% agarose gel containing 3% ethidium bromide.

3.2.12 Luciferase assay

UM-22b cells were transfected with an NFκB-luciferase construct using Lipofectamine 2000 (Invitrogen, Carlsbad, CA) in OPTIMEM 1 medium (Invitrogen, Carlsbad, CA) for 4 hours. DMEM/10% FBS was then replaced. The following day, cells were treated with guggulsterone (10 μM) for 4 hours, collected, and lysed, using a syringe. The Luciferase Reporter 1000 Assay System (Promega) was used, according to the manufacturer's instructions and a luminometer to measure relative light units (RLU). Protein assay solution (Bio-Rad Laboratories, Hercules, CA) was used to quantify the amount of protein in each sample, for comparison to RLUs.

3.2.13 In vivo tumor xenograft studies

3.2.13.1 Guggulsterone study, pretreatment model

Female nude mice (6-8 wks old; 8 in each of 2 groups) were treated daily, by oral gavage, with 2 mg guggulsterone (Steraloids, Inc., Newport, RI) suspended in 200 μl saline, for two weeks prior to tumor cell inoculation or with saline, as a vehicle control. One million 1483 and UM-22b cells, in 100 μl Hank's balanced salt solution (Invitrogen, Carlsbad, CA), were subcutaneously injected into the animals left and right flanks, respectively. Daily treatments with guggulsterone

or saline continued for another three weeks. Mice were euthanized one week after the last guggulsterone treatment. Tumors were fixed in 10% formalin and sectioned onto glass slides. Slides were stained with TUNEL or with an antibody specific for STAT3 (Cell Signaling Technology). Slides were scored by a pathologist (Dr. Raja Seethala) who was blinded to treatment groups. Immunohistochemical score=(%of tumor section scored as 1+) x 1 + (% of tumor section scored as 2+) x 2+ (percent of tumor section scored as 3+) x 3.

3.2.13.2 *Guggulipid* studies, therapy model

Experiment 1. 1483 cells: 16 female nude mice (6-8 weeks old) were subcutaneously injected with one million 1483 cells. After tumor outgrowth, mice were randomized to two groups, based on tumor volumes and treated daily by oral gavage, with 25.9 mg Guggulipid (7.73% guggulsterone; Sabinsa Corporation, Piscataway, NJ), resuspended in corn oil/5% ethanol to a total of 200 µl, or with the vehicle alone. Blinded tumor measurements were taken three times per week.

Experiment 2. UM-22b cells and combination with cetuximab: 40 Female nude mice (6-8 wks old) were subcutaneously injected into each animal's right flank with two million UM-22b cells, in 100 µl Hank's balanced salt solution (Invitrogen, Carlsbad, CA). After tumor outgrowth, 10 days later, mice were randomized to four groups, based on tumor volumes and treated, depending on the group, daily by oral gavage, with 25.9 mg Guggulipid (7.73% guggulsterone; Sabinsa Corporation, Piscataway, NJ), resuspended in corn oil/5% ethanol to a total of 200 µl, twice per week with 0.8 mg cetuximab (ImClone, New York, NY), by intraperitoneal injection in 100 µl saline, with both drugs, or with the corresponding vehicles. Treatments continued for three weeks. Blinded tumor measurements were taken three times per week.

3.2.14 Statistical analyses

All statistical analyses of *in vitro* results and tissue stains were done using the nonparametric Mann-Whitney or Wilcoxon tests. All tests were two-tailed and exact. The *in vivo* tumor xenograft experiments were analyzed with a general linear model that assumed animals were random effects. Data were examined for the interaction between treatment group and day of observation, testing whether the slopes of the growth curves (volume vs. day of observation) were significantly different for the control and treatment groups.

3.3 RESULTS

3.3.1 Guggulsterone inhibits the growth of HNSCC cell lines

To begin to identify a compound with anti-cancer activity in HNSCC cells, a series of naturally-occurring compounds or analogues of naturally occurring compounds, including isothiocyanates, ginsenosides and guggulsterone, which has two stereoisomers, E and Z, were screened *in vitro* for growth in two human HNSCC cell lines, 1483 and UM-22b (Chapter 2). Trypan blue dye exclusion assays demonstrated that, E-guggulsterone, Z-guggulsterone, and an even mixture of the two stereoisomers decreased numbers of viable cells in a dose-dependent manner after 24 hours of treatment (Figure 6a, 6b and 6c). Trypan blue dye exclusion assays also demonstrated that after 72 hours of treatment of 1483, UM-22b or PCI-37a cells with the even mixture of guggulsterone's stereoisomers, inhibition of HNSCC cell growth *in vitro* occurred with EC_{50}s of 7.0 μM for 1483, 8.3 μM for UM-22b, and 5.1 μM for PCI-37a (Figure 6d). These

concentrations are comparable to those observed in guggulsterone treatment of various other cancer cell lines, including other HNSCC cell lines (187, 188, 190). Furthermore, the concentrations required to inhibit the growth of HNSCC cell lines are physiologically attainable *in vivo*. Even though pharmacokinetic parameters for guggulsterone have not been determined in humans, the maximal plasma concentration of guggulsterone (C_{max}) in rats was shown to be about 3.3 μM following oral gavage with 50 mg guggulsterone/kg body weight (201). The plant extract, sold as a nutraceutical dietary supplement, contains both stereoisomers of guggulsterone in nearly equal amounts (data from the laboratory of Dr. Shivendra Singh). Since the plant extract is more likely than the synthetic compound to be used as a clinical formulation and because, based on our observations, there does not seem to be an advantage to using one stereoisomer over the other, subsequent *in vitro* studies were performed using an even mixture of the two stereoisomers. Of note, the cell lines used in the following studies were found to be the most sensitive to guggulsterone (10 μM) in a panel of cell lines treated for 72 hours and assessed for viability with an MTT assay (Figure 6e), which we have found is less sensitive than the trypan blue dye exclusion assay.

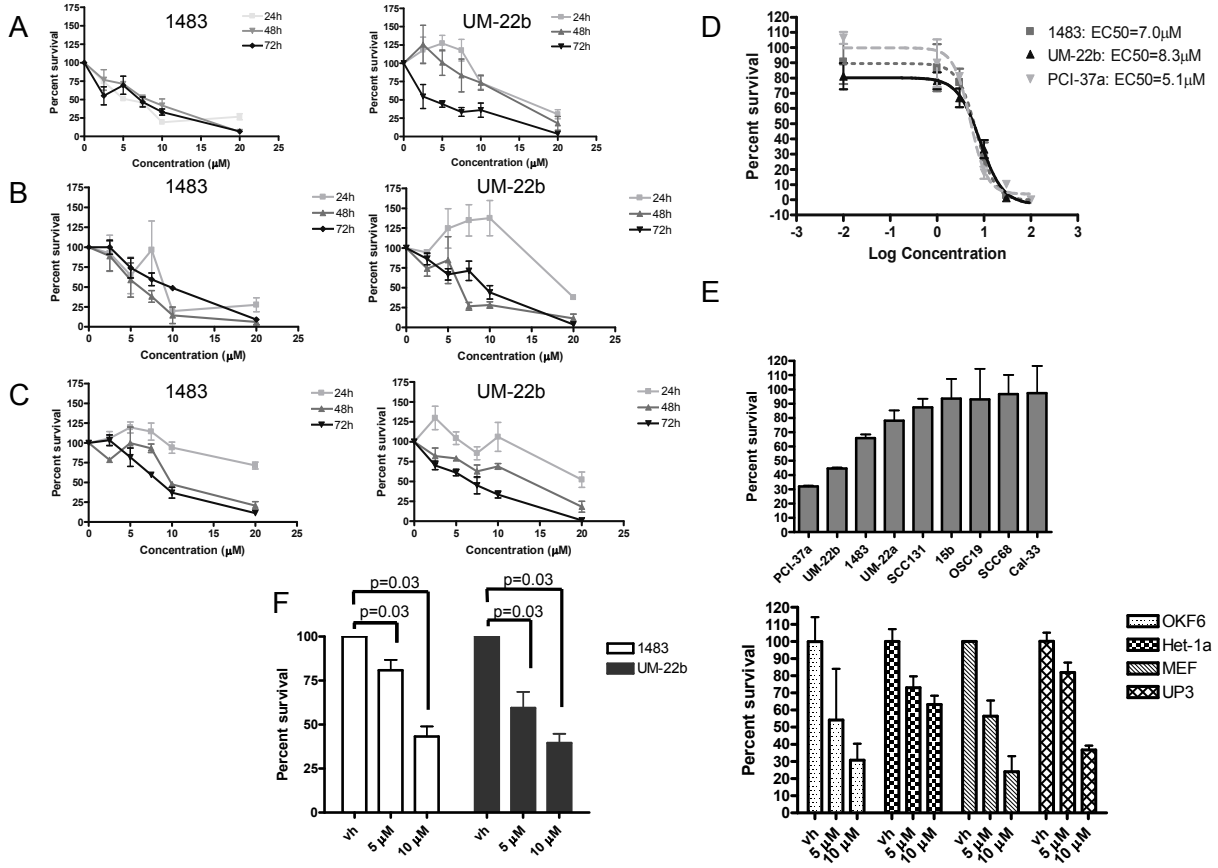

Figure 6. ***In vitro*** **growth inhibition with guggulsterone treatment. 1483 (left) and UM-22b (right) cells were treated with (A) an even mixture of guggulsterone's stereoisomers (B) Z-guggulsterone or (C) E-guggulsterone, for 24, 48 and 72 hours, stained with trypan blue dye and counted. (D) UM-22b, 1483 and PCI-37a cells were treated with an even mixture of guggulsterone's isomers for 72 hours, trypan blue survival assays performed, and EC_{50}s calculated. (E) A panel of HNSCC cell lines were treated with an even mixture of guggulsterone's isomers for 72 hours. MTT assays were performed to determine viability. (F) Four non-tumor cell lines, including primary oral keratinocytes (OKF6), immortalized esophageal epithelial cells (Het-1a), mouse embryonic fibroblasts (MEF), and fibroblasts cultured from benign uvuloplasty tissue (UP3), were all treated with an even mixture of guggulsterone's isomers for 72 hours, stained with trypan blue dye and counted.**

We were interested in determining whether or not guggulsterone's *in vitro* growth inhibitory effects were specific for cancer cells. Despite data showing that, at very high concentrations, primary cultures of normal prostate epithelial cells are insensitive to guggulsterone (188), primary oral keratinocytes (OKF6), immortalized esophageal epithelial cells (Het-1a), mouse embryonic fibroblasts, and primary pharyngeal fibroblasts (UP3), were all sensitive to guggulsterone-induced growth inhibition at similar concentrations as HNSCC cell lines (Figure 6e). We did observe that the rate of UP3 cell growth, which increased as the cells were in culture for a longer period of time, affected their sensitivity to guggulsterone, such that slower growing UP3 cells appeared insensitive to guggulsterone. If guggulsterone had never been used in the clinic, these results, demonstrating nonspecific growth inhibition of normal cell lines, would certainly indicate a potential for toxicity and side effects from this drug. However, as guggulsterone has been found to be safe, these *in vitro* results are less relevant and concerning.

3.3.2 Guggulsterone induces apoptosis and cell cycle arrest and inhibits invasion in HNSCC cell lines.

Guggulsterone has been reported to induce apoptosis in other cancer cell lines, including prostate carcinoma (188), monocytic leukemia (190) and multiple myeloma (194). We therefore tested the ability of guggulsterone to induce apoptosis in HNSCC cell lines. We first looked at guggulsterone's effect on DNA degradation, a marker of apoptosis. This was examined through detection of histone-associated DNA fragments in cell lysates. Treatment of UM-22b cells with guggulsterone at 10 μM induced a time-dependent increase in histone-associated DNA

fragments. 12 hours of treatment resulted in a 3.2-fold increase in histone-associated DNA fragments ($p=0.03$, all time points up to 12 hours) (Figure 7a). The enrichment factor on the y axis is a measure of the levels of histone-associated DNA fragments in lysates of treated cells compared to the vehicle control. In UM-22b cells, levels of histone-associated DNA fragments were also found to increase, dose dependently after 24 and 48 hours of treatment (Figure 7b). We also examined levels of caspase 3, an enzyme mediator of apoptosis that is inactive in its pro-form and cleaved upon activation. 1483 and UM-22b cell lines were treated with guggulsterone for 72 hours. Immunoblots demonstrated that 72-hour guggulsterone treatment of both 1483 and UM-22b results in a relatively modest, but statistically significant by densitometric analysis, decrease in pro-caspase 3, indicating cleavage to the active form and an increase in apoptosis ($p=0.03$ for both cell lines, Figure 7c). Furthermore, this effect was found to be dose dependent in 1483 cells treated for 48 and 72 hours (Figure 7d). These results indicate that guggulsterone induces apoptosis in HNSCC cell lines.

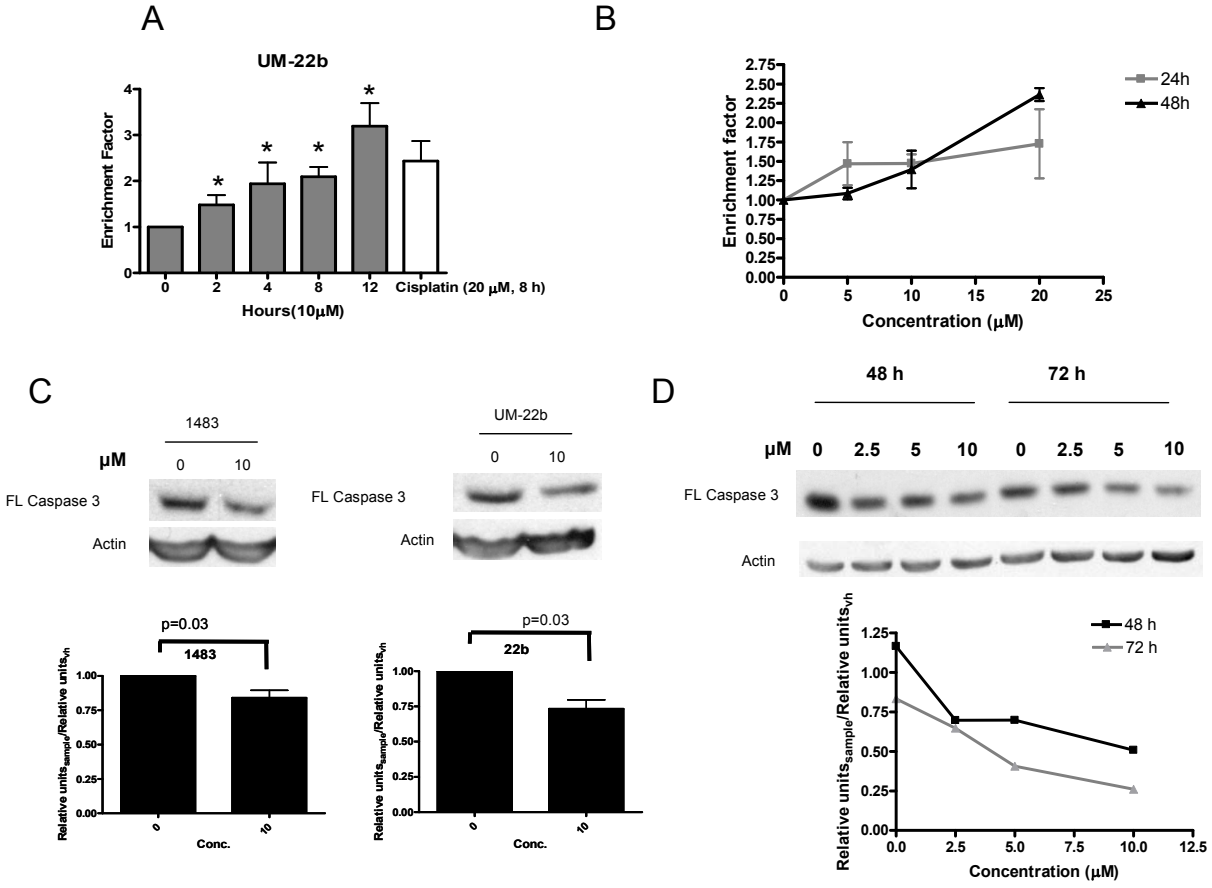

Figure 7. Guggulsterone induces apoptosis in HNSCC cell lines. (A and B) UM-22b cells were treated with guggulsterone (10 μM). Histone-associated DNA fragments were detected through ELISA of cell lysates. (*For all timepoints in (A), p=0.03). UM-22b (C) and 1483 (C and D) cells were treated with guggulsterone (10 μM) for 48 (D) and 72 (C and D) hours. Whole cell lysates were probed for full-length caspase 3. Graphs of densitometric analyses accompany each western blot. (p=0.03 for both experiments in (C)).

We next examined the effects of guggulsterone on the cell cycle, which is often aberrantly regulated in cancer cells. Both 1483 and UM-22b cell lines were treated with the even mixture of guggulsterone stereoisomers for 24 hours. Staining of treated cells with propidium iodide followed by flow cytometric analysis revealed a dose-dependent increase in the proportion of cells in the G0/G1 phases of the cell cycle as compared to vehicle control. This population

increased by 13.3% and 53.6% at 10 and 20 μM, respectively, in 1483 cells and by 9.5% and 33.2%, respectively, in UM-22b cells (Figures 8a and 8b). These results were statistically significant at 20 μM guggulsterone ($p=0.008$ for 1483 and $p=0.03$ for UM-22b). Similar results have previously been reported in human monocytic leukemia and multiple myeloma cells (190, 194). We have found the cell cycle inhibitory effect to be reversible as, after replacing the guggulsterone containing medium (20 μM, 24 h) with drug free medium for an additional 24 hours, the cell cycle profile of guggulsterone-treated cells resembled that of vehicle treated cells (Figure 8c). In UM-22b cells, expression levels of proteins that promote the transition from the G1 to the S phase of the cell cycle, including phosphorylated Rb, Cyclin dependent kinase (CDK) 4, and Cyclin D1, which is a target gene for both STAT3 and NFκB (129, 202), showed a subtle decrease following 16 hours of guggulsterone (10 μM) treatment (Figure 8d).

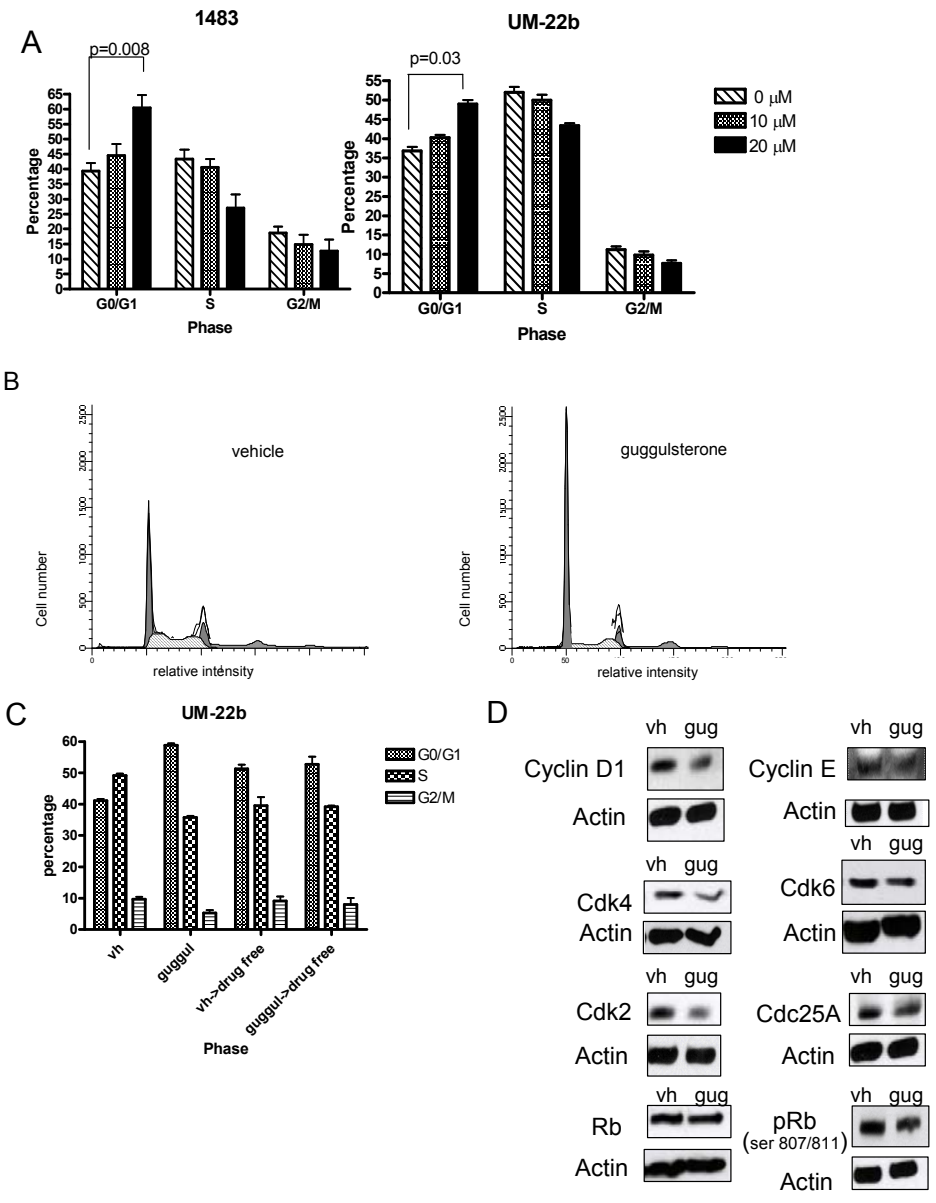

Figure 8. Guggulsterone induces cell cycle arrest in HNSCC cells. (A) HNSCC cell lines, 1483 and UM-22b were treated with guggulsterone (10 and 20 μM) for 24 hours. Cells were fixed with 70% ethanol/PBS, stained with propidium iodide and analyzed by flow cytometry. The y axis represents the percentage of the entire cell population within each sample currently in each phase of the cell cycle. All experiments were done with triplicate samples. Each experiment was performed at least 4 times with similar results. (p=0.008 for 1483 and p=0.03 for UM-22b). (B) Representative cell cycle histograms of 1483 cells treated with vehicle or guggulsterone (20 μM). (C) UM-22b cells were treated either with vehicle or

guggulsterone and then collected or were treated with vehicle or guggulsterone, switched to drug-free medium for 24 hours, and collected, followed by propidium iodide staining and cell cycle analysis. (D) UM-22b cells were treated with guggulsterone (10 μM) for 16 hours. Whole cell lysates were probed with antibodies for cell cycle regulating proteins: cyclin D1, cyclin E, CDK4, CDK6, CDK2, Cdc25a, Rb and pRb. The experiments in part D were performed twice with similar results.

The invasive properties of HNSCC cells contribute to the morbidity and mortality associated with this neoplasm. An *in vitro* matrigel invasion assay was used to determine the effect of guggulsterone treatment on the invasive potential of UM-22b, a cell line derived from a cervical lymph node HNSCC metastasis. Epidermal growth factor (EGF) was used to stimulate invasion and 10% FBS added to the lower well as a chemoattractant for cells to invade through the matrigel, which resembles an extracellular matrix. Cells were treated with 8.3 μM guggulsterone, the 72-hour EC_{50}, which results in only small decreases in viability of UM-22b cells after 24 hours, for 24 hours before matrigel inserts were fixed and stained. Guggulsterone treatment resulted in a 56.8% decrease in average numbers of invasive cells, bringing numbers of invaded cells close to those for EGF-unstimulated samples (Figure 9).

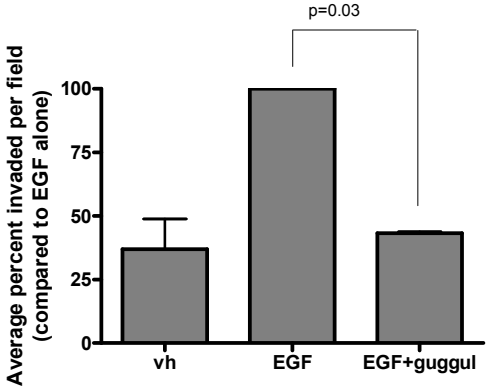

Figure 9. Guggulsterone inhibits invasiveness of HNSCC cells. UM-22b cells were plated, in serum-free DMEM, on top of matrigel inserts in wells containing DMEM/10% FBS. Both inserts and outer wells contained EGF (10ng/ml) and guggulsterone (8.3 μM) or DMSO as a vehicle control. Matrigel inserts were fixed and stained after 24 hours. Numbers of cells invading the matrigel were counted. The experiment was performed 4 times, using duplicate samples and counting at least 4 fields per well (p=0.03).

3.3.3 Guggulsterone enhances the growth inhibitory and anti-invasion activities of HNSCC therapies.

Guggulsterone has recently been shown to inhibit drug efflux transporters involved in multi-drug resistance to cancer therapies (203). Therefore, we examined the effect of combining guggulsterone with two different therapies for HNSCC, the widely used chemotherapeutic drug, cisplatin, and the small molecule EGFR tyrosine kinase inhibitor, erlotinib (Tarceva^{TM}), which is in advanced stages of clinical testing (Figure 10a). A different EGFR-inhibiting therapy, cetuximab, has been approved for treatment of HNSCC but is known to only inhibit growth *in vivo*, and not *in vitro*, perhaps because its efficacy relies on the presence of extracellular factors. Combining the approximate EC_{50} concentration of each drug (1.5 μM for cisplatin and 10 μM for erlotinib) with guggulsterone at its EC_{50} (7.0 μM in 1483 cells) significantly enhanced each drug's growth inhibitory effect ($p=0.03$ for both drugs; Figure 10b). Similar results were seen in UM-22b cells. The inhibitory effect that both erlotinib (5 μM) and cetuximab (4 μg/ml) have on HNSCC invasion was also enhanced with the addition of guggulsterone at its EC_{50} (8.3 μM in UM-22b cells) ($p=0.03$) (Figure 10b).

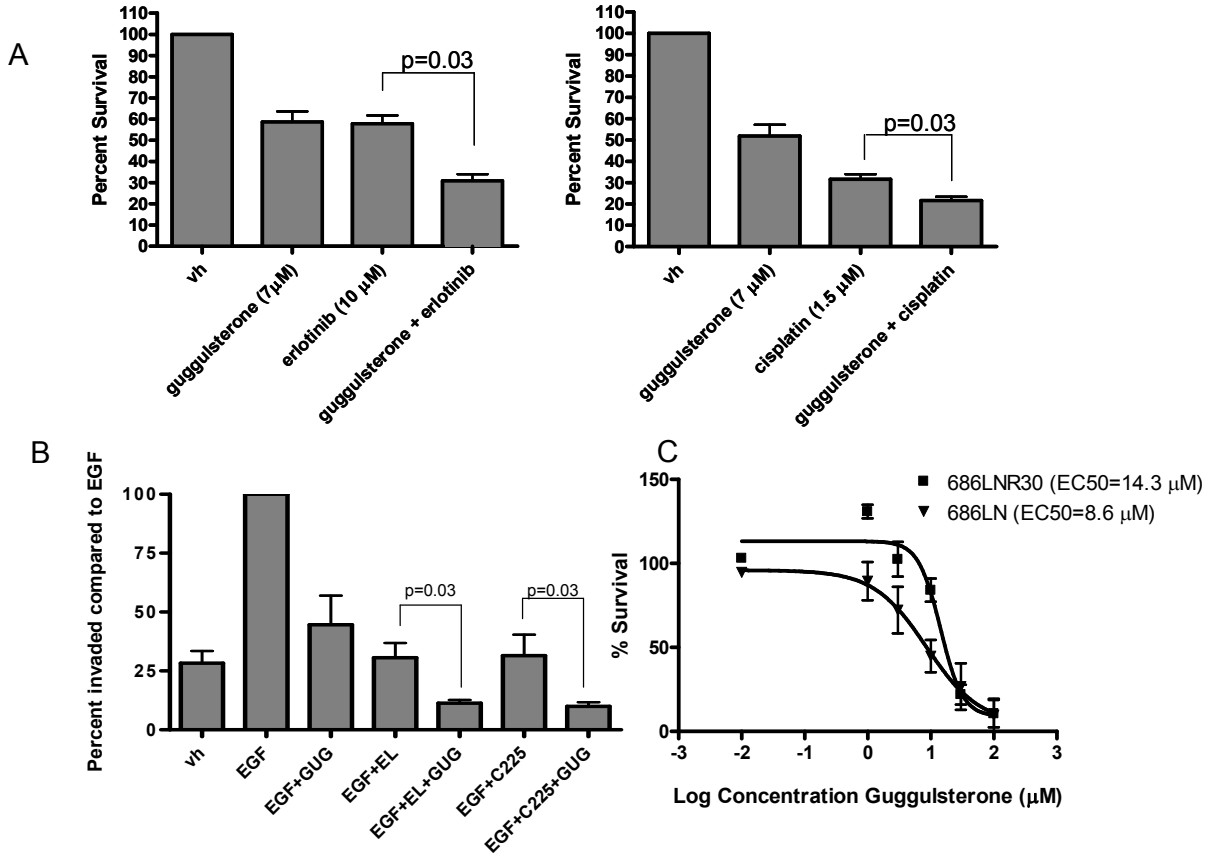

Figure 10. Guggulsterone enhances the activities of cisplatin, erlotinib and cetuximab in HNSCC cells. (A) 1483 cells were treated with guggulsterone (7 μM) and/or erlotinib (10 μM) or cisplatin (1.5 μM). After 72 hours, cells were trypsinized, stained with trypan blue dye and counted. Each experiment was performed with triplicate samples a total of 4 times with similar results (p=0.03 for both experiments) (B) UM-22b cells were plated in serum-free DMEM, on top of matrigel inserts in wells containing DMEM/10% FBS. Both inserts and outer wells contained EGF (10 ng/ml) and either an even mixture of guggulsterone's isomers (8.3 μM) or DMSO as a vehicle control, with or without erlotinib (5 μm) or cetuximab (4 μg/ml). Matrigel inserts were fixed and stained after 24 hours. Numbers of cells invading the matrigel were counted. The experiment was performed 4 times, using duplicate samples and counting 4 fields per well (p=0.03 for both drugs). (C) 686LN and 686LN-R30 cells were treated with guggulsterone (0.01-100 μM) for 72 hours, stained with trypan blue dye, and counted.

A clone (686LN-R30) that arose from selective pressure inducing resistance to EGFR-targeting TKIs (204), in which erlotinib has an EC_{50} of over 40 μM as compared to an EC_{50} of ~4 μM in the parental cell line (686LN) (204) (134.70 μM and 15.13 μM, respectively, in the Grandis lab; personal communications, Kelly Quesnelle). This erlotinib-resistant clone is also relatively resistant to guggulsterone-induced growth inhibition having an EC_{50} of 14.3 μM, as compared to 8.6 μM in the parental cell line (Figure 10c). Although the mechanisms resulting in resistance to EGFR inhibition in this clone are not completely overcome by guggulsterone, these cells are much more sensitive to guggulsterone than to erlotinib.

3.3.4 Guggulsterone decreases total and phosphotyrosine STAT3 expression levels in HNSCC cell lines.

STAT3 contributes to oncogenic signaling in HNSCC and interacts with NFκB, another transcription factor that has been found to be inhibited by guggulsterone (187). Therefore, we chose to assess the effects of guggulsterone on STAT3 expression and activity in HNSCC cell lines. 1483, UM-22b, and PCI-37a cells were treated with the even mixture of guggulsterone's stereoisomers followed by assessment of phosphotyrosine STAT3 and total STAT3 protein levels. All three cell lines demonstrated dose-dependent decreases in both phosphotyrosine STAT3 and total STAT3 that were statistically significant, upon densitometric analysis ($p=0.03$) (Figure 11a). This effect, though less pronounced, was seen as early as 24 hours after treatment (Figure 11b). In contrast to results reported by Ahn et al, who demonstrated decreases in phosphotyrosine STAT3, but not total STAT3, upon treatment of HNSCC cells with the Z but not the E isomer (194), in our study, decreases in both phosphotyrosine and total STAT3 were seen with each stereoisomer of guggulsterone alone (Figure 11c). STAT1, which is thought to be

a tumor suppressor in HNSCC and which is known to have a very similar protein sequence and structure to STAT3, does not decrease with guggulsterone treatment of 1483 cells treated with guggulsterone for 48 or 72 hours (Figure 11d). Guggulsterone's effects on phosphotyrosine and total STAT3 suggest that the anti-proliferative properties of guggulsterone may be due, at least in part, to abrogation of STAT3 signaling.

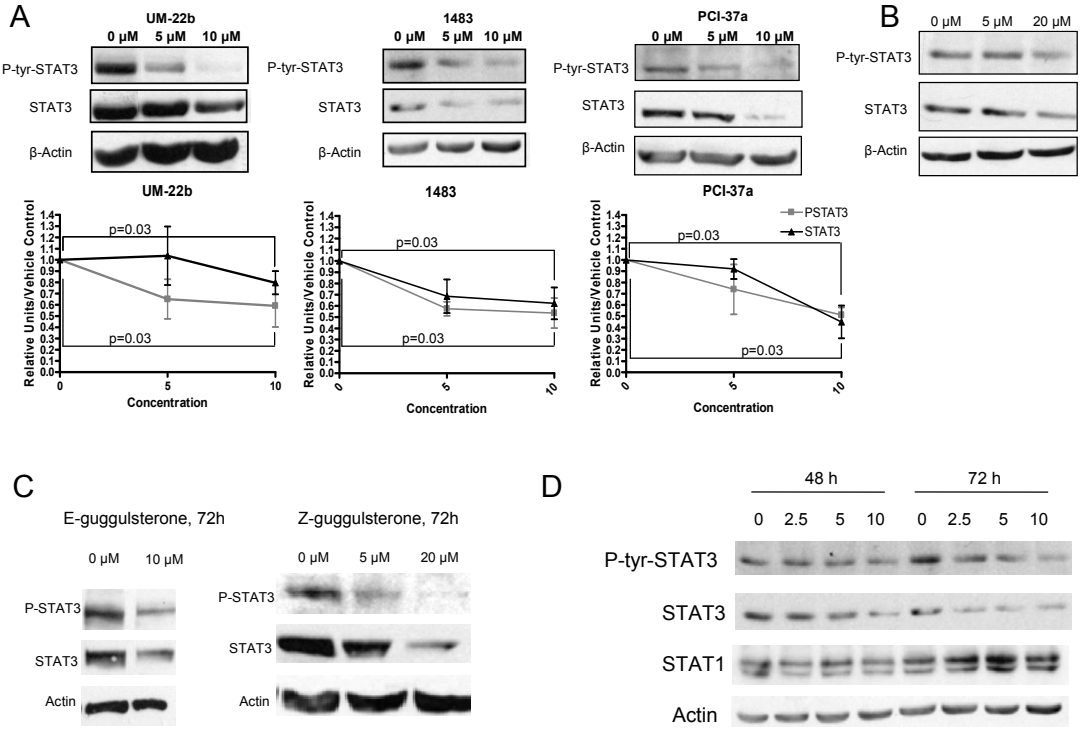

Figure 11. Guggulsterone treatment decreases levels of total and phosphotyrosine STAT3 in HNSCC cell lines. (A) HNSCC cell lines, 1483, UM-22b and PCI-37a were treated with an even mixture of guggulsterone's isomers (5 or 10 μM) for 72 hours. (B) UM-22b cells were treated with an even mixture of guggulsterone's isomers (5 or 20 μM) for 24 hours. (C) UM-22b cells were treated with either E- or Z-guggulsterone (5-20 μM) for 72 hours. (D) 1483 cells were treated with an even mixture of guggulsterone's stereoisomers (2.5-10 μM) for 48 and 72 hours. Whole cell lysates were probed, on immunoblot, with antibodies specific for total and phosphotyrosine STAT3 and STAT1. β-actin was used as a loading control. For (A), densitometric analyses of blots, normalized to β-actin, appear below each blot. Each experiment in (A) was performed 4 times with similar results (p=0.03 for all three cell lines).

3.3.5 STAT3 contributes to the growth inhibitory effects of guggulsterone in HNSCC cell lines.

To determine whether or not the observed decrease in STAT3 contributes to guggulsterone's anticancer activity in HNSCC cell lines, STAT3-specific siRNA was used to knock down STAT3. Transient transfection of both 1483 and PCI-37a cells with STAT3-specific siRNA results in optimal knockdown of STAT3 by 48 hours (Figure 12a). 1483, PCI-37a, and UM-22b cells were treated with guggulsterone 48 hours after transfection with STAT3 or GFP siRNA and harvested at 96 hours after transfection, resulting in 48 hours of guggulsterone treatment. Cells were then stained with trypan blue dye and counted. At this time point, STAT3 siRNA transfection results in a small effect on cell viability. To account for this, the percent survival of each guggulsterone-treated sample was calculated as a comparison to the vehicle control sample transfected with the corresponding siRNA. 1483 cells transfected with GFP siRNA (negative control), showed a 32.5% decrease in the number of viable cells after 48 hours of guggulsterone treatment, but only a 9.7% decrease in cell viability in STAT3 siRNA-transfected cells treated with guggulsterone. PCI-37a cells transfected with GFP siRNA demonstrated a 43.0% decrease in cell viability with guggulsterone treatment compared with a 22.0% decrease in cell viability in the same cells transfected with STAT3 siRNA (Figure 12b; $p=0.015$ for 1483, $p=0.03$ for PCI-37a). The effects of guggulsterone treatment, therefore, were abrogated by siRNA-mediated knockdown of STAT3. Thus, effects on STAT3 signaling are required, at least in part, for the growth inhibitory effect of guggulsterone in 1483 and PCI-37a

cells. On the other hand, under these conditions, STAT3 siRNA transfection did not abrogate the growth inhibitory effects of guggulsterone in UM-22b cells (Figure 12b).

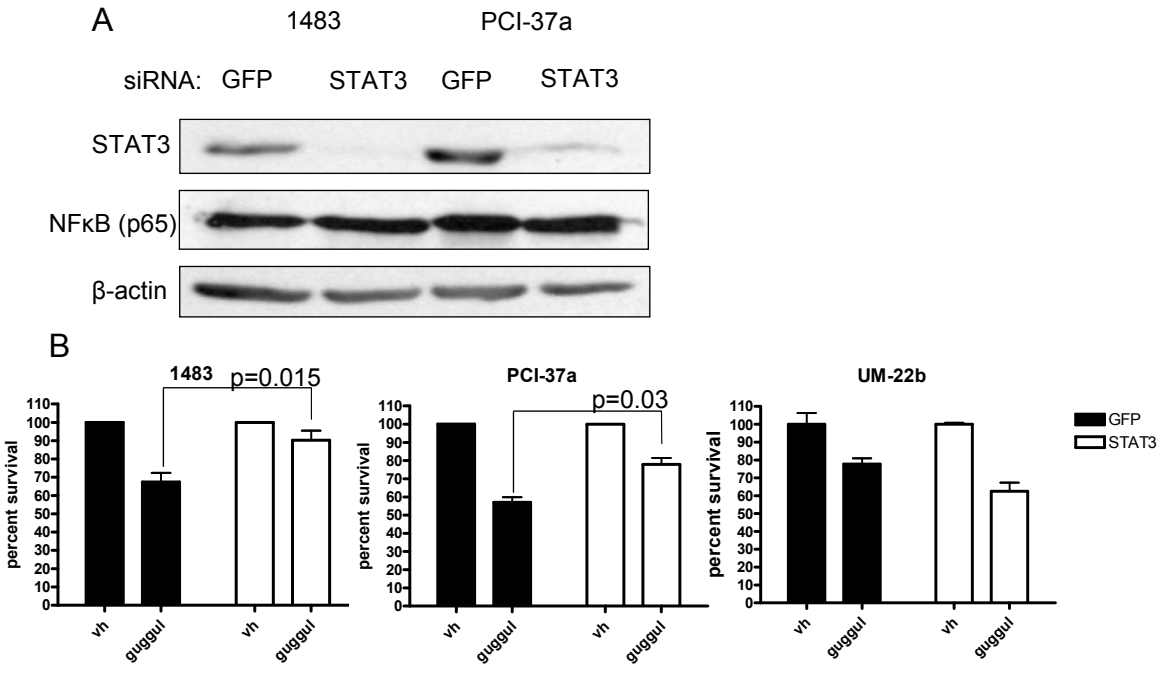

Figure 12. Knockdown of STAT3 inhibits guggulsterone's effect on viability of HNSCC cells. (A) 1483 and PCI-37a cells were transfected with STAT3 siRNA, or GFP siRNA as a control, for 48 hours. Whole cell lysates were probed, on immunoblot, with an antibody specific for total STAT3. β-actin was used as a loading control and NFκB as a negative control for protein knockdown by siRNA. (B) 1483, PCI-37a and UM-22b cells were transfected with STAT3 siRNA, or GFP siRNA as a control, for 48 hours. Cells were then treated with guggulsterone (10 μM) for an additional 48 hours. Attached and floating cells were collected and stained with trypan blue dye. Live cells were counted. The y axis represents the percentage of live cells in each sample compared to a vehicle control. All experiments were done with triplicate samples. The experiments shown in (B) were performed 5 times for 1483 and 4 times for PCI-37a with similar results (p=0.015 for 1483 and p=0.03 for PCI-37a).

3.3.6 Guggulsterone inhibits the expression of HIF-1α

Levels of tumor hypoxia have been found to have prognostic significance in many cancers, including HNSCC (205, 206). HIF-1α is a transcription factor that is induced under hypoxic conditions and whose expression has been shown to correlate with invasiveness of HNSCC cell lines, including UM-22b (207), resistance of HNSCC to radiotherapy and poor clinical prognosis in HNSCC patients (208). HIF-1α overexpression has also been found to be an early change in preneoplastic tissue and is thought to be important in carcinogenesis (209). HIF-1α is known to be regulated by both NFκB (210, 211) and c-Jun-N-terminal kinase (JNK) (212), which has also been implicated in guggulsterone's anticancer activity (11, 34). Therefore, we chose to investigate guggulsterone's effect on HIF-1α. Upon 48 hours of treatment of UM-22b and 1483 cells with guggulsterone (10 μM), protein levels of HIF-1α decreased dramatically (Figure 13a). A similar trend was also observed under hypoxia in UM-22b cells (Figure 13b).

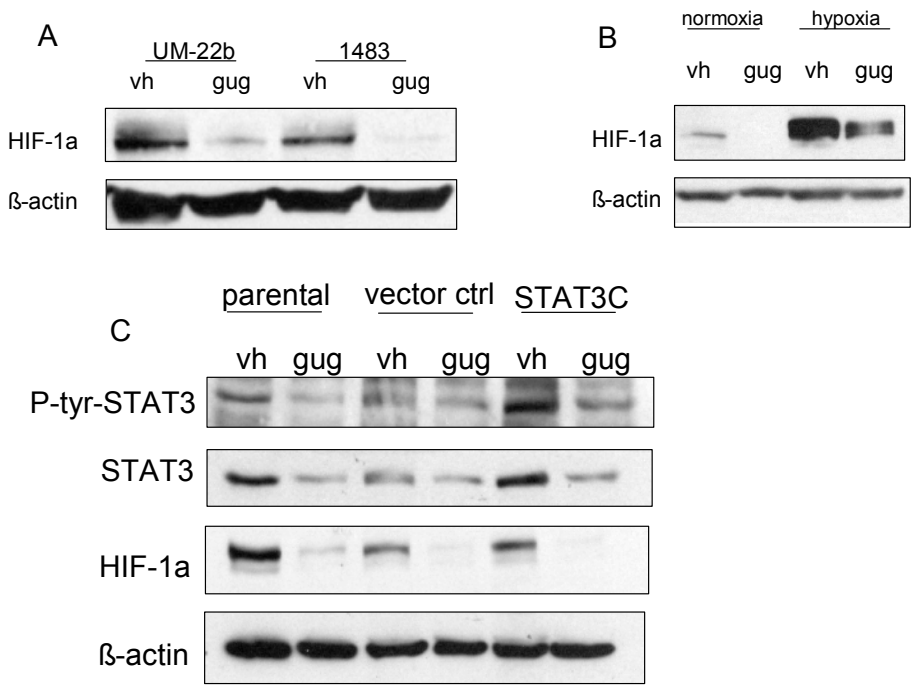

Figure 13. Guggulsterone inhibits expression of HIF-1α in HNSCC cells. (A) UM-22b and 1483 cells were treated with guggulsterone (10 μM), under normoxia, for 48 hours. (B) UM-22b cells were treated under normoxia and hypoxia with an even mixture of guggulsterone's isomers (10 μM) for 48 hours. (C) UM-22b cells, including the parental line, those stably transfected with the constitutively active STAT3 (STAT3C) construct and those stably transfected with the vector control were treated, under normoxia, with an even mixture of guggulsterone's isomers (10 μM) for 48 hours. Whole cell lysates were probed, on immunoblot, with antibodies specific for HIF-1α and β-actin, which was used as a loading control. The experiment in (A) was repeated at least twice for each cell line.

We attempted to discern whether or not guggulsterone's effect on HIF-1α was dependent on inhibition of STAT3 signaling. HNSCC cells transfected with STAT3 siRNA and fibroblasts derived from embryonic STAT3 knockout mice do not express HIF-1α (data not shown) and thus were not useful as models in this case. UM-22b cells stably transfected with the constitutively active STAT3 construct (STAT3C), in which STAT3 molecules exist as constitutive dimmers (51), do express HIF-1α. However, treating these cells with guggulsterone decreases levels of total and phosphotyrosine STAT3 as well as HIF-1α (Figure 13c). The STAT3C model, therefore, is also not useful in determining whether guggulsterone-induced downregulation of HIF-1α is dependent on effects on STAT3 signaling.

3.3.7 Guggulsterone's effects on mRNA levels of other STAT3 target genes

Standard RT-PCR for two STAT3 target genes, cyclin D1 and Bcl-x_L, was performed on mRNA from guggulsterone-treated HNSCC cells. Detectable changes in expression of either target gene were extremely modest and inconsistent between 1 and 72 hours of guggulsterone (10 μM) treatment. At later time points, subtle decreases in cyclin D1 and Bcl-X_L could be visualized in certain individual experiments (Figure 14).

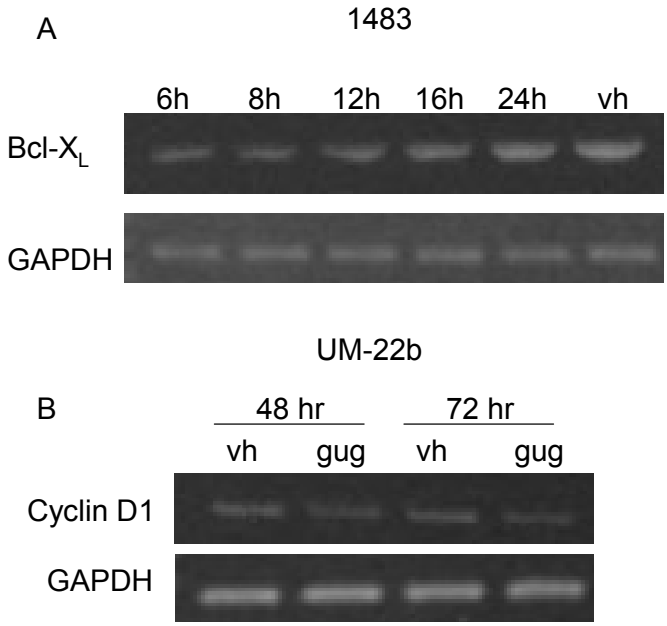

Figure 14. Changes in STAT3 target gene expression with guggulsterone treatment (A) 1483 and (B) UM-22b cells were treated with guggulsterone (10 μM) for up to 72 hours. After RNA extraction and reverse transcription, cDNA transcripts of bcl-X_L and cyclin D1 were amplified by PCR and resolved on an agarose gel containing ethidium bromide. GAPDH, a housekeeping gene, was used as a control.

3.3.8 Potential mechanisms of STAT3 inhibition by guggulsterone

The mechanism of guggulsterone's inhibition of STAT3 reported by Ahn et al. was induction of the protein tyrosine phosphatase SHP-1. This mechanism explains changes in phosphotyrosine STAT3 but does not account for the decreases in total STAT3 that we have observed. The cellular mechanisms of regulating STAT3 levels through transcription, translation and degradation are incompletely understood. Using Realtime PCR of mRNA from 1483 and UM-22b cells treated with guggulsterone (10 μM) for up to 24 hours, we were unable to detect

changes in mRNA levels of STAT3 with guggulsterone treatment (Figure 15), indicating that guggulsterone may affect either translation or degradation of the STAT3 protein. Studies have demonstrated STAT3 degradation by caspases (213), calpain (214), the proteosome (214-217), and serine proteases (218, 219). Small molecule proteosome inhibitors, MG132 and velcade (bortezomib), were not found to abrogate guggulsterone-induced down-regulation of STAT3 (Figure 16a and 16b), suggesting that proteosomal degradation may not be the mechanism of guggulsterone-induced STAT3 downregulation. Cyclohexamide, an inhibitor of translation, clearly affects levels of STAT3 but does not abrogate the STAT3 targeting effect of guggulsterone (Figure 16c).

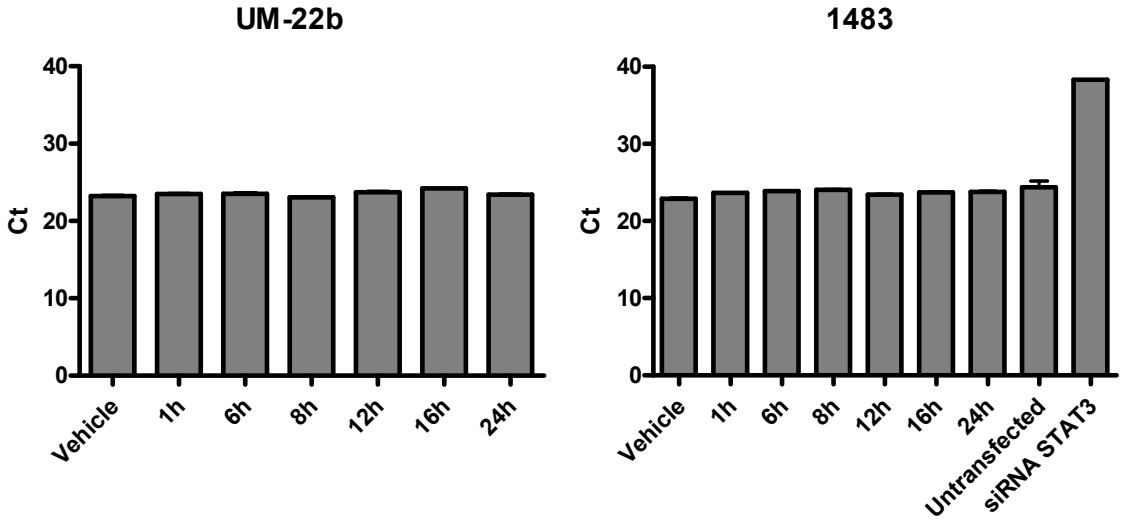

Figure 15. Guggulsterone does not induce a change in STAT3 mRNA levels. 1483 and UM-22b cells were treated with guggulsterone (10 µM) for 1, 6, 8, 12, 16 and 24 hours. After RNA extraction and reverse transcription, quantitative (Realtime) PCR was performed to amplify the STAT3 cDNA transcript. The y axis displays C_t values, which represent the cycle at which a threshold of amplification was reached, such that higher C_t values represent lower amounts of transcript. 48-hour transfection with STAT3 siRNA was used as a negative control for levels of STAT3 transcript. Similar results were seen at 4 hours of guggulsterone treatment.

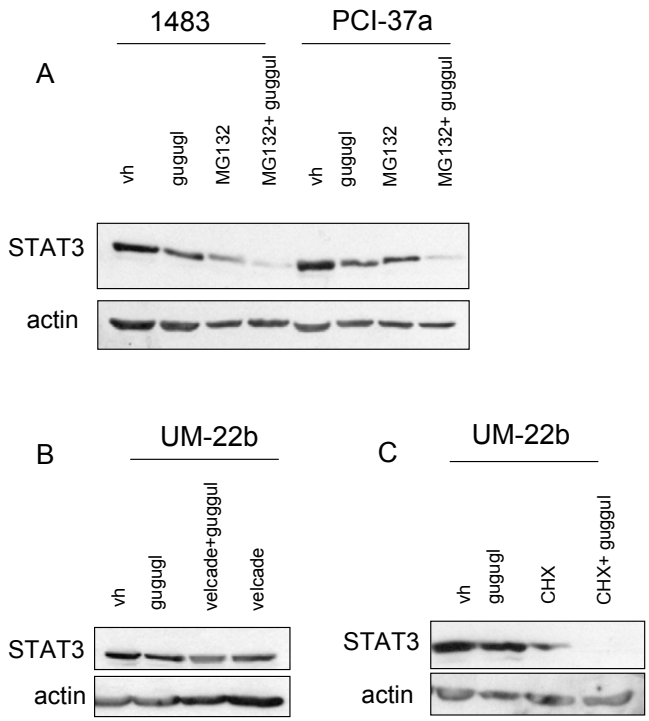

Figure 16. Investigating mechanisms of guggulsterone-induced decreases in total STAT3. HNSCC cell lines were treated with proteosome inhibitors (A) MG132 (50 μM) (B) velcade (bortezomib; 20 nM) or (C) the translation inhibitor, cyclohexamide (10 μg/ml) alone or in combination with guggulsterone (10 μM). For MG132 and cyclohexamide, cells were treated with the inhibitor for 24 hours, after which cell medium was changed to contain either the inhibitor alone or the inhibitor in combination with guggulsterone. After an additional 48 hours, cells were lysed and whole-cell lysates probed for STAT3 and β-actin, as a loading control. Velcade was used concurrently with guggulsterone for 48 hours.

We hypothesized that guggulsterone-induced STAT3 inhibition may be related to effects on some of the known targets of guggulsterone. The molecular target that has gained the most attention in studies of guggulsterone's anticancer activity is NFκB. In a reporter assay with UM-22b cells transiently transfected with a vector containing luciferase downstream of the NFκB promoter, guggulsterone treatment (4 hr, 10 μM) did not induce a decrease in promoter activity, with a very slight decrease at higher concentrations (20 μM) (Figure 17). While Shishodia et al. had shown dramatic decreases in NFκB DNA binding in an HNSCC cell line, this was with

guggulsterone at 50 μM, a concentration that is unlikely to be relevant to the mechanism of STAT3 inhibition at much lower concentrations.

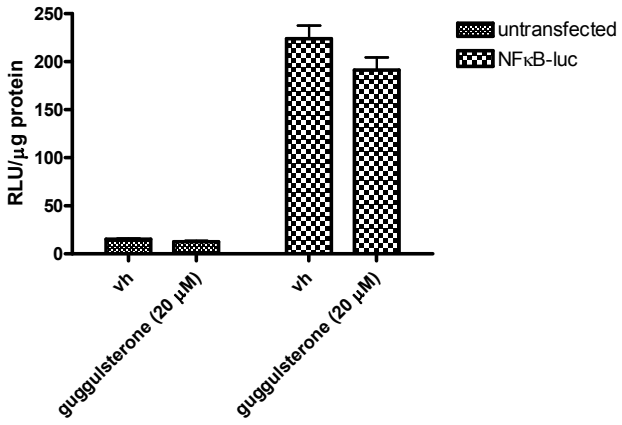

Figure 17. Guggulsterone's effect on NFκB promoter binding. Guggulsterone (10 μM) causes little or no decrease in NFκB promoter activity in UM-22b cells. UM-22b cells were transfected with an NFκB-luciferase construct and, the following day, treated with guggulsterone (10 μM) for 4 hours, collected, lysed and assayed for promoter activity using the Luciferase Reporter 1000 Assay System (Promega). Relative light units (RLU) are compared to total protein in each sample.

Guggulsterone antagonizes the farnesoid X receptor (FXR), a nuclear receptor, which is known as a regulator of bile acid and lipid metabolism but also known to play a role in the invasive properties of breast cancer cells (220). The FXR has also been implicated in guggulsterone-induced apoptosis in a Barrett's esophagus cell line (221). We observed FXR expression in 1483, UM-22b, UM-22a and PCI-37a HNSCC cell lines (Figure 18), suggesting only the possibility of an FXR-mediated effect of guggulsterone in HNSCC cells.

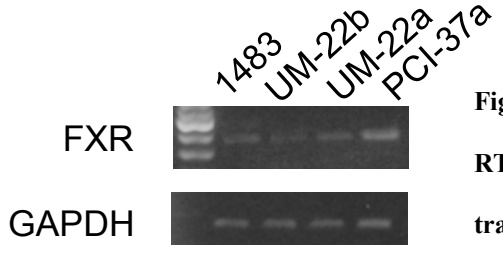

Figure 18. FXR is expressed in HNSCC cell lines. RT-PCR was used to amplify the FXR cDNA transcript in four human HNSCC cell lines.

3.3.9 Guggulsterone's and *Guggulipid*'s in vivo effects on HNSCC tumor xenografts

A xenograft model of HNSCC was used to investigate the *in vivo* effects of guggulsterone in this neoplasm, specifically on STAT3. In each study with the xenograft model, at least 8 mice per group were used, in order to detect a 30% or greater change in average tumor volume with a power of 0.8 and a power of 0.9 to detect a 40% or greater change. Although the xenograft model, which requires already-transformed cancer cells, is inadequate for the study of prevention, we attempted to make the model slightly more relevant to prevention by pretreating the animals for two weeks with guggulsterone before tumor inoculation, as described in Figure 19a.

We later determined, through studies described below, that separating mice into treatment groups, prior to tumor cell inoculation, which precludes randomization to groups by tumor volume, is problematic. In the two studies performed with this pre-treatment model, tumor volumes reflected the order of inoculation by cage (Figure 19b), probably due to decreases in cell viability over time before injection, invalidating our studies of differences in tumor volume using the "pretreatment model." Following this observation, all other studies were done using the standard "therapy model," inoculating and randomizing mice by tumor volume before beginning treatments (Figure 19c).

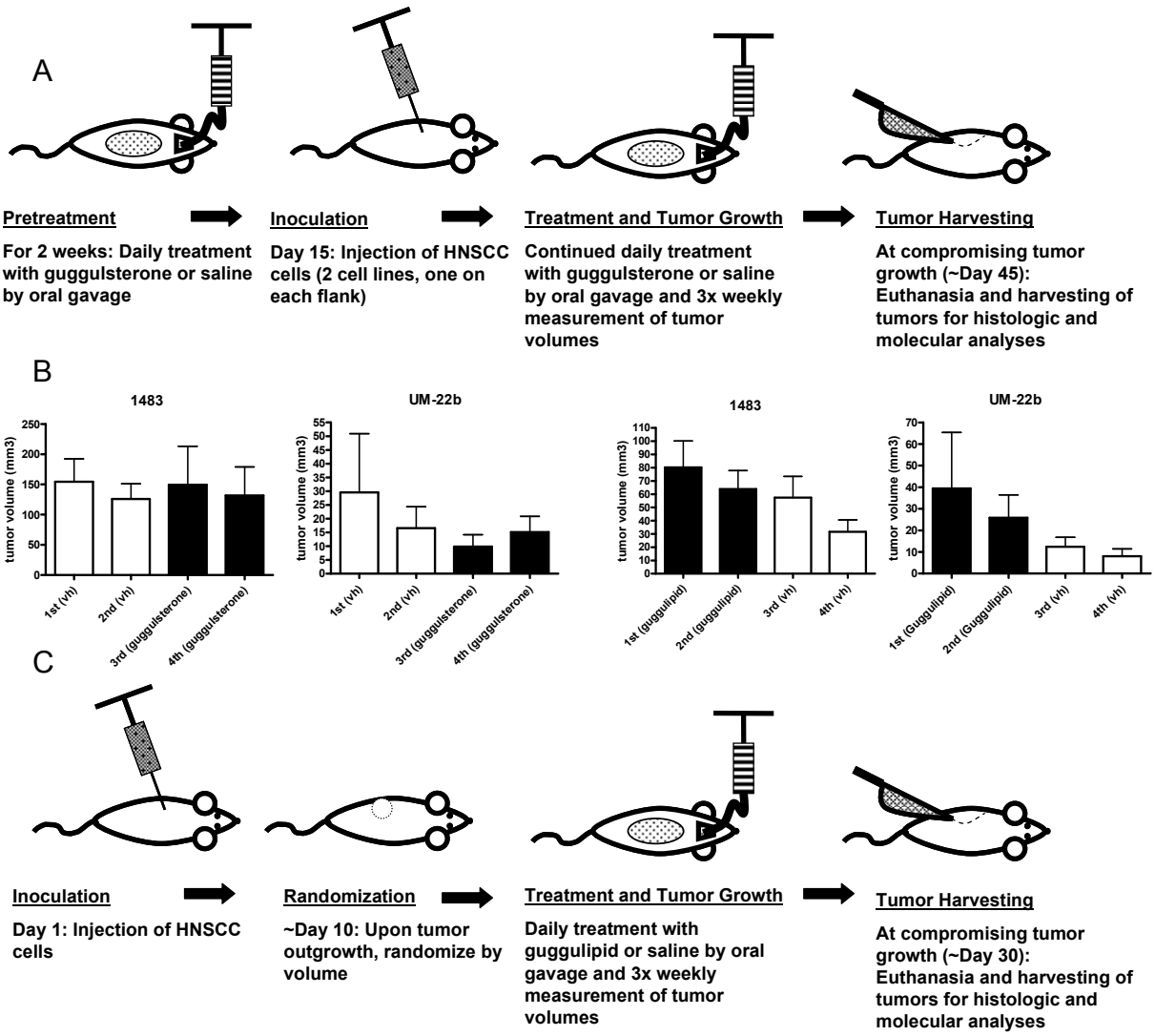

Figure 19. HNSCC pretreatment versus therapy xenograft models. (A) Design of the pretreatment model. (B) Tumor volumes on last day of measurement for two studies done using the pretreatment model. Mice were pretreated for two weeks by daily oral gavage with guggulsterone (2 mg/mouse, left) or saline in the first study and *Guggulipid* (25.9 mg/mouse=2mg/mouse guggulsterone, right) or the vehicle (5% ethanol/corn oil) in the second study. Mice were then inoculated with 1 x 10^6 1483 and UM-22b cells into the left and right flanks, respectively. Blinded tumor measurements were taken 3 times per week. Tumor volumes are shown compared to order of inoculation in each experiment. (C) Design of the HNSCC therapy xenograft model.

In our first study with the "pretreatment model", 8 athymic nude mice per group were treated with an even mixture of the two guggulsterone stereoisomers, or with saline as a vehicle control, by daily oral gavage of 2 mg guggulsterone for two weeks prior to tumor inoculation. Oral administration was selected as it resembles the most likely eventual usage of guggulsterone for cancer therapy. After two weeks of treatment, mice were inoculated subcutaneously with 1 x 10^6 1483 cells or UM-22b cells on either flank. Daily guggulsterone treatments continued for an additional 3 weeks. Tumor volumes were measured, by an investigator blinded to treatment group, three times per week. Synthetic guggulsterone (Steraloids, Inc), which was used in this study, was very expensive and was expended after 3 weeks post inoculation, 5 weeks total of treatment. One week after completing treatment, the animals were sacrificed and tumors stained with TUNEL for detection of apoptosis and, by immunohistochemistry, for total STAT3. Slides were also stained, by immunohistochemistry, for total STAT3 but were unusable due to poor staining quality with this antibody. Slides stained for TUNEL were scored based on the percentage of positively staining nuclei in the overall section. Slides stained for STAT3 were scored by assigning a subjective score related to the darkness of the stain, ranging from 1+ to 3+, multiplying the approximate percentage of the tumor sample composed by the corresponding scored area by the assigned score, and adding together these normalized scores for all regions of the tumor section (i.e. score=(%of tumor section scored as 1+) x 1 + (% of tumor section scored as 2+) x 2+ (percent of tumor section scored as 3+) x 3). This scoring was performed by a head and neck pathologist (Dr. Raja Seethala) who was blinded to treatment groups. Percentages of TUNEL-positive cells increased 2.2-fold in 1483 xenografts and 4-fold in UM-22b xenografts from mice treated with guggulsterone versus vehicle, indicating that guggulsterone induced

apoptosis in these xenografts (Figure 20a). In this tumor model, we observed a decrease in total STAT3 of 87.3% in UM-22b- derived tumors and of 44.3% in 1483-derived tumors (Figure 21b). These results suggest that guggulsterone downregulates total STAT3 *in vivo* as well as *in vitro*. Note that one UM-22b tumor in each group did not form so that results for the UM-22b cell line represent 7, rather than 8, tumors. A second study was performed with the "pretreatment model," employing *Guggulipid* (described below) instead of synthetic guggulsterone, but was clearly affected, in both cell lines, by order of inoculation (Figure 19b).

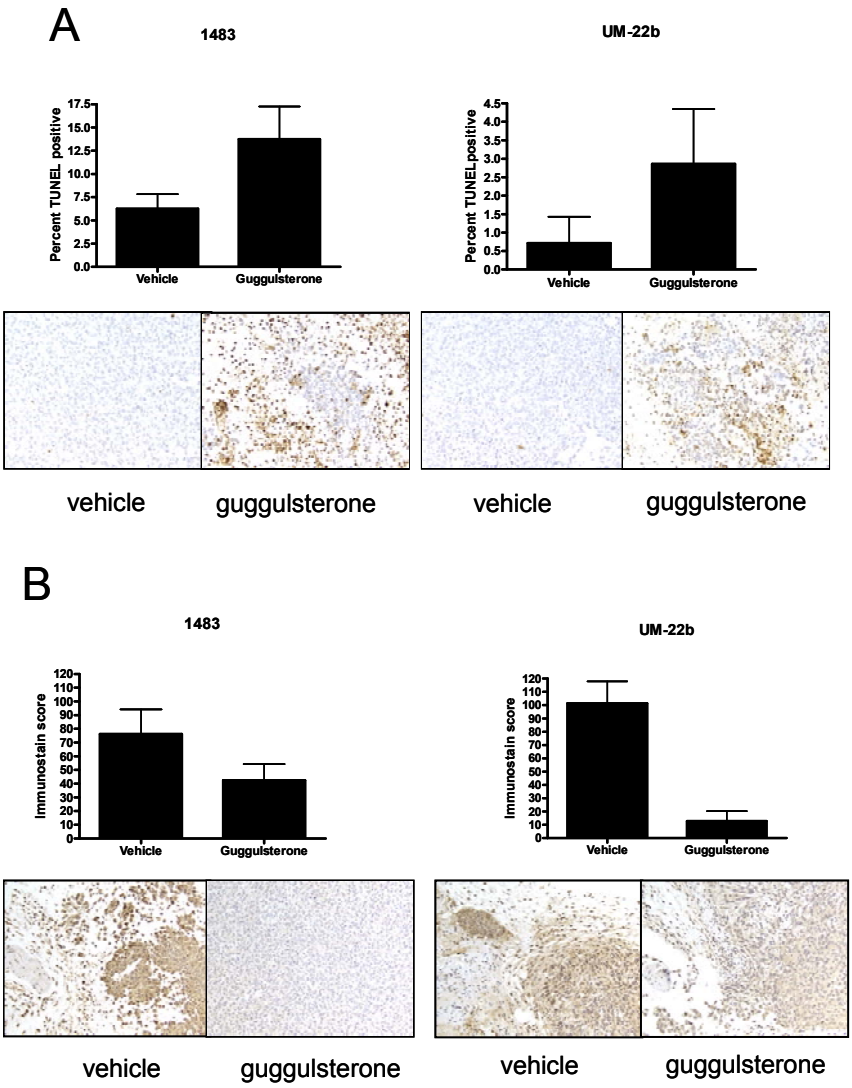

Figure 20. Guggulsterone's *in vivo* effects in the HNSCC pretreatment model. (A) and (B) Nude mice (8 per group) were treated orally with 2 mg/mouse/day of guggulsterone or with saline. After two weeks, mice were inoculated with 1 x 10^6 UM-22b and 1483 cells, in the right and left flank, respectively. Treatments continued for 3 weeks following inoculation. One week after discontinuation of treatment, mice were sacrificed and tumors harvested, sectioned, and stained with (A) TUNEL and (B) by immunohistochemistry, for STAT3 (20x photomicrographs). Internal controls for STAT3 include vascular endothelial cells, inflammatory cells (positive), and nerves (negative). Immunohistochemical score= (% tumor section scored as 1+) x 1 + (% tumor section scored as 2+) x 2+ (% tumor section scored as 3+) x 3.

Guggulipid (Sabinsa Corp.) represents one of several guggulsterone-containing dietary supplements. It is a standardized extract of *C. Mukul,* and is sold by General Nutrition Centers (GNC). Because *Guggulipid* is more likely to be administered clinically than the synthetic guggulsterone used in our *in vitro* studies and in our first xenograft study with the "pretreatment model," we chose to test the *in vivo* effects of *Guggulipid* in the xenograft model of HNSCC, both alone and in combination with the EGFR-targeting antibody approved for use in HNSCC, cetuximab. Correcting for the amount of guggulsterone present in *Guggulipid,* this extract inhibited the growth of HNSCC cell lines *in vitro* with EC_{50}'s slightly lower than those observed for synthetic guggulsterone (Figure 21a) and decreased expression levels of phosphotyrosine STAT3 and total STAT3 at the same concentrations and to a comparable degree as synthetic guggulsterone (Figure 21b).

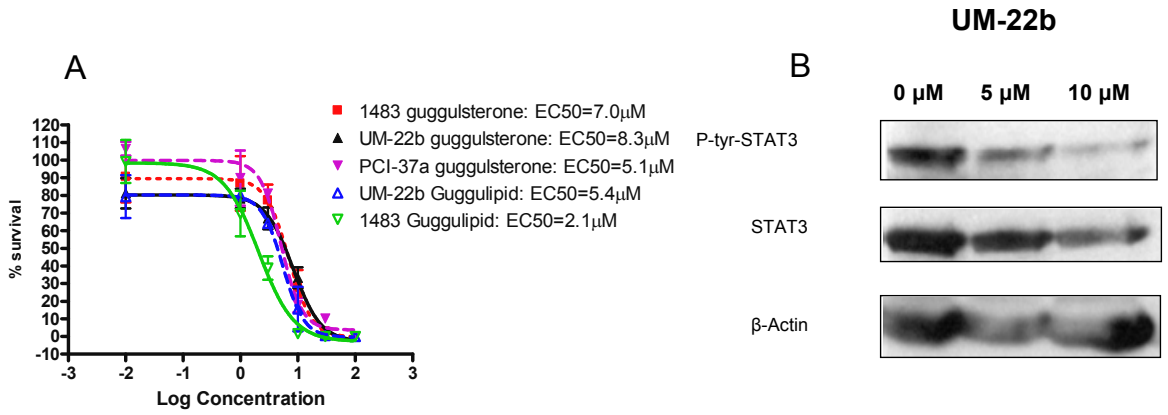

Figure 21. *Guggulipid* inhibits growth and decreases total and phosphotyrosine STAT3 in HNSCC cells. (A) 1483 and UM-22b cells were treated with *Guggulipid* (to equal 0.01-100µM guggulsterone) for 72 hours, stained with trypan blue dye and counted. Data are shown compared to growth curves for cells treated with the even mixture of synthetic guggulsterone isomers (from Figure 6d). (B) UM-22b cells were treated with *Guggulipid* (to equal 5-10 µM guggulsterone) for 72 hours. Whole cell lysates were probed for phosphotyrosine and total STAT3. β-actin was used as a loading control.

In the first study treating with *Guggulipid* in the "therapy model," 8 athymic nude mice were inoculated with 1 x 10^6 1483 cells and after tumor outgrowth, randomized to two groups. In all xenograft studies with *Guggulipid,* mice received daily oral treatments of 25.9 mg/mouse/day of *Guggulipid*, the equivalent of 2 mg/mouse of guggulsterone (7.73% of *Guggulipid*), suspended in corn oil/5% ethanol. Blinded measurements of tumor volume were taken three times per week. On its own, *Guggulipid* did not inhibit the growth of 1483 xenografts (Figure 22a).

In the study investigating the combination of *Guggulipid* and cetuximab, forty athymic nude mice were inoculated subcutaneously with 2 x 10^6 UM-22b cells and, following tumor outgrowth, randomized to four groups. The groups were treated either orally with 25.9 mg/mouse/day of *Guggulipid*, the equivalent of 2 mg/mouse of guggulsterone (7.73% of *Guggulipid*), suspended in corn oil/5% ethanol, twice weekly with 0.8 mg cetuximab in saline by intraperitoneal injection, with both drugs or with the corresponding vehicles. A suboptimal dose of cetuximab was purposely chosen so that a combination effect would be detectable. Treatments continued for 3 weeks. Blinded measurements of tumors were taken three times per week (Figure 22b). The average rate of tumor growth for the vehicle only group was 35.0 mm^3/day. The average rate of tumor growth for the *Guggulipid*-treated group was 24.3 mm^3/day, a 30.7% decrease in growth rate. The average rate of tumor growth for the cetuximab/*Guggulipid* combination group was 18.9 mm^3/day compared to 24.3 mm^3/day for the group treated with cetuximab alone, representing a 27.0% decrease in growth rate. Using a general linear model analysis, rates of tumor growth were found to be significantly different for the vehicle and *Guggulipid* alone groups ($p=0.0007$) and between the cetuximab and cetuximab/*Guggulipid*

combination groups (p=0.0017). In this study, tumors from the vehicle and *Guggulipid* groups were harvested and stained with TUNEL and, by immunohistochemistry, for total STAT3, as was done in our first study with the "pretreatment model." In this study, however, *Guggulipid* did not induce an increase in apoptosis or a decrease in STAT3 expression, contradicting what was seen in both cell lines in the "pretreatment model" study with synthetic guggulsterone (Figures 20a and 20b).

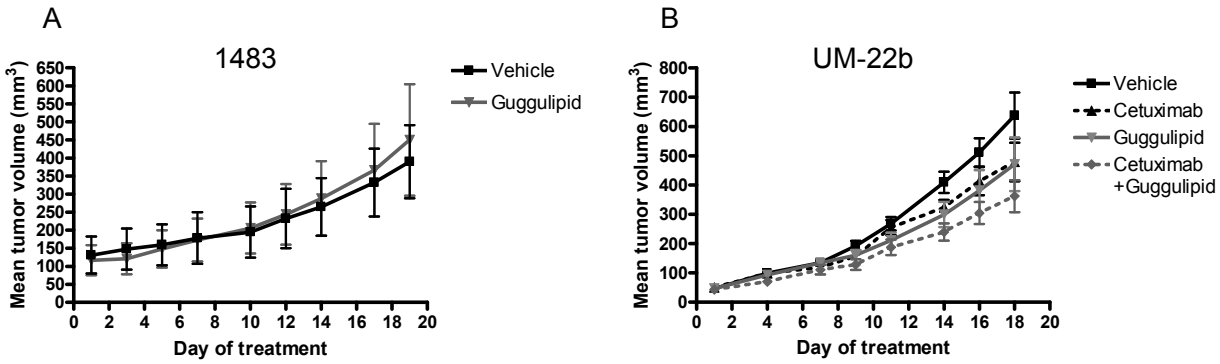

Figure 22. *Guggulipid*'s effect on tumor growth in the xenograft model of HNSCC. (A) Nude mice (N=16) were subcutaneously inoculated with 1 x 10^6 1483 cells and, after tumor outgrowth, randomized into two groups of 8. Mice were then treated daily, by oral gavage, with 25.9 mg *Guggulipid* (Sabinsa Corporation), which is the equivalent of 2 mg/mouse/day of guggulsterone, suspended in 200 µl corn oil/5% ethanol or with vehicle alone. Tumors were measured three times per week. (B) Nude mice (N=40) were subcutaneously inoculated with 2 x 10^6 UM-22b cells and, after tumor outgrowth, randomized into four groups of 10. Mice were then treated daily, by oral gavage, with 25.9 mg *Guggulipid* as in (A), with 0.8 mg cetuximab in 100 µl saline, twice weekly by intraperitoneal injection, with a combination of both drugs or with the corresponding vehicles. Tumors were measured three times per week. Average rates of tumor growth were found to be significantly decreased in the *Guggulipid*-treated group compared to vehicle (p=0.0007) and in the cetuximab/*Guggulipid* combination group compared to cetuximab alone (p=0.0017).

3.4 DISCUSSION

Guggulsterone is a widely available natural compound that has been shown to have hypolipidemic activity (222, 223). The safety profile of this drug (183, 185) makes it a good candidate for complementary and preventive therapy. In the present study, guggulsterone was found to induce growth inhibition in HNSCC cell lines associated with apoptosis, cell cycle arrest, decreased invasiveness and enhancement of the effects of current therapies including the chemotherapy agent cisplatin and EGFR inhibitors cetuximab and erlotinib. The growth inhibitory effect of guggulsterone is mediated, at least in part, through inhibition of STAT3 signaling. Guggulsterone also abrogated expression of HIF-1α, a therapeutic target downstream of STAT3. *In vivo,* guggulsterone treatments resulted in increased apoptosis and decreased expression of STAT3, as well as growth inhibition and enhancement of the efficacy of the EGFR-targeting antibody, cetuximab, when given in the form of *Guggulipid,* a plant extract that contains guggulsterone.

We investigated the effect of combining guggulsterone with cisplatin, erlotinib and cetuximab. Because cetuximab, which is FDA approved for the treatment of HNSCC and has been clinically efficacious, does not inhibit HNSCC growth *in vitro*, here we investigated guggulsterone's effect on cetuximab's anti-invasion activity *in vitro* (Figure 10b) and growth-inhibitory activity *in vivo* (Figure 23), finding that both were at least modestly enhanced by the addition of guggulsterone, as were the *in vitro* growth-inhibitory effects of cisplatin and erlotinib (Figure 10a). *In vivo, Guggulipid* alone was found to inhibit UM-22b tumor growth as compared to the vehicle control and also to enhance the activity of cetuximab (Figure 22b). As HNSCC treatments are often limited by side-effects and/or resistance to therapy, a compound that

enhances the effect of a particular dose of each drug may potentially have an important clinical impact. Resistance to EGFR-inhibiting therapies like cetuximab is thought to result, partially, from alternative pathways of STAT3 activation, including signaling through Src kinases and IL-6, which are known to play a role in HNSCC. Figure 23 outlines the potential mechanism behind the observed enhancement of erlotinib's and cetuximab's activities. Guggulsterone decreases levels of total STAT3, an effect that precludes STAT3 activation through alternate pathways.

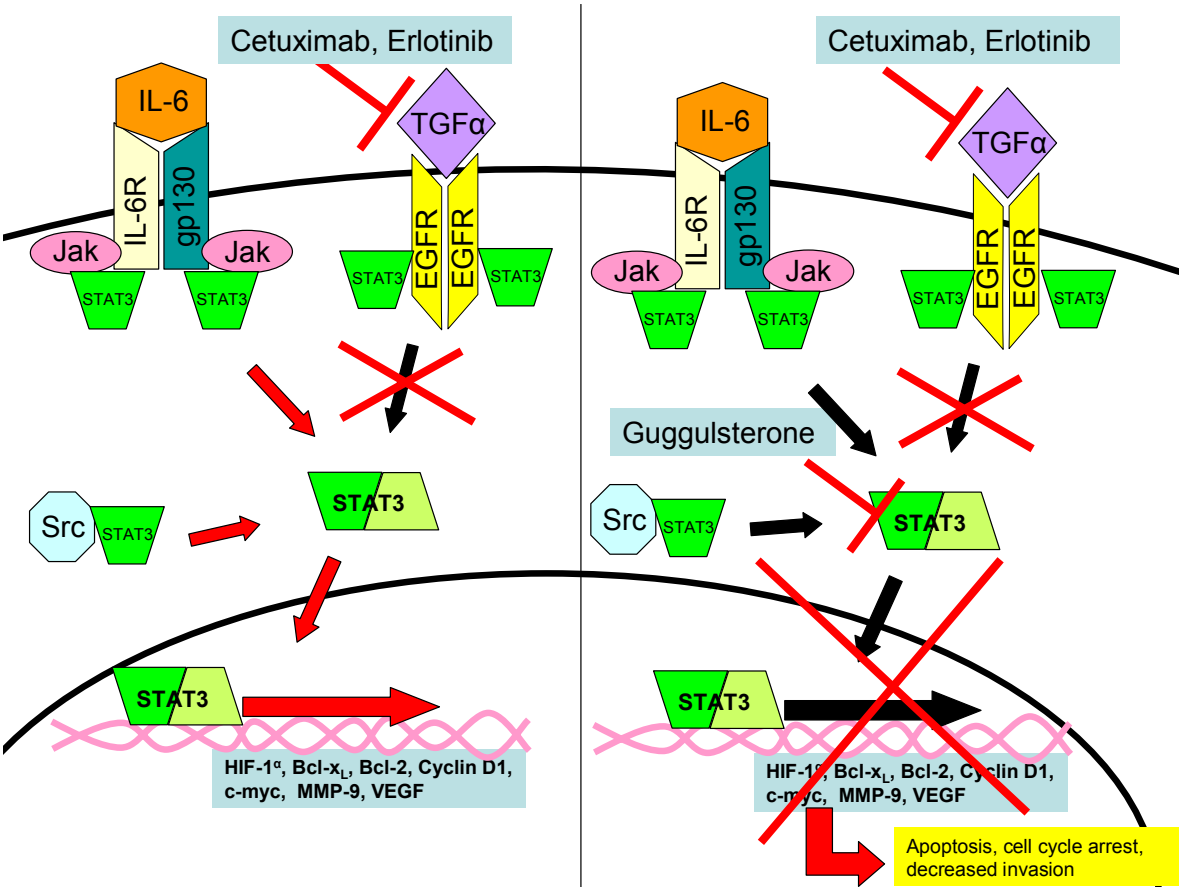

Figure 23. Rationale for combining guggulsterone with EGFR inhibitors. (Left) Therapeutic resistance to EGFR inhibition is thought to result partly from signaling through alternative pathways that activate STAT3 (e.g. IL-6 and Src). (Right) Direct inhibition of STAT3 by guggulsterone may preclude STAT3 activation through alternative pathways, inhibiting the transcription of STAT3 target genes and resulting in enhancement of antitumor activities associated with EGFR inhibition.

The *in vivo* anticancer activity of synthetic guggulsterone, as opposed to a *C. mukul* extract like *Guggulipid*, has been previously shown in a model of prostate cancer, employing matrigel plugs containing prostate carcinoma cells grown as xenografts (192), and in a chemical carcinogenesis model of skin cancer (193). Here, we chose to test the guggulsterone-containing nutraceutical, *Guggulipid*, whose anticancer activity has not previously been demonstrated *in vivo*, because pure, synthetic guggulsterone is expensive and currently unavailable as a clinical formulation.

Xenograft tumor models are limited by the requirement for cells that are already fully transformed, rendering them inappropriate for study of an agent's chemopreventive potential. Furthermore, as we found in our studies employing the "pretreatment model," even if we hope to use xenografts to demonstrate any chemopreventive activity through effects on extracellular factors (e.g. extracellular matrix and establishment of tumor, tumor angiogenesis) the clear importance of randomizing mice before treatment makes this pseudo-prevention model impractical. The model is also inappropriate for studying prevention as tumors are established and grow quickly, which, while a toxic chemotherapeutic drug may be able to inhibit this process, the effect of a non-toxic, less potent natural compound may be obscured by the speed of tumor growth. This is combined with other complicating factors such as large variance in tumor sizes within groups and frequent necrosis of tumors over time. Investigation of the potential *in vivo* chemopreventive effects of guggulsterone in HNSCC will require the use of transgenic and carcinogen-induced animal models of HNSCC, as is described in Chapter 4.

Our interest in guggulsterone's potential for targeting STAT3 in HNSCC stemmed from evidence of this compound's ability to inhibit NFκB (187). Molecular crosstalk between STAT3 and NFκB has been observed in HNSCC cell lines (141). Furthermore, STAT3 and NFκB have been found to affect one another's binding to other gene regulatory elements (141) and to form a complex in certain systems (144-146). As STAT3 has been found to play an important role in many cancers, including HNSCC, a compound that targets STAT3 may be especially useful in cancer therapy.

Our findings suggest that guggulsterone inhibits the growth of HNSCC, at least in part, via decreases in STAT3 (Figure 12b). Ahn et al. (194) have reported decreases in phosphotyrosine but not total STAT3 induced by the Z but not the E stereoisomer of guggulsterone. This is in contrast to our observations that either stereoisomer alone (Figure 11b) as well as the even mixture decrease levels of both total STAT3, which was seen *in vitro* (Figure 11a) and *in vivo* (Figure 20b), as well as phosphotyrosine STAT3 (Figure 11a). Guggulsterone's effect on total STAT3 levels is of interest, particularly in light of evidence that STAT3's translocation to the nucleus may occur independently of tyrosine phosphorylation and that STAT3 activity may be regulated by other posttranslational modifications, aside from tyrosine phosphorylation (40, 41, 43, 60). Using Realtime PCR of mRNA from 1483 and UM-22b cells treated, for up to 24 hours, with guggulsterone, we were unable to detect changes in mRNA levels of STAT3 with guggulsterone treatment (Figure 15). Our investigations, using small molecule inhibitors of the proteosome (Figures 16 a and 16b) and cyclohexamide (Figure 16c), which inhibits translation, have been unsuccessful in revealing the mechanism of guggulsterone-induced decreases in total STAT3. Future mechanistic studies will require more specific

methods, such as S35-methionine pulse chase experiments to detect changes in STAT3 translation and assays to detect ubiquitination of STAT3, as well as investigations of other potential mechanisms and enzymes involved. HNSCC cell lines transfected with STAT3 siRNA (Figure 12a) were significantly less susceptible to guggulsterone-induced growth inhibition (Figure 12b), demonstrating that in these cell lines, a decrease in STAT3 is at least partly responsible for guggulsterone's effect on viability, lending relevance to demonstrations of guggulsterone-induced inhibition of STAT3 signaling.

Several cancer therapies that are currently under investigation in preclinical studies, including various natural compounds, inhibit STAT3 tyrosine phosphorylation (96, 118-125, 138). With many of these natural compounds, inhibition of STAT3 tyrosine phosphorylation has been shown to be mediated through effects on signaling mediators upstream of STAT3 (96, 118-125, 138). To our knowledge, these natural compounds have several targets and have not been shown to induce a decrease in total STAT3 levels as we have observed with guggulsterone treatment of HNSCC (Figure 11). Synthetically enhanced compounds that resemble naturally-occurring compounds are also under study as potential cancer therapeutics, including two synthetic triterpenoids found to inhibit STAT3 and prevent lung tumorigenesis *in vivo* (224).

Mechanisms of guggulsterone's anti-cancer activity upstream of STAT3 and its direct inhibitor, SHP-1, have not been studied in HNSCC. Guggulsterone is known for its ability to antagonize the FXR, prompting studies of its hypolipidemic activity. The FXR, which is involved in the invasive properties of breast cancer cells (220) and in guggulsterone-induced apoptosis in a Barrett's esophagus cell line (221), was found to be expressed in HNSCC cell

lines (Figure 18). Guggulsterone is also an agonist of the pregnane X receptor (PXR) (225), which regulates expression of CYP3a, an enzyme involved in carcinogen metabolism and whose expression is decreased in HNSCC tumors compared to adjacent normal tissue (226). Agonists of the retinoid X receptor (RXR), which dimerizes with both the FXR and PXR, have been found to inhibit STAT3 in HNSCC cell lines (126) and have shown promise as chemopreventive therapies for HNSCC, albeit with unacceptable toxicity. Investigation into guggulsterone's effects on the FXR, PXR and RXR in HNSCC cell lines may possibly help to elucidate the mechanisms of guggulsterone's anti-cancer activity in HNSCC. Figure 24 outlines a model for guggulsterone's general mechanism of action downstream of one of these nuclear receptors.

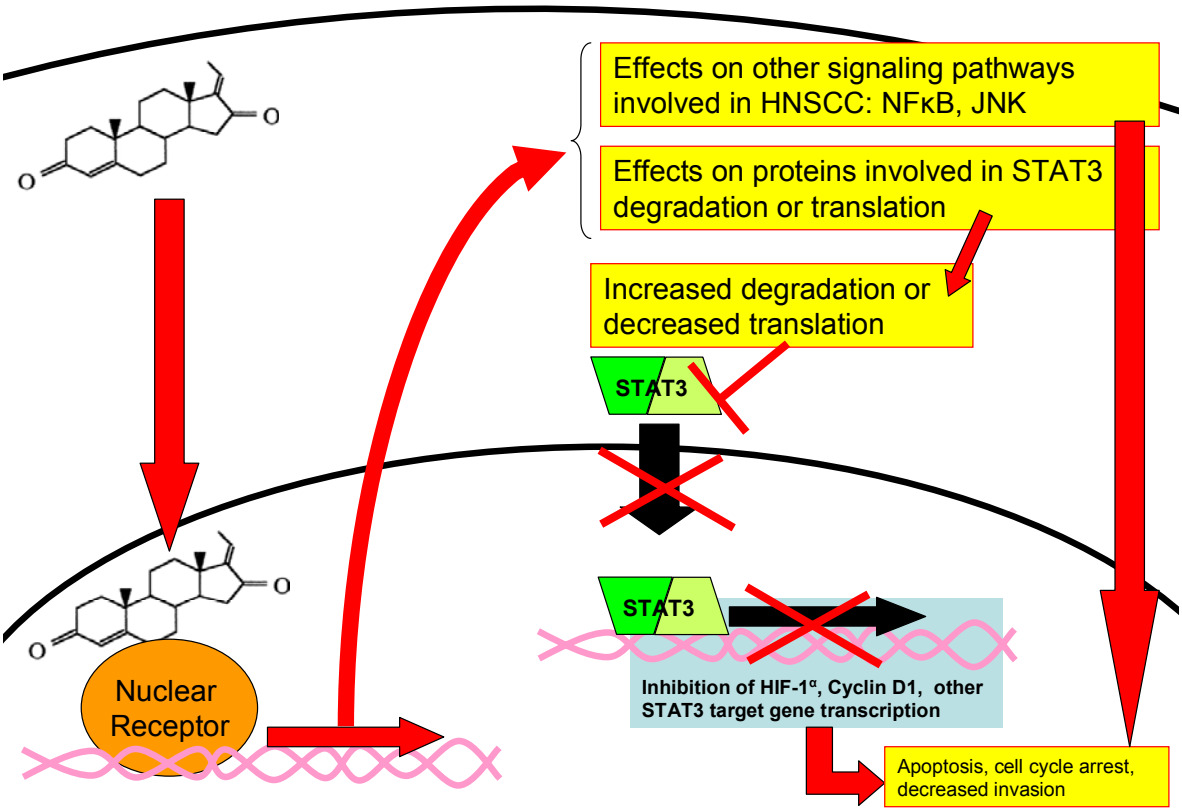

Figure 24. General model of guggulsterone's mechanism of action in HNSCC cells. Guggulsterone is known to bind various nuclear receptors. Genes regulated by one or more of these affected nuclear receptors may result in complex signaling changes in the cell, affecting proteins involved in regulation of STAT3 translation and/or degradation as well as other signaling pathways. STAT3 inhibition combined with effects on JNK and NFκB result in guggulsterone's antitumor activities, including apoptosis, cell cycle arrest and decreased invasiveness.

Guggulsterone's effect on inflammation may contribute to its effects on HNSCC growth and apoptosis. In addition to directly regulating the expression of oncogenes, both NFκB and STAT3 have been shown to promote tumorigenesis via their role in inflammation (227-229), which plays an important role in HNSCC (228, 230). Guggulsterone's use, in Ayurvedic medicine, for treatment of arthritis, as well as a study demonstrating guggulsterone's ability to inhibit nitric oxide production by lipopolysaccharide (LPS)-stimulated macrophages (186), were

early clues leading to investigation into the effect of guggulsterone on NFκB activity (187). Furthermore, guggulsterone has been found to ameliorate dextran sulfate sodium (DSS)-induced murine colitis and to inhibit activation of NFκB in this model (231). The involvement of reactive oxygen species (ROS) in HNSCC carcinogenesis has also been found to be associated with the actions of inflammatory mediators, including NFκB (232). Guggulsterone has been shown to function as an antioxidant (233, 234) as well as induce *increases* in ROS in prostate carcinoma and acute myeloid leukemia cells (189, 191). Guggulsterone may have complex effects on levels of ROS that depend on the individual system and have implications for guggulsterone's therapeutic potential.

HIF-1α is a transcription factor whose expression is directly correlated with increased invasiveness (207), resistance to radiotherapy and poor clinical outcome (208). A recent study has shown that STAT3 is required for the expression of HIF-1α in a human melanoma cell line (168). In our study, dramatic abrogation of HIF-1α expression was seen in treatment of UM-22b cells with guggulsterone (Figure 13). To our knowledge, this is the first evidence of guggulsterone's effect on HIF-1α. Various pre-clinical studies have been devoted to targeting HIF-1α with specific inhibitors and natural products (235-237).

Further investigation is required to determine both the mechanism of guggulsterone-induced decreases in total STAT3 and guggulsterone's potential for use as a chemopreventive therapy in HNSCC. The data presented here, demonstrating guggulsterone's ability to target STAT3 and HIF-1α and to enhance the efficacies of therapies for HNSCC, are suggestive of the

clinical utility of guggulsterone, a safe and inexpensive nutraceutical, as a potential complementary therapy for the treatment of HNSCC.

4.0 GUGGULSTERONE'S AND ERLOTINIB'S EFFECTS IN A PREVENTION MODEL OF HNSCC

4.1 INTRODUCTION

4.1.1 Animal models of cancer

One common way to model cancer in animals is through xenografts, cancer cells introduced into an immunodeficient host, often of a different species. In the case of our studies of HNSCC, we use human HNSCC cell lines injected into athymic nude mice. If we want to investigate the anatomic spread of the tumor, we can, to some extent, approximate an actual HNSCC tumor by injecting the tumor cells into the floor of the animal's mouth. Xenograft models are useful in examining the effects of potential therapeutics in already-formed tumors and, because they employ actual human cancer cell lines, may best reflect the molecular phenotype of a human tumor. As described in Chapter 3, however, because these models require cancer cells that are already transformed and able to propagate *in vivo*, xenografts carry serious limitations in their relevance to the process of carcinogenesis. Other animal models of cancer include transgenic models, in which specific genes are altered, resulting in tumor formation, and carcinogen-induced models, in which a chemical is used to induce carcinogenesis. Many of these models are characterized by gradual progression from normal tissue, through dysplasia, carcinoma *in situ*

and invasive carcinoma. These models, therefore, more closely resemble tumor formation in humans and are more useful in studies of potential chemopreventive agents that may target some of the molecular mechanisms involved in early stages of carcinogenesis, such as DNA damage, tumor initiation and promotion.

4.1.2 Animal models of HNSCC

4.1.2.1 Transgenic models:

Cyclin D1/p53

An early transgenic model employed the Epstein-Barr virus lytic promoter (ED-L2), as the Epstein-Barr virus specifically infects the squamous mucosa of the oropharynx. This was used to induce expression of the cyclin D1 transgene in the upper aerodigestive tract of mice. However, after 16 months, these animals developed dysplasia but not tumors. HNSCC was produced by crossing these mice with p53 heterozygotes. The major disadvantage of this model was that p53 heterozygosity was not tissue specific, so that animals were compromised by tumors that arose from various organ sites (238, 239).

TGFβRII/K-ras

A more tissue-targeted transgenic model is the inducible *K-ras*$^{12D/+}$*/TGFβRII*$^{-/-}$ mouse. Upon treatment of this mouse with the progesterone receptor antagonist, RU-486, a Cre recombinase/progesterone receptor fusion protein driven by the *keratin 5* promoter induces deletion of *TGFβRII* and mutation of *K ras,* specifically in the upper aerodigestive tract epithelium. Tumors that bear great microscopic and molecular resemblance to human HNSCC

arise around 5 weeks after RU-486 application (240). Increased protein levels of the oncogenic proteins *H ras* and *K ras* have been shown to occur in human HNSCC (241). In mice, *K ras* activation has been shown to induce the formation of benign squamous papillomas of the oral cavity (242). The role that TGFβ receptor II plays in HNSCC has yet to be determined, though it has been associated with the pathogenesis of other squamous cell carcinomas (243). The phenotype of this transgenic mouse, however, suggests that is may be important in HNSCC pathogenesis as well (240). Additionally, tumors resulting from this model demonstrate changes in other proteins known to play important roles in human HNSCC, including epidermal growth factor receptor (EGFR), STAT3 and the cell cycle regulators p15, p21 and cyclin D1 (240).

We considered using this model to assess the chemopreventive activities of guggulsterone and erlotinib. Dr. Xiao-Jing Wang, OHSU Cancer Institute had offered to collaborate with us and provide us with these mice. One problem with using this model is that guggulsterone promiscuously binds various steroid receptors, including the progesterone receptor (225). However, the amount of RU-486 that would be used, which is sufficient for induction of Cre recombinase fusion protein activity, is 1000-fold lower than the amount of the drug required to antagonize a steroid receptor and does not cause abortion in pregnant mice co-treated with progesterone (244). To ensure that guggulsterone was not interfering with the Cre recombinase/progesterone receptor fusion protein, we had planned to test tissue samples for the *TGFβRII* deletion after sacrificing the mice. Dr. Eva Szabo, an expert on clinical trials of chemopreventive agents, advised us that a chemical carcinogenesis model would be more appropriate, as it is more relevant to human carcinogenesis.

4.1.2.2 Carcinogen induced models:

Hamster cheek pouch

Traditionally, the most commonly used animal model of HNSCC was the chemically induced Syrian hamster cheek pouch model. This model involved topical application of the carcinogen, 7,12-dimethybenzanthracene (DMBA) to the cheek pouch, but resulted in tumors that did not resemble human HNSCC, possibly because the anatomic site is so different from the human oral cavity (239).

4-nitroquinoline-1-oxide

Another carcinogen-induced model employs 4-nitroquinoline-1-oxide (4-NQO), a carcinogen that resembles some of the carcinogens present in tobacco smoke and, like those compounds, causes DNA adducts. Oral administration of this compound to mice has been shown to result in temporally progressive carcinogenesis forming dysplastic lesions and, eventually, neoplasia (245). Additionally, the resulting oral squamous cell carcinomas have been found to resemble human HNSCC both histologically and in terms of molecular changes that often characterize human HNSCCs, including changes in levels of EGFR and the cell cycle regulator p16 (246). This carcinogen has been used to induce HNSCC in rats and mice, through topical application. More recently, optimal tumor formation has been attained through administration in the animals' drinking water (246).

We are collaborating with Dr. Mark Lingen from the University of Chicago, who has extensive experience using this model. Though Dr. Lingen's group is still currently determining

the kinetics of this model, he has provided us with protocols for 4-NQO administration to mice in their drinking water, information about expected toxicity and methods for tissue analysis.

4.1.3 Agents under study

We are using the 4-NQO chemical carcinogenesis model to investigate the chemopreventive properties of both guggulsterone and erlotinib. Using HNSCC cell lines and xenografts, we have demonstrated the anticancer and STAT3-targeting activities of guggulsterone, the natural compound in the extract of *C. mukul* (Chapter 3). These data are supportive of the potential for use of guggulsterone as a chemopreventive agent. Furthermore, guggulsterone's safety in clinical trials and availability in inexpensive clinical formulations, such as *Guggulipid* (Sabinsa Corporation, Piscataway, NJ), makes it a good candidate for chemopreventive use.

Erlotinib (Tarceva^{TM}) is an EGFR-targeting tyrosine kinase inhibitor (TKI) that has shown promise in clinical trials with HNSCC and is currently in advanced stages of clinical testing for treatment of this disease. EGFR, which is upstream of the STAT3 signaling pathway, is overexpressed in over 80% of HNSCCs (247) and is also overexpressed in the 4-NQO model of HNSCC (245). It is an important therapeutic target in HNSCC. Cetuximab (C225), an EGFR-inhibiting antibody, is approved for use in the treatment of HNSCC. Erlotinib is currently in advanced stages of clinical testing. Clinical trials investigating the chemopreventive activity of EGFR inhibitors, including erlotinib, in patients with pre-malignant lesions of the upper aerodigestive tract are currently underway. To our knowledge, there is no data from animal studies indicating the chemopreventive activity of EGFR inhibition for HNSCC.

4.2 MATERIALS AND METHODS

4.2.1 Reagents: drugs and animal diets

4-NQO (Sigma Chemical) was dissolved in 100% DMSO (final concentration 50 mg/ml) and kept at -20°C. *Guggulipid* (solid, 2.65% guggulsterones by hplc) was provided by Sabinsa Corporation (Piscataway, NJ) and erlotinib by OSI Pharmaceuticals (New York, NY). Harlan Teklad prepared custom erlotinib (diet 08141, 300 mg/kg) and *Guggulipid* (diet 08142, 28.3 g/kg, equivalent of 750 mg/kg guggulsterone) containing formulations in their 18% rodent diet. Assuming diet consumption of 3 g/mouse/day and average mouse weight of 22.5 g (both change as mice age), mice would receive 2.25 mg guggulsterone/day, 3.77 g/kg *Guggulipid* (equivalent to 100 mg/kg guggulsterone) or 40 mg/kg erlotinib. Diets were stored in vacuum-sealed bags at 4°C.

4.2.2 Study design and statistics

The study was designed to detect a 25% or greater difference in incidence of preneoplastic and neoplastic lesions in the treated mice versus controls with a power of 0.85. This design requires 75 mice per group, relying on the presence of preneoplastic or neoplastic lesions in at least 80% of the control group at the end of the experiment. As, based on the

observations of Dr. Mark Lingen, ~5% of mice are expected to die from 4-NQO toxicity, 80 mice were used per treatment group. Additionally, as the kinetics of the 4-NQO model have not been conclusively determined, we employed an adaptive study design. 50 more mice were added to the control group so that over time, 10 at a time could be sacrificed at various time points. If 10/10 mice have preneoplastic or neoplastic lesions, there is a probability of 0.89 that at least 80% of mice in the control group should have lesions as well. These samples are necessary because, while it is important, in order for us to have enough power to detect a difference, that at least 80% of the control group have lesions by the time of sacrifice, it is also important not to wait too long, until all mice in both treatment and control groups have lesions, obscuring any effect of the drugs under investigation. In immunohistochemistry studies, quantitative scores will be assigned to each histologic section and groups compared using a Wilcoxon test. Results will be judged for significance at an α of 0.05.

4.2.3 Animal treatments

Female CBA/J mice (5-6 weeks; Jackson Laboratories) mice were treated with either the control diet or one of the drug-containing diets for 2 weeks prior to initiating 4-NQO treatments and for 1.5 weeks of 4-NQO treatment. Administration of drug-containing diets was stopped at this point, due to unforeseen toxicity of combining 4-NQO with either erlotinib or *Guggulipid* (see *Results*). 4-NQO water was prepared by thawing stock solutions, diluting to 12.5 mg/ml in propylene glycol and adding 2 ml to each bottle of 250 ml sterilized water (final concentration is 100 μg/ml). 4-NQO water was made and changed once per week and continued for 8 weeks. 5

mice in each treatment group received the special diet but no 4-NQO in their water. Figure 25 outlines the study design.

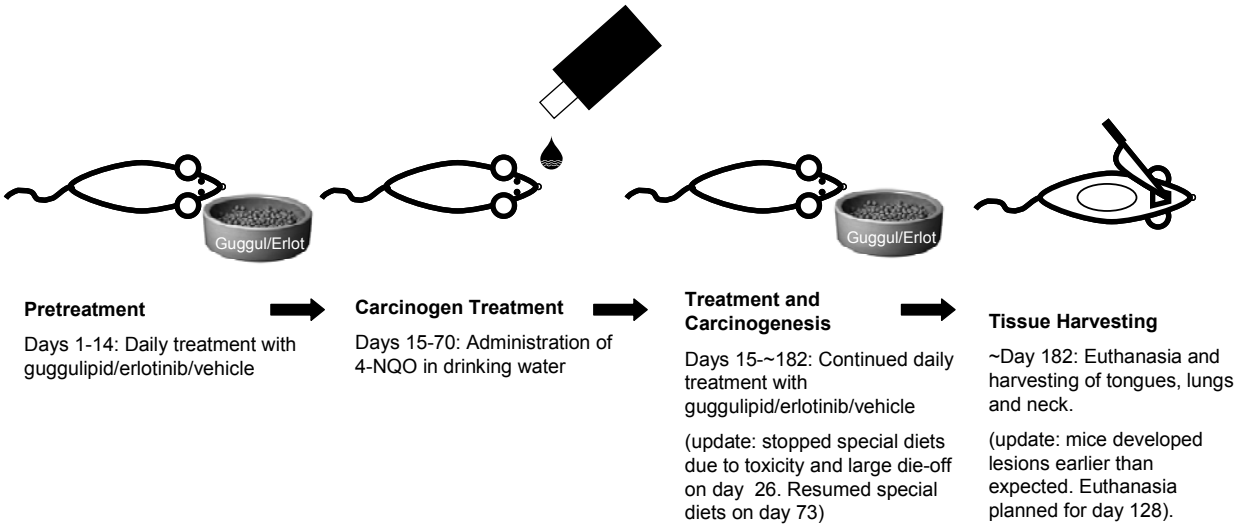

Figure 25. Design of the study of erlotinib's and *Guggulipid*'s *in vivo* chemopreventive activities

4.2.4 Dissection and tissue processing

Tongues of euthanized mice were removed by cutting through the angle of the mouth, thus disconnecting the jaw, and removing the tongue by cutting through connective tissue on the ventral side of tongue and making one cut at the root of the tongue. The lungs, as well as the entire neck will also be removed to later examine metastases to lungs and lymph nodes. All tissues will be fixed in 10% formalin. Ventral tongues will be inked and tongues cut in multiple horizontal sections. Tongues will then be processed, paraffin embedded, sectioned completely and every tenth slide stained with hematoxylin & eosin. Multiple slides per mouse will be kept for immunostaining. Tongues will be categorized (mild/moderate dysplasia, severe dysplasia/carcinoma *in situ,* or invasive SCC) by the most advanced lesion seen in reviewing

multiple sections. The lungs and lymph nodes from the necks of mice with invasive SCC will be processed and stained with hematoxylin & eosin in order to detect micrometastases. The investigator reviewing slides will be blinded to treatment groups.

4.2.5 Immunostaining

Immunostaining will be performed using antibodies specific for STAT3, phosphotyrosine STAT3, NFκB, HIF-1α, phosphoEGFR, total EGFR and cyclin D1. Immunohistochemical score=(%of tumor section scored as 1+) x 1 + (% of tumor section scored as 2+) x 2+ (percent of tumor section scored as 3+) x 3. The investigator scoring slides will be blinded to treatment group.

4.3 RESULTS

4.3.1 Preliminary studies

Although Dr. Mark Lingen employs male mice in his studies, we planned to use female mice, based on the methods used by Tang et al. in their original study administering 4-NQO, in drinking water, to female mice (246). Therefore, 4-NQO treatment of 5 female mice was performed in order to test for overwhelming toxicity and for differences in the kinetics of tumor development in females. These 5 mice were treated with 4-NQO water for 8 weeks. By 16

weeks, all 5 had preneoplastic or neoplastic lesions, one with severe dysplasia, 2 with carcinoma *in situ*, and 2 with invasive oral SCC. Representative photomicrographs are shown in Figure 26a.

Another preliminary study was performed in order to test average consumption and toxicity of both the erlotinib and *Guggulipid*-containing diets. The mice ate both drug-containing diets in amounts comparable to control diet (~2-3 g/mouse/day), with no discernible weight loss or toxicity over one month of treatment.

4.3.2 Ongoing study of *Guggulipid* and erlotinib in the 4-NQO model

When Dr. Lingen employs the 4-NQO model to investigate a potential chemopreventive therapy, compounds under investigation are administered following the 8-week period of 4-NQO treatment. In the current study, in order to maximize exposure to erlotinib and *Guggulipid*, mice were treated for two weeks prior to 4-NQO administration. We had intended to continue administering the special diet with 4-NQO. However, after 1.5 weeks of 4-NQO treatment, 28 mice in the erlotinib group and 5 mice in the *Guggulipid* group died suddenly. None of the mice in either the group treated with the control diet nor in either cage treated with the special diet, without 4-NQO, died. We concluded, therefore, that the deaths resulted from unforeseen toxicity of combining 4-NQO with either *Guggulipid* or erlotinib. We promptly took all mice receiving 4-NQO treatments off of the drug-containing diets until completion of the course of 4-NQO, at which point the drug-containing diets were resumed. Although the death rate slowed dramatically after withdrawal of the drug-containing diets, more mice died over the course of the

experiment. Necropsy of one of the mice that died after combining 4-NQO with erlotinib indicated, according to DLAR veterinarians, that it had died of hemorrhagic gastroenteritis.

Based on observations by Dr. Mark Lingen, we had not expected mice to develop any preneoplastic lesions until 12 weeks after the end of 4-NQO treatments, at the earliest, and had planned to sacrifice our first sample group of 10 mice at 10 weeks after 4-NQO. However, at 5 weeks after completing 4-NQO treatment, some of the mice were noted to have lost a lot of weight. This prompted examination of mouse tongues and, though only one out of the 5 that had lost considerable amounts of weight had a visible tumor on its tongue, surprisingly, so did several other mice, including 9 in the control group and 5 in the *Guggulipid* group (~7% of each), but none in the erlotinib group. Figure 26b shows representative tumors from the control group. The 5 mice that had lost weight were sacrificed and their tongues harvested, sectioned and H & E stained. Of these 5 mice, 4 had preneoplastic or neoplastic lesions. At 6 weeks after 4-NQO treatment, 10 more mice, the first real sample, were sacrificed.

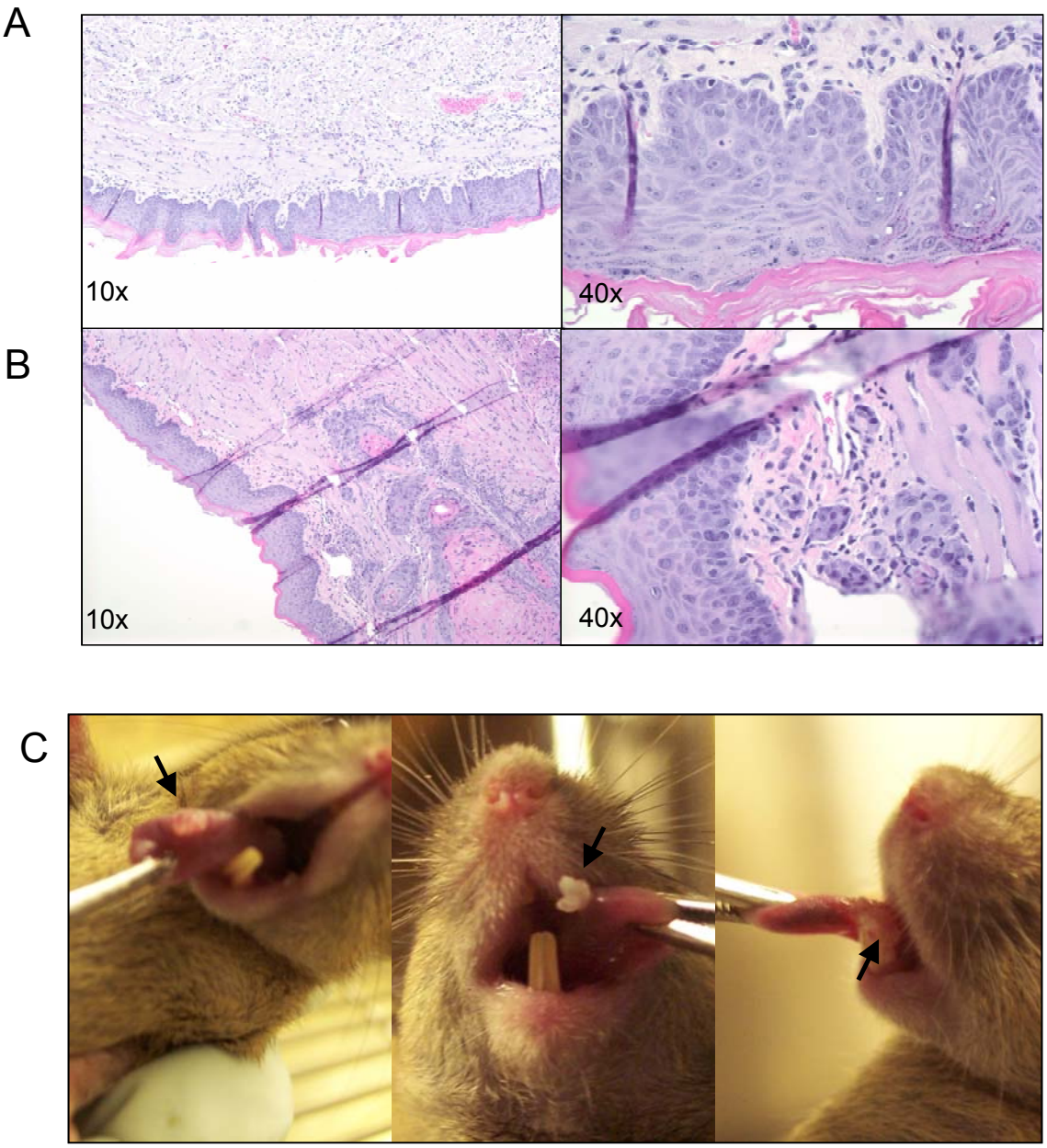

Figure 26. Representative tumors derived from the 4-NQO-induced model of HNSCC. (A) and (B) Histologic sections of tongues harvested from mice in a preliminary study of 4-NQO's activity, at 16 weeks post-carcinogen treatment. (A) Severe/moderate dysplasia (B) Invasive SCC (C) Representative tumors from the control group of the chemoprevention study, 7 weeks post carcinogen treatment, on dorsal tongue (left), right lateral border (middle), and left lateral border (right). Arrow heads indicate tumors.

4.4 DISCUSSION

The 4-NQO model of oral carcinogenesis provides us with the opportunity to examine the chemopreventive activities of different agents. The current study examines guggulsterone, in the form of *Guggulipid*, and erlotinib, as potential chemopreventive therapies. The primary endpoint is detection of a difference in incidence of pre-malignant and malignant lesions of 4-NQO treated mice receiving either drug, compared to the control group. We will also examine differences in expression of certain biomarkers that serve as intermediate endpoints regarding the antitumor and chemopreventive activities of the drugs administered. These will include phosphotyrosine and total STAT3, HIF-1α, NFκB, phosphoEGFR, total EGFR and cyclin D1. Finally, we will examine the lungs and cervical lymph nodes of animals that have invasive SCC at the time of sacrifice, in order to investigate the ability of each drug to prevent metastasis.

The results of this study are pending. If either drug is efficacious in the 4-NQO model of oral SCC, this will provide a rationale for clinical study of this compound as a chemopreventive agent. In the case of erlotinib, it would justify ongoing clinical studies targeting the EGFR as a strategy for chemoprevention. In the case of *Guggulipid*, it would suggest that this inexpensive and safe natural product be investigated in clinical trials to prevent HNSCC. Potential clinical trials are discussed in Chapter 6.

5.0 HONOKIOL TARGETS STAT3 AND ENHANCES EGFR-INHIBITION IN THE TREATMENT OF HNSCC

*Note: Contributions to this chapter represent experiments performed by Dr. Quan Cai.

5.1 INTRODUCTION

5.1.1 Honokiol's therapeutic potential

Honokiol is a natural compound derived from the bark of the magnolia tree and used in traditional Chinese medicine. The structure of honokiol is shown in Figure 27. Studies have demonstrated various ways in which honokiol may have a therapeutic benefit, including its ability to behave as a muscle relaxant (248), to have anti-inflammatory (249-251), antimicrobial (252) and antioxidant (253) activity, and indications that it may be useful in protecting against hepatotoxicity (254), neurotoxicity (255), thrombosis (256) and angiopathy (257). Interest in the role that honokiol may fill in cancer therapy began with a study demonstrating prevention of skin papillomas in mice (258). Several studies have

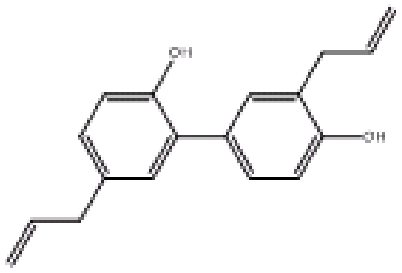

Figure 27. Chemical structure of honokiol

demonstrated the anticancer activities of honokiol in cancer cell lines (259-269) and xenograft tumor models (257, 259, 261, 263, 267, 270-272).

5.1.2 Honokiol's anticancer activity

In cancer models, honokiol has been found to alter various molecular targets that are known to affect tumor cell growth and survival. One of the most commonly proposed mechanisms of honokiol's antitumor activity is inhibition of the nuclear factor kappa B (NFκB) signaling pathway. NFκB is a transcription factor that contributes to several physiological processes (e.g. inflammation) but also regulates the expression of genes that are involved in cancer, including genes that control the cell cycle, apoptosis, tumor angiogenesis, and invasion (130-132). NFκB and upstream signaling mediators have been found to be inhibited by honokiol treatment of human monocytes (250), embryonic kidney cells (273), endothelial cells (257), lymphoma (268, 273), promyelocytic leukemia (268), multiple myeloma (273), breast cancer (268), cervical cancer (268), and HNSCC cells (273).

5.1.3 Rationale and hypothesis

In HNSCC cell lines, NFκB has been reported to interact with STAT3 (141), which is a potential molecular target for the treatment of HNSCC. In addition to regulating several genes involved in cancer (138), including some that are also regulated by NFκB, STAT3 has been found to be important for growth and survival of HNSCC cell lines and tumor xenografts (53, 90, 92) and is the target of many cancer therapies currently under investigation in preclinical models (138).

Honokiol has been shown to inhibit several proteins that are known to interact with STAT3 including, Src (259) and the IL-6 receptor (264), each of which directly activate STAT3 in HNSCC (91, 93), and NFκB (250, 257, 268, 273). Additionally, honokiol has been found to decrease the expression of various STAT3 target genes, including cyclin D1 (273-276), p21Waf1 (275, 277), c-Myc (273, 276), Mcl-1 (260, 263), Bcl-x_L (263), survivin (263), and VEGF (265, 273). STAT3 inhibition by honokiol in a multiple myeloma cell line has been reported (264). To our knowledge, the effect of honokiol on STAT3 in epithelial malignancies has not been determined. We hypothesized that honokiol can be used to target STAT3 in the treatment of HNSCC.

5.2 MATERIALS AND METHODS

5.2.1 Reagents and cells

HNSCC cell lines Cal-33, derived from an oral squamous cell carcinoma (SCC) (278), UM-22B, from a cervical lymph node metastasis of hypopharyngeal SCC (279), and 1483, from an oropharyngeal SCC (197), were maintained in DMEM/10% heat-inactivated FBS at 37˚C in a humidified incubator with 5% CO_2. Cal-33 cells were provided by Dr. Gerard Milano (Centre Anotoine-Lacassagne, Nice, France) (278), UM-22b cells by Dr. Thomas Carey (University of Michigan, Ann Arbor, MI) and 1483 cells by Dr. Gary Clayman (MD Anderson Cancer Center,

Houston TX). Honokiol is a natural product extracted from the seed cone of *Magnolia grandiflora* as previously described (259). In treatments of cell cultures, honokiol was dissolved in 100% ethanol as a vehicle and in 20% Intralipid (Baxter Healthcare, Deerfield, IL) for animal treatments. Erlotinib (OSI Pharmaceuticals, Melville, NY), was dissolved in 100% dimethyl sulfoxide (DMSO) as a vehicle.

5.2.2 Trypan blue dye exclusion assay

HNSCC cells were cultured overnight and treated with honokiol, erlotinib or the corresponding vehicles, in DMEM/1% serum, the following day. After 72 hours, cells were harvested by trypsinization and live cells counted after staining for trypan blue dye exclusion. Each experiment was performed with triplicate samples and the average percent survival calculated as a comparison to cells treated with the vehicle alone. The EC_{50} was calculated using Prism software version 4.03 (GraphPad Software Inc).

5.2.3 Annexin V apoptosis assay

Cal-33 cells were plated and, the following day, treated with either honokiol (10 μM) or ethanol, as the vehicle, for 72 hours. Cells were then harvested and stained with Cy3 labeled annexin V, according to the manufacturer's instructions (Annexin V-Cy3 Apoptosis Detection Kit, BioVision). Stained cells were imaged using a fluorescent microscope (Nikon) and the numbers of annexin V-positive cells counted (at least 3 fields per sample) using ImageJ software (NIH).

5.2.4 Matrigel invasion assay

The invasion assay was performed as previously described (199). Briefly, HNSCC cells were plated in serum-free DMEM containing epidermal growth factor (EGF) alone (10 ng/ml), EGF with honokiol (5 μM) and/or erlotinib (5 μM) or the corresponding vehicles, in a matrigel invasion chamber insert (BD Biosciences, San Diego, California). The outer well contained DMEM/10% FBS, as a chemoattractant. After 24 hours incubation, uninvaded cells were removed and the invaded cells in the matrigel were fixed, stained with Hema 3 (Fisher Scientific) and counted.

5.2.5 Western blotting

Immunoblotting was performed as previously described (199). Briefly, the proteins from whole cell lysates were resolved by SDS-PAGE and transferred onto nitrocellulose membranes (Bio-Rad, Hercules, CA) by a semi-dry transfer apparatus (Bio-Rad, Hercules, CA). The membrane was blocked with 5% skim milk in Tris-buffered saline-Tween (TBS-T) solution (100 mM Tris, 150 mM NaCl and 0.125% Tween 20). Membranes were incubated overnight with primary antibodies with 5% skim milk in TBS-T. After washing in TBS-T, membranes were incubated with secondary antibodies (anti-rabbit or anti-mouse IgG-horseradish peroxidase conjugate from Bio-Rad Laboratories, Hercules, CA). The blots were washed and developed with a luminol kit (Santa Cruz Biotechnology, Santa Cruz, CA). Primary antibodies for STAT3 and

phosphotyrosine STAT3 (Cell Signaling Technology, Boston, MA) and β-actin (CalBiochem, Gibbstown, NJ) were used. Densitometry was performed using DigiDoc1000 software (Alpha Innatech Corporation, San Leandro, CA).

5.2.6 *In vivo* tumor xenograft studies

Female athymic nude mice (5-6 weeks old, N=8) were inoculated with 1483 and UM-22b cells (1×10^6) into the right and left flank of each mouse, respectively. Upon outgrowth of palpable tumors (2 to 3 mm in diameter), 14 days following tumor cell inoculation, mice were randomized, by tumor volume, to two groups of four. The treatment group received intraperitoneal injections of honokiol (3 mg/mouse/day, five days/week) in 20% Intralipid (Baxter Healthcare, Deerfield, IL). The control group received the 20% Intralipid vehicle. Tumors were measured using digital calipers (Control Company, Friendswood, TX) at least three times per week and tumor volumes calculated using the following formula: volume= $L \times (W)^2/2$ (L: longest diameter; W: shorter diameter).

5.2.7 Statistical analyses

All statistical analyses of *in vitro* results were done using the nonparametric Mann-Whitney or Wilcoxon tests. For matrigel invasion assays, p values were calculated using EGF alone as 100% invasion for the comparison of EGF versus honokiol and EGFR plus erlotinib as 100% invasion for the comparison of erlotinib versus the honokiol/erlotinib combination.

5.3 RESULTS

5.3.1 Honokiol inhibits growth and induces apoptosis in HNSCC cells

The *in vitro* growth inhibitory and pro-apoptotic activities of honokiol have been demonstrated in several cancer cell lines (259-269, 280). In the current study, 3 HNSCC cell lines, 1483, UM-22b and Cal-33, were treated for 72 hours, with honokiol at concentrations ranging from 0.01 μM to 100 μM and compared to the vehicle (ethanol) alone. EC_{50} values were 7.44 μM for 1483, 7.36 μM for UM-22b and 3.90 μM for Cal-33 (Figure 28a). These values are comparable or lower than EC_{50} values seen in other cancer cell types (260, 263, 267, 269, 276). Honokiol was not found to be specific for cancer cells as it induces growth inhibition in a normal, immortalized esophageal cell line, Het-1a, with an EC_{50} of 3.09 μM (Figure 28b)

To determine the role of programmed cell death in the growth inhibitory effects of honokiol, HNSCC cells were treated with honokiol, followed by annexin V staining. As shown in Figure 28c, some of the growth inhibitory properties of honokiol in HNSCC cell lines can be attributed to increased apoptosis, as a 7.4-fold increase in apoptotic cells was detected after 72 hours of treatment with 10 μM honokiol, compared to the vehicle ($p=0.03$).

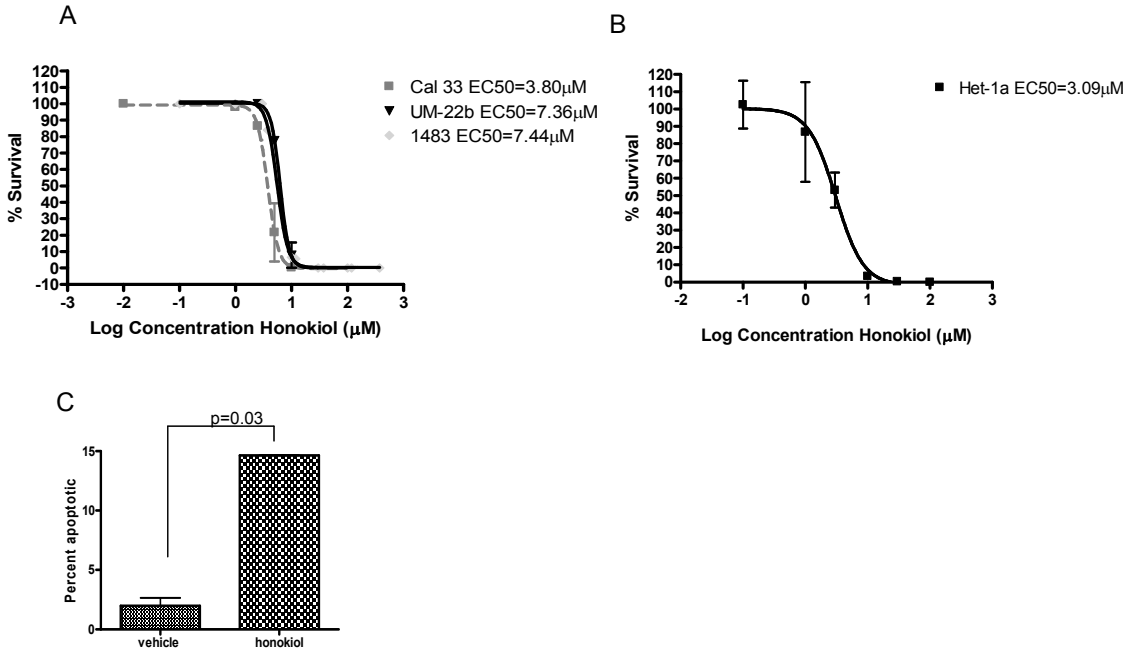

Figure 28. Honokiol inhibits growth and induces apoptosis in HNSCC cell lines. (A) HNSCC cells (UM-22b, 1483, and Cal-33) and (B) Het-1a cells were treated with honokiol or vehicle, stained in trypan blue dye and counted. The experiment was performed twice for each HNSCC cell line with similar results. (C) Cal-33 cells were treated with either honokiol (10 μM) or vehicle for 72 hours. Cells were then harvested and stained with Cy3-labeled annexin V. Images of stained cells were obtained with a fluorescent microscope and the percentage of annexin V positive cells counted. The experiment was repeated 4 times with triplicate samples and similar results.

5.3.2 Honokiol decreases levels of phosphotyrosine STAT3 in HNSCC cells

STAT3, an oncogenic transcription factor, represents a promising therapeutic target in the treatment of HNSCC. Various potential therapeutics that target STAT3, including oligonucleotides, peptidomimetics, and natural compounds, are currently under preclinical investigation (138). Treatment of UM-22b and Cal-33 induced a decrease in phosphotyrosine STAT3, after 24 hour serum starvation followed by 24 hours of honokiol (10 μM) treatment

(Figure 29). Average densitometric values are shown below each western blot and indicate a 63.3% and 35.5% decrease in UM-22b cells and Cal-33 cells, respectively, treated with honokiol as compared to the vehicle (p=0.03 for Cal-33 and p=0.05 for UM-22b). Similar results were seen in 1483 cells (data not shown). As STAT3 is known to play a key role in HNSCC growth both *in vitro* and *in vivo* (53, 90, 92), these data indicate that honokiol may have potential utility in the treatment of HNSCC.

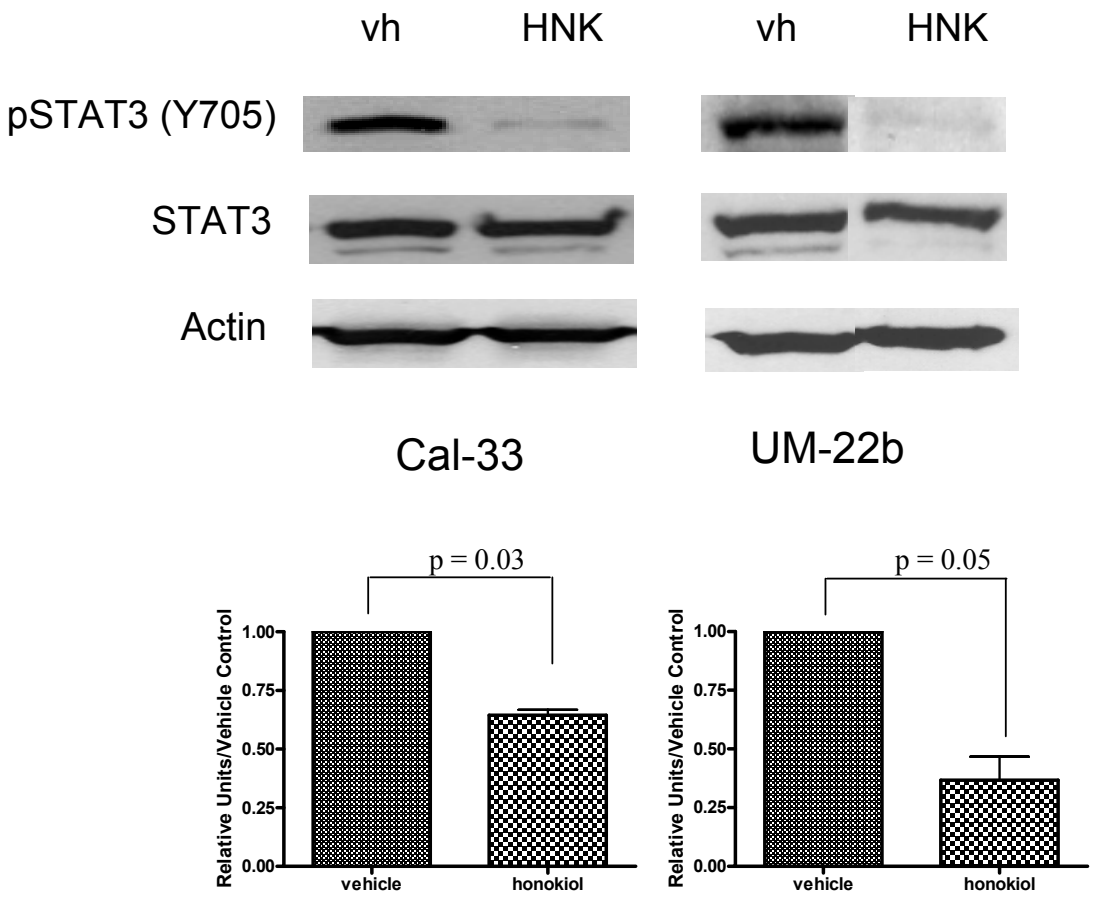

Figure 29. Honokiol inhibits STAT3 in HNSCC. Cells were cultured in serum containing medium for 24 hours, in serum free medium for another 24 hours, followed by 24 hour treatment with either honokiol (10 μM) or vehicle in serum free medium. Whole cell lysates were probed for phosphotyrosine STAT3 and total STAT3, with β-actin as a loading control.

5.3.3 Honokiol enhances the activity of erlotinib in HNSCC cells

Honokiol has been shown to enhance the effects of bortezomib (264), fludarabine (260), cladribine (260), chlorambucil (260), doxorubicin (272, 273), adriamycin (281, 282), paclitaxel (272, 273), docetaxel (267), SAHA (272), lapatinib (276), rapamycin (276) or cisplatin (270) in different cancer models. Erlotinib is an epidermal growth factor (EGFR)-targeting small-molecule tyrosine kinase inhibitor that has shown promise, in clinical trials, as a treatment for HNSCC. A different EGFR-targeting therapy, the anti-EGFR antibody, cetuximab, is FDA approved for the treatment of HNSCC. Cetuximab is known to inhibit HNSCC growth *in vivo*, but not *in vitro*, perhaps due to reliance on extracellular matrix components or the immune system. Therefore, in our studies of honokiol's effect in combination with EGFR inhibition *in vitro*, we used erlotinib instead. Combining honokiol at its EC_{50} (7.4 μM) with the approximate EC_{50} for erlotinib (10μM) resulted in a 77.0% growth inhibition, compared to 46.1% growth inhibition for erlotinib alone, a 1.7-fold enhancement of growth inhibition (Figure 30a; p=0.03).

Honokiol has been shown to decrease the invasiveness of fibrosarcoma (283) and breast cancer cells (276). We assayed the invasiveness of UM-22b cells, which are derived from an HNSCC lymph node metastasis, using matrigel invasion assays. Cells were plated in serum-free medium containing EGF (10 ng/ml) as a stimulant and either honokiol (5 μM), erlotinib (10 μM), a combination of both drugs or their corresponding vehicles. Medium containing 10% serum was present in the lower chamber as a chemoattractant. After 24 hours, honokiol was found to inhibit invasion on its own and also to enhance the anti-invasion activity of erlotinib. Considering the large impact of invasion and metastasis on the clinical outcome of HNSCC, these data suggest

that honokiol may have a role in HNSCC treatment, especially in combination with other therapies.

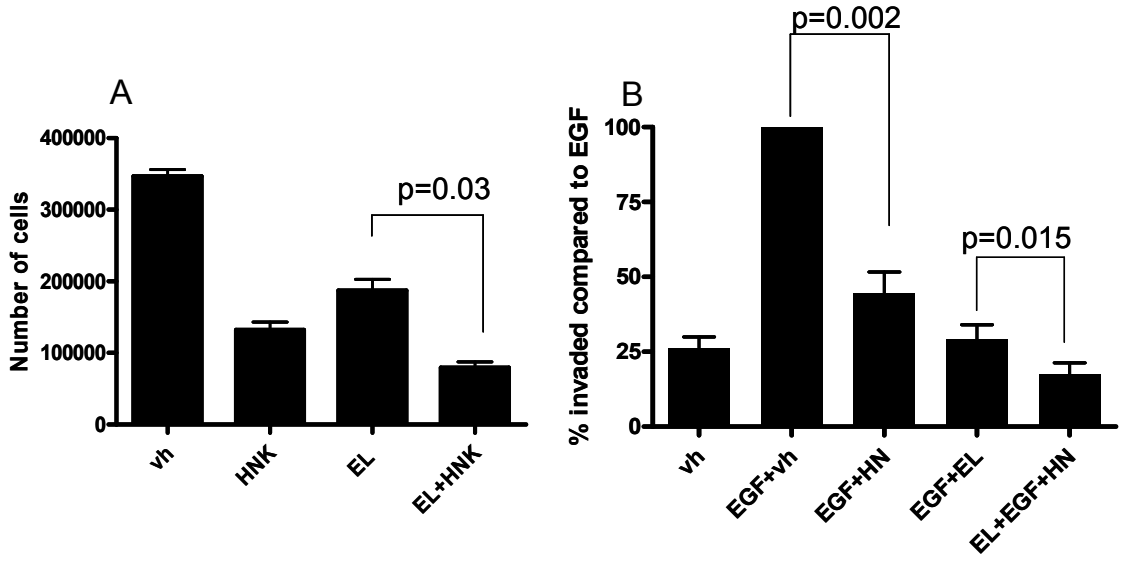

Figure 30. Honokiol enhances the effects of erlotinib. (A) UM-22B cells were treated with either honokiol at its EC_{50} (7.4 µM) or erlotinib (10 µM), both drugs, or their corresponding vehicles. After 72 hours, cells were stained with trypan blue dye and counted. The experiment was performed 4 times with triplicate samples and similar results (p=0.03). (B) UM-22b cells were plated in serum-free DMEM, on top of matrigel inserts in wells containing DMEM/10% FBS. Both inserts and outer wells contained EGF (10 ng/ml) and either honokiol (5 µM), with or without erlotinib (5 µm), or the vehicle. Matrigel inserts were fixed and stained after 24 hours. Numbers of cells invading the matrigel were counted. The experiment was performed 6 times, using duplicate samples and counting at least 4 fields per well (p=0.002 for EGF versus EGF+honokiol; p=0.015 for EGF+erlotinib versus EGF+combination).

5.3.4 Honokiol's *in vivo* effect in the xenograft model of HNSCC

Honokiol has been found to prevent the formation of skin papillomas *in vivo* (258) and to inhibit growth of xenografts derived from angiosarcoma (259), colorectal (261), prostate (263, 267), gastric (266), breast (272), lung (270), and ovarian (265, 271) cancer cells, *in vivo*. Using an HNSCC xenograft model, 1 x 10^6 1483 cells and UM-22b cells were injected into the animals right and left flanks, respectively. Mice were then randomized to two groups by tumor volume and treated, 5 days per week, with 3 mg/mouse of honokiol, by intraperitoneal injection, or with 20% intralipid, as the vehicle control. Although, due to small numbers of animals and a modest treatment effect, differences in tumor volume were not statistically significant between the two groups, growth rates of xenografts derived from both cell lines were slightly lower in animals treated with honokiol compared to the vehicle (Figure 31). 1483-derived xenografts in the honokiol-treated group grew at an average rate of 14.31 mm^3/day, 28.0% slower than the control group, which grew at a rate of 19.87 mm^3/day. The UM-22b-derived xenografts in the honokiol group grew 21.6% slower, at a rate of 15.01 mm^3/day, compared to 19.14 mm^3/day for the control group. To our knowledge, this is the first study demonstrating the *in vivo* anticancer activity of honokiol in HNSCC.

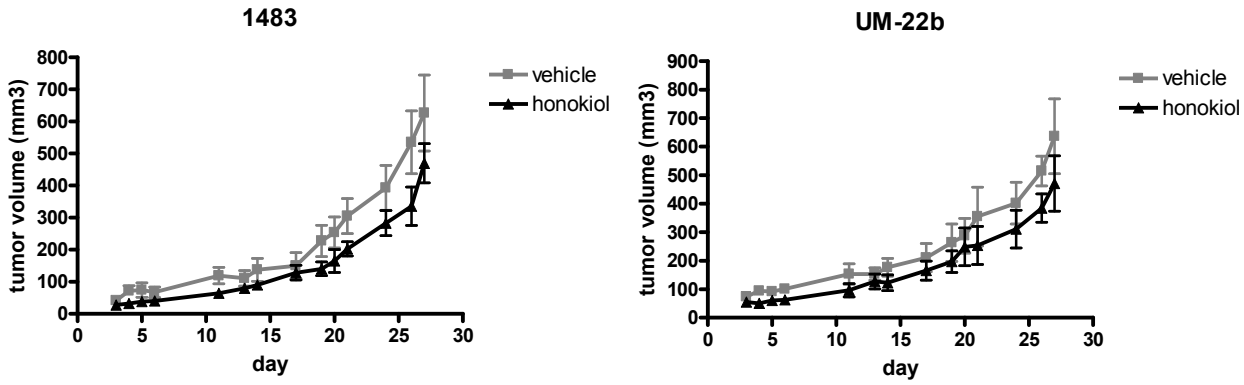

Figure 31. Honokiol's *in vivo* effects in the HNSCC xenograft therapy model. Nude mice (4 per group) were inoculated with 1 x 10 ^{6} UM-22b and 1483 cells, subcutaneously, into opposite flanks. After tumor outgrowth, 14 days later, mice were randomized to two groups, based on tumor volume and 5 times per week with intraperitoneal injections of honokiol (3 mg/mouse) dissolved in Intralipid or with Intralipid alone. Tumor measurements were taken at least three times per week.

5.4 DISCUSSION

The therapeutic potential, including antitumor activity of honokiol, a natural product derived from the magnolia plant and used in traditional Chinese medicine, has been reported in various preclinical trials. In the current study, we investigated honokiol's potential utility in the treatment of HNSCC. Honokiol was found to inhibit growth and induce apoptosis in HNSCC cell lines and to enhance the growth-inhibitory and anti-invasion activities of EGFR-targeting therapies. Furthermore, STAT3, a potential therapeutic target in HNSCC, was inhibited upon honokiol treatment. Finally, honokiol was found to inhibit the growth of xenografts derived from two HNSCC cell lines, *in vivo*.

Many preclinical studies have focused on targeting STAT3 with engineered oligonucleotides, peptidomimetics and other molecules (138). Several natural compounds have also been found to inhibit STAT3 in different models (96, 118-125, 138, 194). Our rationale for investigating the ability of honokiol to target STAT3 included evidence of STAT3 inhibition in honokiol treatment of a multiple myeloma cell line (264) and of honokiol-induced inhibition of signaling molecules upstream of STAT3, including Src (259) and the IL-6 receptor (264), inhibition of NFκB (250, 257, 268, 273), which is known to experience crosstalk with STAT3 in HNSCC (141), and downregulation of STAT3 target genes, including cyclin D1 (273-276),

p21Waf1 (275, 277), c-Myc (273, 276), Mcl-1 (260, 263), Bcl-x_L (263), survivin (263), and VEGF (265, 273). Future studies of honokiol's activity should focus on both the upstream mechanism of STAT3 inhibition, which may include effects on receptor tyrosine kinases (e.g. EGFR), non-receptor tyrosine kinases (e.g. Src), or phosphatase inhibitors of STAT3 (e.g. SHP-1), and on whether or not the reported decreases in expression of STAT3 target genes, which are regulated by other transcription factors, as well, actually depend on alterations in STAT3 signaling.

Currently available treatments for HNSCC are themselves responsible for much of the morbidity and mortality associated with this disease and are also often limited by drug resistance. Therefore, administration of a compound that enhances the activity of an HNSCC treatment may be useful in complementary therapy. In this study we investigated honokiol's ability to enhance the activity of erlotinib (Tarceva^{TM}), a small molecule inhibitor that has shown promise in clinical trials in HNSCC. The problem of resistance to EGFR-targeting therapy is thought to stem partly from activation of STAT3 through alternative signaling pathways, including Src and the IL-6 receptor, which both play a role in HNSCC. A molecule that targets one of these alternative pathways, like honokiol, which inhibits Src and the IL-6 receptor, may potentially be useful in overcoming resistance to EGFR inhibition. Liu *et al*. have shown that honokiol synergizes with lapatinib, another EGFR-targeting therapeutic, in the treatment of HER2-overexpressing breast cancer cells (276). Honokiol was found to enhance both the growth inhibitory and anti-invasion activities of erlotinib in HNSCC cells.

An *in vivo* study of honokiol's growth inhibitory activity in HNSCC xenografts demonstrated decreases in tumor growth rates. Future *in vivo* studies should use larger numbers of animals, allowing for sufficient power to detect a significant difference in growth rates, and should investigate the *in vivo* efficacy of combining honokiol with EGFR-inhibiting therapies in HNSCC. Our observations of a modest growth-inhibitory effect *in vivo,* coupled with demonstrations of honokiol's ability to target STAT3 and enhance erlotinib's activity *in vitro*, suggest a potential role for honokiol in the treatment of HNSCC, particularly in combination with EGFR-inhibiting therapy.

6.0 GENERAL DISCUSSION

This thesis focused on the use of STAT3-targeting natural compounds in HNSCC treatment and chemoprevention. The studies described reveal the STAT3-targeting, anticancer activity of two natural compounds, guggulsterone and honokiol. One study, the results of which are still pending, focuses on the potential chemopreventive properties of two agents, *Guggulipid* and erlotinib.

6.1 STAT3 TARGETING BY NATURAL COMPOUNDS

STAT3, an oncogenic transcription factor is a plausible therapeutic target for the treatment and prevention of HNSCC. This is true for many other malignancies, in which STAT3 is constitutively activated, as well. Various preclinical studies have focused on the development of specific STAT3 inhibitors for the treatment of cancer. Natural compounds, like guggulsterone and honokiol, are not specific molecular inhibitors, which can be either a disadvantage or an advantage, depending on which other molecules are affected. One advantage of guggulsterone over oligonucleotide and peptidomimetic STAT3 inhibitors is that it is known to be safe and can be easily administered. In this study, guggulsterone was found to decrease phosphotyrosine and total STAT3 levels *in vitro* and total STAT3 levels *in vivo*. Honokiol was found to decrease

levels of phosphotyrosine STAT3 *in vitro*. Most natural compounds known to inhibit STAT3, like honokiol, only affect levels of phosphotyrosine STAT3, implying that the mechanism is indirect and involves either increases in activity of the physiological inhibitors of STAT3 (e.g. SOCS-1, SOCS-3, GRIM-19, PIAS and PTPRT) or decreases in signaling through upstream molecules (e.g. EGFR, Src, IL-6 receptor). Guggulsterone, on the other hand, is unique in that it affects levels of total STAT3. Although, to my knowledge, there are no published reports of natural compounds that decrease total STAT3, total STAT3 was also found to decrease slightly in a single experiment treating UM-22b cells with the aromatic isothiocyanate, PBITC (Figure 5), so this may not be so uncommon in natural compounds but merely unreported.

Although, in the case of guggulsterone, inhibition of STAT3 signaling was found to be responsible for part of guggulsterone's *in vitro* growth inhibitory activity, the mechanism of STAT3 inhibition was not determined. Realtime PCR did not demonstrate changes in levels of STAT3 mRNA. Inhibitors of proteosomal degradation and translation did not abrogate guggulsterone-induced STAT3 inhibition, though the nonspecific nature of these inhibitors is problematic and future studies should employ more specific methods for investigation of these potential mechanisms, in addition to investigating the possible involvement of other enzymes, aside from the proteosome, which are known to degrade STAT3. In addition to proteosomal degradation, studies have previously reported STAT3 degradation by caspases, calpain and serine proteases in certain systems (213-219). In general, however, while mechanisms of STAT3 phosphorylation and dephosphorylation have received a lot of attention, very little is known about cellular mechanisms of regulating STAT3 protein levels.

Honokiol, on the other hand, affects phosphotyrosine but not total STAT3 levels. Some of the signaling molecules upstream of STAT3, IL-6 receptor and Src, are also inhibited by honokiol (259, 264). Whether or not honokiol's STAT3 inhibition relies on alterations in these signaling pathways, or on others (e.g. EGFR, NFκB), remains to be determined. Because guggulsterone seems to cause somewhat more dramatic decreases in phosphotyrosine than in total STAT3 (Figure 11), it's possible that a second mechanism, which inhibits phosphorylation of STAT3, may also result from guggulsterone treatment. Possible mechanisms include increases in activity of the phosphatase SHP-1, as was reported by Ahn et al. (194), or decreases in the IL-6-mediated crosstalk between NFκB and STAT3, which was demonstrated, in HNSCC, by Squarize et al. (141).

Although the mechanisms of guggulsterone's activity upstream of STAT3 have not been revealed, I would speculate that the ultimate upstream target is a nuclear receptor, perhaps more than one. Brobst et al. have found that guggulsterone, a steroid-like molecule, promiscuously binds various steroid receptors (284). In fact, although guggulsterone's antagonism of the FXR has gained the most attention, as a mechanism for guggulsterone's hypolipidemic activity (223), and more recently for its involvement in breast cancer cell migration (220) and survival of Barrett's esophagus cell lines (221), guggulsterone binds various other steroid receptors even more strongly. Guggulsterone is a strong agonist of the progesterone receptor (PR), estrogen receptor (ER)-α, and pregnane x receptor (PXR). (284) The PXR regulates the CYP3A genes, which are involved in drug and carcinogen metabolism (226). Recent evidence indicates negative crosstalk between FXR and NFκB in hepatocytes (285). Whether or not this information is relevant to signaling in epithelial malignancies is unknown. FXR also dimerizes with the RXR,

the target of retinoids originally identified as potential chemopreventive agents for HNSCC (126). The possibility of multiple steroid receptor targets suggests a very complex, non-specific downstream signaling mechanism that may differ between cell types.

One likely mechanism of honokiol's activity, on the other hand, is direct scavenging of reactive oxygen species. Honokiol's structure contains two phenolic groups that can scavenge free radicals, which has been shown by Dikalov et al. (286). As NFκB is induced by reactive oxygen species, the aforementioned crosstalk between NFκB and STAT3, via IL-6 (141) may decrease after scavenging of free radicals by honokiol. Guggulsterone has been found to increase or decrease levels of reactive oxygen species, depending on the system, though it has been hypothesized that this is an indirect effect, involving signaling through cellular proteins, rather than direct scavenging of free radicals (189, 191, 233, 234).

6.2 ANTICANCER EFFECTS OF GUGGULSTERONE AND HONOKIOL IN PRECLINICAL MODELS OF HNSCC

In the described studies, two STAT3-targeting natural compounds, guggulsterone and honokiol, have been found to have anticancer activity in preclinical models of HNSCC. Both compounds were found to induce apoptosis and to inhibit invasiveness of HNSCC cell lines. Guggulsterone was also found to induce cell cycle arrest, associated with decreases in various cell cycle regulating proteins (Figure 8). Both compounds enhanced the activities of HNSCC therapies,

particularly EGFR-targeting molecules. This enhancement was also demonstrated in *in vivo* combination of *Guggulipid* and cetuximab.

These data are supportive of a clinical use for guggulsterone and honokiol in HNSCC treatment. Based on our observations, particularly *in vivo,* neither compound is potent enough to be used as a single agent. However, both may have a role in complementary therapy. Combining guggulsterone, a direct STAT3 inhibitor, with an EGFR-targeting therapy may preclude activation of alternate pathways that are thought to lead to therapeutic resistance to EGFR inhibition (Figure 23). Honokiol, on the other hand, may inhibit one or more of these alternate pathways, IL-6 receptor and/or Src signaling. While guggulsterone has already been used and found to be safe in clinical trials investigating its potential hypolipidemic activity, to my knowledge, honokiol has not been used in any published clinical trial. Honokiol has been commonly used in Chinese medicine, however, suggesting that it is also probably safe and a good candidate for combination treatment.

Guggulsterone's effects varied between cell lines, both *in vitro*, in examining growth inhibition, levels of apoptosis and the role of STAT3 inhibition, and in its *in vivo* effects on tumor growth, suggesting that guggulsterone may only be useful in a subset of patients. Despite guggulsterone's safety in clinical trials, another important concern is its activation of various steroid receptors, particularly the PXR, as this may alter the metabolism of other therapies. Indeed, *Guggulipid*, has already been shown to decrease plasma levels of diltiazem and propranolol in humans (183).

6.3 HNSCC CHEMOPREVENTION

The original aim of this project was to identify and characterize a potential chemopreventive agent for HNSCC, as a great clinical need for such a therapy exists. Based on evidence of its role in HNSCC carcinogenesis, STAT3 was chosen as an appropriate molecular target for HNSCC chemoprevention. The preclinical models typically used to investigate HNSCC therapies were inadequate for testing an agent's chemopreventive activity. Therefore, we chose to use a carcinogen-induced animal model for this purpose. The results of this study, investigating the chemopreventive activities of *Guggulipid* and the EGFR-targeting TKI, erlotinib, are pending.

The relevance of my studies of guggulsterone's anticancer activity as a treatment for HNSCC, *in vitro* and in the xenograft model, to guggulsterone's potential chemopreventive activity is unclear. These models employ cells that have already progressed through the process of carcinogenesis. However, demonstrating inhibition of a molecular target, STAT3, in these preclinical models, is helpful in providing a rationale for studying guggulsterone as a chemopreventive agent. Furthermore, evidence that guggulsterone inhibits the cellular processes that cause cancer cells to proliferate, suggests that it may also be able to target these processes in precancerous cells that have molecular alterations predisposing them to uncontrolled growth, thus inhibiting tumor promotion.

If either compound decreases the incidence of preneoplastic or neoplastic lesions in the oral mucosa of 4-NQO treated mice, these data will justify the compound's use in a clinical trial for chemoprevention of HNSCC. In fact, erlotinib is already in clinical trial for chemoprevention, despite the lack of supporting data in an animal model. Clinical trials

investigating chemopreventive agents are plagued by logistical problems, including, for example, the fact that they require patients who do not have cancer and also the large numbers and long periods of time required to draw conclusions about whether or not administration of a compound actually decreases the incidence of cancer. For these reasons, many chemoprevention trials rely on intermediate endpoints, such as expression of biomarkers or rates of recurrence in a population that has previously had cancer.

If *Guggulipid* is found to have chemopreventive activity in the 4-NQO model, we will propose a clinical chemoprevention study using changes in certain biomarkers as an intermediate endpoint. Patients with oral leukoplakia, a premalignant lesion that can progress to HNSCC, will be treated with *Guggulipid* for a short period of time. After excision of the lesion, we will use the tissue to assay levels of certain biomarkers of progression to HNSCC, perhaps STAT3 and phosphotyrosine STAT3 or others identified in our animal study.

6.4 CONCLUSIONS

Improvements in the therapeutic approach to HNSCC, a common and devastating disease with a 50% mortality rate and frequent second primary tumors (SPTs), are greatly needed. One possible method of improving therapy is to enhance currently available treatments. Another is to prevent the initial malignancy, recurrence, or SPT. In the studies described in this thesis, we have identified two natural compounds that target STAT3, a therapeutic target for the treatment and prevention of HNSCC. Our data from preclinical models provide a rationale for use of either

guggulsterone or honokiol in combination with current HNSCC therapies. Results of an ongoing study may reveal the potential for use of either guggulsterone or the EGFR-targeting molecule, erlotinib, in HNSCC chemoprevention.

7.0 BIBLIOGRAPHY

1. Jemal, A., Siegel, R., Ward, E., Murray, T., Xu, J., Smigal, C., and Thun, M. J. Cancer statistics, 2006. CA Cancer J Clin, *56:* 106-130, 2006.
2. Parkin, D. M., Pisani, P., and Ferlay, J. Estimates of the worldwide incidence of 25 major cancers in 1990. Int J Cancer, *80:* 827-841, 1999.
3. Sturgis, E. M. A review of social and behavioral efforts at oral cancer preventions in India. Head Neck, *26:* 937-944, 2004.
4. Fan, C. Y. Genetic alterations in head and neck cancer: interactions among environmental carcinogens, cell cycle control, and host DNA repair. Curr Oncol Rep, *3:* 66-71, 2001.
5. Marchand, J. L., Luce, D., Leclerc, A., Goldberg, P., Orlowski, E., Bugel, I., and Brugere, J. Laryngeal and hypopharyngeal cancer and occupational exposure to asbestos and man-made vitreous fibers: results of a case-control study. Am J Ind Med, *37:* 581-589, 2000.
6. Laforest, L., Luce, D., Goldberg, P., Begin, D., Gerin, M., Demers, P. A., Brugere, J., and Leclerc, A. Laryngeal and hypopharyngeal cancers and occupational exposure to formaldehyde and various dusts: a case-control study in France. Occup Environ Med, *57:* 767-773, 2000.
7. Berrino, F., Richiardi, L., Boffetta, P., Esteve, J., Belletti, I., Raymond, L., Troschel, L., Pisani, P., Zubiri, L., Ascunce, N., Guberan, E., Tuyns, A., Terracini, B., and Merletti, F.

Occupation and larynx and hypopharynx cancer: a job-exposure matrix approach in an international case-control study in France, Italy, Spain and Switzerland. Cancer Causes Control, *14:* 213-223, 2003.

8. Gustavsson, P., Jakobsson, R., Johansson, H., Lewin, F., Norell, S., and Rutkvist, L. E. Occupational exposures and squamous cell carcinoma of the oral cavity, pharynx, larynx, and oesophagus: a case-control study in Sweden. Occup Environ Med, *55:* 393-400, 1998.

9. Luce, D., Leclerc, A., Begin, D., Demers, P. A., Gerin, M., Orlowski, E., Kogevinas, M., Belli, S., Bugel, I., Bolm-Audorff, U., Brinton, L. A., Comba, P., Hardell, L., Hayes, R. B., Magnani, C., Merler, E., Preston-Martin, S., Vaughan, T. L., Zheng, W., and Boffetta, P. Sinonasal cancer and occupational exposures: a pooled analysis of 12 case-control studies. Cancer Causes Control, *13:* 147-157, 2002.

10. Scully, C., Field, J. K., and Tanzawa, H. Genetic aberrations in oral or head and neck squamous cell carcinoma (SCCHN): 1. Carcinogen metabolism, DNA repair and cell cycle control. Oral Oncol, *36:* 256-263, 2000.

11. Slaughter, D. P., Southwick, H. W., and Smejkal, W. Field cancerization in oral stratified squamous epithelium; clinical implications of multicentric origin. Cancer, *6:* 963-968, 1953.

12. Vikram, B. Changing patterns of failure in advanced head and neck cancer. Arch Otolaryngol, *110:* 564-565, 1984.

13. Do, K. A., Johnson, M. M., Doherty, D. A., Lee, J. J., Wu, X. F., Dong, Q., Hong, W. K., Khuri, F. R., Fu, K. K., and Spitz, M. R. Second primary tumors in patients with upper

aerodigestive tract cancers: joint effects of smoking and alcohol (United States). Cancer Causes Control, *14:* 131-138, 2003.

14. Moffat, B. A., Chenevert, T. L., Lawrence, T. S., Meyer, C. R., Johnson, T. D., Dong, Q., Tsien, C., Mukherji, S., Quint, D. J., Gebarski, S. S., Robertson, P. L., Junck, L. R., Rehemtulla, A., and Ross, B. D. Functional diffusion map: a noninvasive MRI biomarker for early stratification of clinical brain tumor response. Proc Natl Acad Sci U S A, *102:* 5524-5529, 2005.

15. Wolbach, S. B. and Howe, P. R. Nutrition Classics. The Journal of Experimental Medicine 42: 753-77, 1925. Tissue changes following deprivation of fat-soluble A vitamin. S. Burt Wolbach and Percy R. Howe. Nutr Rev, *36:* 16-19, 1978.

16. Hong, W. K., Endicott, J., Itri, L. M., Doos, W., Batsakis, J. G., Bell, R., Fofonoff, S., Byers, R., Atkinson, E. N., Vaughan, C., and et al. 13-cis-retinoic acid in the treatment of oral leukoplakia. N Engl J Med, *315:* 1501-1505, 1986.

17. Hong, W. K., Lippman, S. M., Itri, L. M., Karp, D. D., Lee, J. S., Byers, R. M., Schantz, S. P., Kramer, A. M., Lotan, R., Peters, L. J., and et al. Prevention of second primary tumors with isotretinoin in squamous-cell carcinoma of the head and neck. N Engl J Med, *323:* 795-801, 1990.

18. Khuri, F. R., Lee, J. J., Lippman, S. M., Kim, E. S., Cooper, J. S., Benner, S. E., Winn, R., Pajak, T. F., Williams, B., Shenouda, G., Hodson, I., Fu, K., Shin, D. M., Vokes, E. E., Feng, L., Goepfert, H., and Hong, W. K. Randomized phase III trial of low-dose isotretinoin for prevention of second primary tumors in stage I and II head and neck cancer patients. J Natl Cancer Inst, *98:* 441-450, 2006.

19. Lippman, S. M., Lee, J. J., Karp, D. D., Vokes, E. E., Benner, S. E., Goodman, G. E., Khuri, F. R., Marks, R., Winn, R. J., Fry, W., Graziano, S. L., Gandara, D. R., Okawara, G., Woodhouse, C. L., Williams, B., Perez, C., Kim, H. W., Lotan, R., Roth, J. A., and Hong, W. K. Randomized phase III intergroup trial of isotretinoin to prevent second primary tumors in stage I non-small-cell lung cancer. J Natl Cancer Inst, *93:* 605-618, 2001.

20. Schwartz, J. L., Baker, V., Larios, E., and Chung, F. L. Molecular and cellular effects of green tea on oral cells of smokers: a pilot study. Mol Nutr Food Res, *49:* 43-51, 2005.

21. Pisters, K. M., Newman, R. A., Coldman, B., Shin, D. M., Khuri, F. R., Hong, W. K., Glisson, B. S., and Lee, J. S. Phase I trial of oral green tea extract in adult patients with solid tumors. J Clin Oncol, *19:* 1830-1838, 2001.

22. Armstrong, W. B., Kennedy, A. R., Wan, X. S., Taylor, T. H., Nguyen, Q. A., Jensen, J., Thompson, W., Lagerberg, W., and Meyskens, F. L., Jr. Clinical modulation of oral leukoplakia and protease activity by Bowman-Birk inhibitor concentrate in a phase IIa chemoprevention trial. Clin Cancer Res, *6:* 4684-4691, 2000.

23. Khuri, F. R. and Shin, D. M. Head and neck cancer chemoprevention gets a shot in the arm. J Clin Oncol, *26:* 345-347, 2008.

24. Silvennoinen, O., Schindler, C., Schlessinger, J., and Levy, D. E. Ras-independent growth factor signaling by transcription factor tyrosine phosphorylation. Science, *261:* 1736-1739, 1993.

25. Stahl, N., Farruggella, T. J., Boulton, T. G., Zhong, Z., Darnell, J. E., Jr., and Yancopoulos, G. D. Choice of STATs and other substrates specified by modular tyrosine-based motifs in cytokine receptors. Science, *267:* 1349-1353, 1995.

26. Darnell, J. E., Jr., Kerr, I. M., and Stark, G. R. Jak-STAT pathways and transcriptional activation in response to IFNs and other extracellular signaling proteins. Science, *264:* 1415-1421, 1994.

27. Chen, E., Gadina, M., Chen, M., and O'Shea, J. J. Advances in cytokine signaling: the role of Jaks and STATs. Transplant Proc, *31:* 1482-1487, 1999.

28. Ihle, J. N. and Kerr, I. M. Jaks and Stats in signaling by the cytokine receptor superfamily. Trends Genet, *11:* 69-74, 1995.

29. Briscoe, J., Kohlhuber, F., and Muller, M. JAKs and STATs branch out. Trends Cell Biol, *6:* 336-340, 1996.

30. Greenlund, A. C., Farrar, M. A., Viviano, B. L., and Schreiber, R. D. Ligand-induced IFN gamma receptor tyrosine phosphorylation couples the receptor to its signal transduction system (p91). Embo J, *13:* 1591-1600, 1994.

31. Schindler, C., Shuai, K., Prezioso, V. R., and Darnell, J. E., Jr. Interferon-dependent tyrosine phosphorylation of a latent cytoplasmic transcription factor. Science, *257:* 809-813, 1992.

32. Quelle, F. W., Thierfelder, W., Witthuhn, B. A., Tang, B., Cohen, S., and Ihle, J. N. Phosphorylation and activation of the DNA binding activity of purified Stat1 by the Janus protein-tyrosine kinases and the epidermal growth factor receptor. J Biol Chem, *270:* 20775-20780, 1995.

33. Darnell, J. E., Jr. STATs and gene regulation. Science, *277:* 1630-1635, 1997.

34. Vignais, M. L., Sadowski, H. B., Watling, D., Rogers, N. C., and Gilman, M. Platelet-derived growth factor induces phosphorylation of multiple JAK family kinases and STAT proteins. Mol Cell Biol, *16:* 1759-1769, 1996.

35. Ruff-Jamison, S., Zhong, Z., Wen, Z., Chen, K., Darnell, J. E., Jr., and Cohen, S. Epidermal growth factor and lipopolysaccharide activate Stat3 transcription factor in mouse liver. J Biol Chem, *269:* 21933-21935, 1994.

36. Shao, H., Cheng, H. Y., Cook, R. G., and Tweardy, D. J. Identification and characterization of signal transducer and activator of transcription 3 recruitment sites within the epidermal growth factor receptor. Cancer Res, *63:* 3923-3930, 2003.

37. Turkson, J., Bowman, T., Garcia, R., Caldenhoven, E., De Groot, R. P., and Jove, R. Stat3 activation by Src induces specific gene regulation and is required for cell transformation. Mol Cell Biol, *18:* 2545-2552, 1998.

38. Danial, N. N., Pernis, A., and Rothman, P. B. Jak-STAT signaling induced by the v-abl oncogene. Science, *269:* 1875-1877, 1995.

39. Shuai, K., Schindler, C., Prezioso, V. R., and Darnell, J. E., Jr. Activation of transcription by IFN-gamma: tyrosine phosphorylation of a 91-kD DNA binding protein. Science, *258:* 1808-1812, 1992.

40. Liu, L., McBride, K. M., and Reich, N. C. STAT3 nuclear import is independent of tyrosine phosphorylation and mediated by importin-alpha3. Proc Natl Acad Sci U S A, *102:* 8150-8155, 2005.

41. Komyod, W., Bauer, U. M., Heinrich, P. C., Haan, S., and Behrmann, I. Are STATS arginine-methylated? J Biol Chem, *280:* 21700-21705, 2005.

42. Mowen, K. A., Tang, J., Zhu, W., Schurter, B. T., Shuai, K., Herschman, H. R., and David, M. Arginine methylation of STAT1 modulates IFNalpha/beta-induced transcription. Cell, *104:* 731-741, 2001.

43. Yuan, Z. L., Guan, Y. J., Chatterjee, D., and Chin, Y. E. Stat3 dimerization regulated by reversible acetylation of a single lysine residue. Science, *307:* 269-273, 2005.

44. Zhong, Z., Wen, Z., and Darnell, J. E., Jr. Stat3: a STAT family member activated by tyrosine phosphorylation in response to epidermal growth factor and interleukin-6. Science, *264:* 95-98, 1994.

45. Aaronson, D. S. and Horvath, C. M. A road map for those who don't know JAK-STAT. Science, *296:* 1653-1655, 2002.

46. Decker, T., Lew, D. J., Mirkovitch, J., and Darnell, J. E., Jr. Cytoplasmic activation of GAF, an IFN-gamma-regulated DNA-binding factor. Embo J, *10:* 927-932, 1991.

47. Schaefer, T. S., Sanders, L. K., and Nathans, D. Cooperative transcriptional activity of Jun and Stat3 beta, a short form of Stat3. Proc Natl Acad Sci U S A, *92:* 9097-9101, 1995.

48. Bugno, M., Graeve, L., Gatsios, P., Koj, A., Heinrich, P. C., Travis, J., and Kordula, T. Identification of the interleukin-6/oncostatin M response element in the rat tissue inhibitor of metalloproteinases-1 (TIMP-1) promoter. Nucleic Acids Res, *23:* 5041-5047, 1995.

49. Calo, V., Migliavacca, M., Bazan, V., Macaluso, M., Buscemi, M., Gebbia, N., and Russo, A. STAT proteins: from normal control of cellular events to tumorigenesis. J Cell Physiol, *197:* 157-168, 2003.

50. Bromberg, J. F., Horvath, C. M., Besser, D., Lathem, W. W., and Darnell, J. E., Jr. Stat3 activation is required for cellular transformation by v-src. Mol Cell Biol, *18:* 2553-2558, 1998.

51. Bromberg, J. F., Wrzeszczynska, M. H., Devgan, G., Zhao, Y., Pestell, R. G., Albanese, C., and Darnell, J. E., Jr. Stat3 as an oncogene. Cell, *98:* 295-303, 1999.

52. Bowman, T., Garcia, R., Turkson, J., and Jove, R. STATs in oncogenesis. Oncogene, *19:* 2474-2488, 2000.

53. Grandis, J. R., Drenning, S. D., Chakraborty, A., Zhou, M. Y., Zeng, Q., Pitt, A. S., and Tweardy, D. J. Requirement of Stat3 but not Stat1 activation for epidermal growth factor receptor- mediated cell growth In vitro. J Clin Invest, *102:* 1385-1392, 1998.

54. Catlett-Falcone, R., Landowski, T. H., Oshiro, M. M., Turkson, J., Levitzki, A., Savino, R., Ciliberto, G., Moscinski, L., Fernandez-Luna, J. L., Nunez, G., Dalton, W. S., and Jove, R. Constitutive activation of Stat3 signaling confers resistance to apoptosis in human U266 myeloma cells. Immunity, *10:* 105-115, 1999.

55. Niu, G., Heller, R., Catlett-Falcone, R., Coppola, D., Jaroszeski, M., Dalton, W., Jove, R., and Yu, H. Gene therapy with dominant-negative Stat3 suppresses growth of the murine melanoma B16 tumor in vivo. Cancer Res, *59:* 5059-5063, 1999.

56. Garcia, R., Bowman, T. L., Niu, G., Yu, H., Minton, S., Muro-Cacho, C. A., Cox, C. E., Falcone, R., Fairclough, R., Parsons, S., Laudano, A., Gazit, A., Levitzki, A., Kraker, A., and Jove, R. Constitutive activation of Stat3 by the Src and JAK tyrosine kinases participates in growth regulation of human breast carcinoma cells. Oncogene, *20:* 2499-2513, 2001.

57. Niu, G., Bowman, T., Huang, M., Shivers, S., Reintgen, D., Daud, A., Chang, A., Kraker, A., Jove, R., and Yu, H. Roles of activated Src and Stat3 signaling in melanoma tumor cell growth. Oncogene, *21:* 7001-7010, 2002.

58. Tumang, J. R., Hsia, C. Y., Tian, W., Bromberg, J. F., and Liou, H. C. IL-6 rescues the hyporesponsiveness of c-Rel deficient B cells independent of Bcl-xL, Mcl-1, and Bcl-2. Cell Immunol, *217:* 47-57, 2002.

59. Dauer, D. J., Ferraro, B., Song, L., Yu, B., Mora, L., Buettner, R., Enkemann, S., Jove, R., and Haura, E. B. Stat3 regulates genes common to both wound healing and cancer. Oncogene, *24:* 3397-3408, 2005.

60. Yang, J., Chatterjee-Kishore, M., Staugaitis, S. M., Nguyen, H., Schlessinger, K., Levy, D. E., and Stark, G. R. Novel roles of unphosphorylated STAT3 in oncogenesis and transcriptional regulation. Cancer Res, *65:* 939-947, 2005.

61. Thomas, S. M. and Grandis, J. R. Pharmacokinetic and pharmacodynamic properties of EGFR inhibitors under clinical investigation. Cancer Treat Rev, *30:* 255-268, 2004.

62. Suzuki, A., Hanada, T., Mitsuyama, K., Yoshida, T., Kamizono, S., Hoshino, T., Kubo, M., Yamashita, A., Okabe, M., Takeda, K., Akira, S., Matsumoto, S., Toyonaga, A., Sata, M., and Yoshimura, A. CIS3/SOCS3/SSI3 plays a negative regulatory role in STAT3 activation and intestinal inflammation. J Exp Med, *193:* 471-481, 2001.

63. Chung, C. D., Liao, J., Liu, B., Rao, X., Jay, P., Berta, P., and Shuai, K. Specific inhibition of Stat3 signal transduction by PIAS3. Science, *278:* 1803-1805, 1997.

64. Lufei, C., Ma, J., Huang, G., Zhang, T., Novotny-Diermayr, V., Ong, C. T., and Cao, X. GRIM-19, a death-regulatory gene product, suppresses Stat3 activity via functional interaction. Embo J, *22:* 1325-1335, 2003.

65. Ford, A. C. and Grandis, J. R. Targeting epidermal growth factor receptor in head and neck cancer. Head Neck, *25:* 67-73, 2003.

66. James, C., Ugo, V., Casadevall, N., Constantinescu, S. N., and Vainchenker, W. A JAK2 mutation in myeloproliferative disorders: pathogenesis and therapeutic and scientific prospects. Trends Mol Med, *11:* 546-554, 2005.

67. Jain, S., Khuri, F. R., and Shin, D. M. Prevention of head and neck cancer: current status and future prospects. Curr Probl Cancer, *28:* 265-286, 2004.

68. Bowman, T., Broome, M. A., Sinibaldi, D., Wharton, W., Pledger, W. J., Sedivy, J. M., Irby, R., Yeatman, T., Courtneidge, S. A., and Jove, R. Stat3-mediated Myc expression is required for Src transformation and PDGF-induced mitogenesis. Proc Natl Acad Sci U S A, *98:* 7319-7324, 2001.

69. Starr, R. and Hilton, D. J. Negative regulation of the JAK/STAT pathway. Bioessays, *21:* 47-52, 1999.

70. Yu, H. and Jove, R. The STATs of cancer--new molecular targets come of age. Nat Rev Cancer, *4:* 97-105, 2004.

71. Yoshikawa, H., Matsubara, K., Qian, G. S., Jackson, P., Groopman, J. D., Manning, J. E., Harris, C. C., and Herman, J. G. SOCS-1, a negative regulator of the JAK/STAT pathway, is silenced by methylation in human hepatocellular carcinoma and shows growth-suppression activity. Nat Genet, *28:* 29-35, 2001.

72. Galm, O., Yoshikawa, H., Esteller, M., Osieka, R., and Herman, J. G. SOCS-1, a negative regulator of cytokine signaling, is frequently silenced by methylation in multiple myeloma. Blood, *101:* 2784-2788, 2003.

73. Komazaki, T., Nagai, H., Emi, M., Terada, Y., Yabe, A., Jin, E., Kawanami, O., Konishi, N., Moriyama, Y., Naka, T., and Kishimoto, T. Hypermethylation-associated inactivation

of the SOCS-1 gene, a JAK/STAT inhibitor, in human pancreatic cancers. Jpn J Clin Oncol, *34:* 191-194, 2004.

74. Nagai, H., Naka, T., Terada, Y., Komazaki, T., Yabe, A., Jin, E., Kawanami, O., Kishimoto, T., Konishi, N., Nakamura, M., Kobayashi, Y., and Emi, M. Hypermethylation associated with inactivation of the SOCS-1 gene, a JAK/STAT inhibitor, in human hepatoblastomas. J Hum Genet, *48:* 65-69, 2003.

75. He, B., You, L., Uematsu, K., Zang, K., Xu, Z., Lee, A. Y., Costello, J. F., McCormick, F., and Jablons, D. M. SOCS-3 is frequently silenced by hypermethylation and suppresses cell growth in human lung cancer. Proc Natl Acad Sci U S A, *100:* 14133-14138, 2003.

76. Zhang, Q., Raghunath, P. N., Xue, L., Majewski, M., Carpentieri, D. F., Odum, N., Morris, S., Skorski, T., and Wasik, M. A. Multilevel dysregulation of STAT3 activation in anaplastic lymphoma kinase-positive T/null-cell lymphoma. J Immunol, *168:* 466-474, 2002.

77. Oka, T., Ouchida, M., Koyama, M., Ogama, Y., Takada, S., Nakatani, Y., Tanaka, T., Yoshino, T., Hayashi, K., Ohara, N., Kondo, E., Takahashi, K., Tsuchiyama, J., Tanimoto, M., Shimizu, K., and Akagi, T. Gene silencing of the tyrosine phosphatase SHP1 gene by aberrant methylation in leukemias/lymphomas. Cancer Res, *62:* 6390-6394, 2002.

78. Chim, C. S., Fung, T. K., Cheung, W. C., Liang, R., and Kwong, Y. L. SOCS1 and SHP1 hypermethylation in multiple myeloma: implications for epigenetic activation of the Jak/STAT pathway. Blood, *103:* 4630-4635, 2004.

79. Endo, T. A., Masuhara, M., Yokouchi, M., Suzuki, R., Sakamoto, H., Mitsui, K., Matsumoto, A., Tanimura, S., Ohtsubo, M., Misawa, H., Miyazaki, T., Leonor, N., Taniguchi, T., Fujita, T., Kanakura, Y., Komiya, S., and Yoshimura, A. A new protein containing an SH2 domain that inhibits JAK kinases. Nature, *387:* 921-924, 1997.

80. Naka, T., Narazaki, M., Hirata, M., Matsumoto, T., Minamoto, S., Aono, A., Nishimoto, N., Kajita, T., Taga, T., Yoshizaki, K., Akira, S., and Kishimoto, T. Structure and function of a new STAT-induced STAT inhibitor. Nature, *387:* 924-929, 1997.

81. Naka, T., Fujimoto, M., and Kishimoto, T. Negative regulation of cytokine signaling: STAT-induced STAT inhibitor. Trends Biochem Sci, *24:* 394-398, 1999.

82. Flowers, L. O., Subramaniam, P. S., and Johnson, H. M. A SOCS-1 peptide mimetic inhibits both constitutive and IL-6 induced activation of STAT3 in prostate cancer cells. Oncogene, *24:* 2114-2120, 2005.

83. Larsen, L. and Ropke, C. Suppressors of cytokine signalling: SOCS. Apmis, *110:* 833-844, 2002.

84. Shuai, K. Modulation of STAT signaling by STAT-interacting proteins. Oncogene, *19:* 2638-2644, 2000.

85. David, M., Chen, H. E., Goelz, S., Larner, A. C., and Neel, B. G. Differential regulation of the alpha/beta interferon-stimulated Jak/Stat pathway by the SH2 domain-containing tyrosine phosphatase SHPTP1. Mol Cell Biol, *15:* 7050-7058, 1995.

86. Jiao, H., Berrada, K., Yang, W., Tabrizi, M., Platanias, L. C., and Yi, T. Direct association with and dephosphorylation of Jak2 kinase by the SH2-domain-containing protein tyrosine phosphatase SHP-1. Mol Cell Biol, *16:* 6985-6992, 1996.

87. Levy, D. E. and Darnell, J. E., Jr. Stats: transcriptional control and biological impact. Nat Rev Mol Cell Biol, *3:* 651-662, 2002.

88. Collum, R. G., Brutsaert, S., Lee, G., and Schindler, C. A Stat3-interacting protein (StIP1) regulates cytokine signal transduction. Proc Natl Acad Sci U S A, *97:* 10120-10125, 2000.

89. Grandis, J. R., Drenning, S. D., Zeng, Q., Watkins, S. C., Melhem, M. F., Endo, S., Johnson, D. E., Huang, L., He, Y., and Kim, J. D. Constitutive activation of Stat3 signaling abrogates apoptosis in squamous cell carcinogenesis in vivo. Proc Natl Acad Sci U S A, *97:* 4227-4232, 2000.

90. Kijima, T., Niwa, H., Steinman, R. A., Drenning, S. D., Gooding, W. E., Wentzel, A. L., Xi, S., and Grandis, J. R. STAT3 activation abrogates growth factor dependence and contributes to head and neck squamous cell carcinoma tumor growth in vivo. Cell Growth Differ, *13:* 355-362, 2002.

91. Sriuranpong, V., Park, J. I., Amornphimoltham, P., Patel, V., Nelkin, B. D., and Gutkind, J. S. Epidermal growth factor receptor-independent constitutive activation of STAT3 in head and neck squamous cell carcinoma is mediated by the autocrine/paracrine stimulation of the interleukin 6/gp130 cytokine system. Cancer Res, *63:* 2948-2956, 2003.

92. Rubin Grandis, J., Zeng, Q., and Drenning, S. D. Epidermal growth factor receptor--mediated stat3 signaling blocks apoptosis in head and neck cancer. Laryngoscope, *110:* 868-874, 2000.

93. Xi, S., Zhang, Q., Dyer, K. F., Lerner, E. C., Smithgall, T. E., Gooding, W. E., Kamens, J., and Grandis, J. R. Src kinases mediate STAT growth pathways in squamous cell carcinoma of the head and neck. J Biol Chem, *278:* 31574-31583, 2003.

94. Nagpal, J. K., Mishra, R., and Das, B. R. Activation of Stat-3 as one of the early events in tobacco chewing-mediated oral carcinogenesis. Cancer, *94:* 2393-2400, 2002.

95. Arany, I., Chen, S. H., Megyesi, J. K., Adler-Storthz, K., Chen, Z., Rajaraman, S., Ember, I. A., Tyring, S. K., and Brysk, M. M. Differentiation-dependent expression of signal transducers and activators of transcription (STATs) might modify responses to growth factors in the cancers of the head and neck. Cancer Lett, *199:* 83-89, 2003.

96. Blaskovich, M. A., Sun, J., Cantor, A., Turkson, J., Jove, R., and Sebti, S. M. Discovery of JSI-124 (cucurbitacin I), a selective Janus kinase/signal transducer and activator of transcription 3 signaling pathway inhibitor with potent antitumor activity against human and murine cancer cells in mice. Cancer Res, *63:* 1270-1279, 2003.

97. Berg, T., Cohen, S. B., Desharnais, J., Sonderegger, C., Maslyar, D. J., Goldberg, J., Boger, D. L., and Vogt, P. K. Small-molecule antagonists of Myc/Max dimerization inhibit Myc-induced transformation of chicken embryo fibroblasts. Proc Natl Acad Sci U S A, *99:* 3830-3835, 2002.

98. Turkson, J., Kim, J. S., Zhang, S., Yuan, J., Huang, M., Glenn, M., Haura, E., Sebti, S., Hamilton, A. D., and Jove, R. Novel peptidomimetic inhibitors of signal transducer and activator of transcription 3 dimerization and biological activity. Mol Cancer Ther, *3:* 261-269, 2004.

99. Turkson, J., Ryan, D., Kim, J. S., Zhang, Y., Chen, Z., Haura, E., Laudano, A., Sebti, S., Hamilton, A. D., and Jove, R. Phosphotyrosyl peptides block Stat3-mediated DNA

binding activity, gene regulation, and cell transformation. J Biol Chem, *276:* 45443-45455, 2001.

100. Ren, Z., Cabell, L. A., Schaefer, T. S., and McMurray, J. S. Identification of a high-affinity phosphopeptide inhibitor of Stat3. Bioorg Med Chem Lett, *13:* 633-636, 2003.

101. Buerger, C. and Groner, B. Bifunctional recombinant proteins in cancer therapy: cell penetrating peptide aptamers as inhibitors of growth factor signaling. J Cancer Res Clin Oncol, *129:* 669-675, 2003.

102. Buerger, C., Nagel-Wolfrum, K., Kunz, C., Wittig, I., Butz, K., Hoppe-Seyler, F., and Groner, B. Sequence-specific peptide aptamers, interacting with the intracellular domain of the epidermal growth factor receptor, interfere with Stat3 activation and inhibit the growth of tumor cells. J Biol Chem, *278:* 37610-37621, 2003.

103. Nagel-Wolfrum, K., Buerger, C., Wittig, I., Butz, K., Hoppe-Seyler, F., and Groner, B. The interaction of specific peptide aptamers with the DNA binding domain and the dimerization domain of the transcription factor Stat3 inhibits transactivation and induces apoptosis in tumor cells. Mol Cancer Res, *2:* 170-182, 2004.

104. Bates, P. J., Kahlon, J. B., Thomas, S. D., Trent, J. O., and Miller, D. M. Antiproliferative activity of G-rich oligonucleotides correlates with protein binding. J Biol Chem, *274:* 26369-26377, 1999.

105. Jing, N., Li, Y., Xu, X., Sha, W., Li, P., Feng, L., and Tweardy, D. J. Targeting Stat3 with G-quartet oligodeoxynucleotides in human cancer cells. DNA Cell Biol, *22:* 685-696, 2003.

106. Jing, N., Sha, W., Li, Y., Xiong, W., and Tweardy, D. J. Rational drug design of G-quartet DNA as anti-cancer agents. Curr Pharm Des, *11:* 2841-2854, 2005.

107. Jing, N. and Tweardy, D. J. Targeting Stat3 in cancer therapy. Anticancer Drugs, *16:* 601-607, 2005.

108. Jing, N., Li, Y., Xiong, W., Sha, W., Jing, L., and Tweardy, D. J. G-quartet oligonucleotides: a new class of signal transducer and activator of transcription 3 inhibitors that suppresses growth of prostate and breast tumors through induction of apoptosis. Cancer Res, *64:* 6603-6609, 2004.

109. Coppelli, F. M. and Grandis, J. R. Oligonucleotides as anticancer agents: from the benchside to the clinic and beyond. Curr Pharm Des, *11:* 2825-2840, 2005.

110. Gao, L. F., Xu, D. Q., Wen, L. J., Zhang, X. Y., Shao, Y. T., and Zhao, X. J. Inhibition of STAT3 expression by siRNA suppresses growth and induces apoptosis in laryngeal cancer cells. Acta Pharmacol Sin, *26:* 377-383, 2005.

111. Konnikova, L., Kotecki, M., Kruger, M. M., and Cochran, B. H. Knockdown of STAT3 expression by RNAi induces apoptosis in astrocytoma cells. BMC Cancer, *3:* 23, 2003.

112. Kawamura, I., Morishita, R., Tsujimoto, S., Manda, T., Tomoi, M., Tomita, N., Goto, T., Ogihara, T., and Kaneda, Y. Intravenous injection of oligodeoxynucleotides to the NF-kappaB binding site inhibits hepatic metastasis of M5076 reticulosarcoma in mice. Gene Ther, *8:* 905-912, 2001.

113. Leong, P. L., Andrews, G. A., Johnson, D. E., Dyer, K. F., Xi, S., Mai, J. C., Robbins, P. D., Gadiparthi, S., Burke, N. A., Watkins, S. F., and Grandis, J. R. Targeted inhibition of Stat3 with a decoy oligonucleotide abrogates head and neck cancer cell growth. Proc Natl Acad Sci U S A, *100:* 4138-4143, 2003.

114. Xi, S., Gooding, W. E., and Grandis, J. R. In vivo antitumor efficacy of STAT3 blockade using a transcription factor decoy approach: implications for cancer therapy. Oncogene, *24:* 970-979, 2005.

115. Chan, K. S., Sano, S., Kiguchi, K., Anders, J., Komazawa, N., Takeda, J., and DiGiovanni, J. Disruption of Stat3 reveals a critical role in both the initiation and the promotion stages of epithelial carcinogenesis. J Clin Invest, *114:* 720-728, 2004.

116. Park, Y. G., Nesterova, M., Agrawal, S., and Cho-Chung, Y. S. Dual blockade of cyclic AMP response element- (CRE) and AP-1-directed transcription by CRE-transcription factor decoy oligonucleotide. gene-specific inhibition of tumor growth. J Biol Chem, *274:* 1573-1580, 1999.

117. Barton, B. E., Murphy, T. F., Shu, P., Huang, H. F., Meyenhofer, M., and Barton, A. Novel single-stranded oligonucleotides that inhibit signal transducer and activator of transcription 3 induce apoptosis in vitro and in vivo in prostate cancer cell lines. Mol Cancer Ther, *3:* 1183-1191, 2004.

118. Wung, B. S., Hsu, M. C., Wu, C. C., and Hsieh, C. W. Resveratrol suppresses IL-6-induced ICAM-1 gene expression in endothelial cells: effects on the inhibition of STAT3 phosphorylation. Life Sci, *78:* 389-397, 2005.

119. Kim, N. H., Lee, M. Y., Park, S. J., Choi, J. S., Oh, M. K., and Kim, I. S. Auranofin blocks interleukin-6 signalling by inhibiting phosphorylation of JAK1 and STAT3. Immunology, *122:* 607-614, 2007.

120. Chen, S. C., Chang, Y. L., Wang, D. L., and Cheng, J. J. Herbal remedy magnolol suppresses IL-6-induced STAT3 activation and gene expression in endothelial cells. Br J Pharmacol, *148:* 226-232, 2006.

121. Bharti, A. C., Shishodia, S., Reuben, J. M., Weber, D., Alexanian, R., Raj-Vadhan, S., Estrov, Z., Talpaz, M., and Aggarwal, B. B. Nuclear factor-kappaB and STAT3 are constitutively active in CD138+ cells derived from multiple myeloma patients, and suppression of these transcription factors leads to apoptosis. Blood, *103:* 3175-3184, 2004.

122. Kim, H. Y., Park, E. J., Joe, E. H., and Jou, I. Curcumin suppresses Janus kinase-STAT inflammatory signaling through activation of Src homology 2 domain-containing tyrosine phosphatase 2 in brain microglia. J Immunol, *171:* 6072-6079, 2003.

123. Chakravarti, N., Myers, J. N., and Aggarwal, B. B. Targeting constitutive and interleukin-6-inducible signal transducers and activators of transcription 3 pathway in head and neck squamous cell carcinoma cells by curcumin (diferuloylmethane). Int J Cancer, *119:* 1268-1275, 2006.

124. Masuda, M., Suzui, M., and Weinstein, I. B. Effects of epigallocatechin-3-gallate on growth, epidermal growth factor receptor signaling pathways, gene expression, and chemosensitivity in human head and neck squamous cell carcinoma cell lines. Clin Cancer Res, *7:* 4220-4229, 2001.

125. Nam, S., Buettner, R., Turkson, J., Kim, D., Cheng, J. Q., Muehlbeyer, S., Hippe, F., Vatter, S., Merz, K. H., Eisenbrand, G., and Jove, R. Indirubin derivatives inhibit Stat3 signaling and induce apoptosis in human cancer cells. Proc Natl Acad Sci U S A, *102:* 5998-6003, 2005.

126. Song, J. I., Lango, M. N., Hwang, J. D., Drenning, S. D., Zeng, Q., Lamph, W. W., and Grandis, J. R. Abrogation of transforming growth factor-alpha/epidermal growth factor

receptor autocrine signaling by an RXR-selective retinoid (LGD1069, Targretin) in head and neck cancer cell lines. Cancer Res, *61:* 5919-5925, 2001.

127. Lango, M., Wentzel, A. L., Song, J. I., Xi, S., Johnson, D. E., Lamph, W. W., Miller, L., and Grandis, J. R. Responsiveness to the retinoic acid receptor-selective retinoid LGD1550 correlates with abrogation of transforming growth factor alpha/epidermal growth factor receptor autocrine signaling in head and neck squamous carcinoma cells. Clin Cancer Res, *9:* 4205-4213, 2003.

128. Nikitakis, N. G., Siavash, H., Hebert, C., Reynolds, M. A., Hamburger, A. W., and Sauk, J. J. 15-PGJ2, but not thiazolidinediones, inhibits cell growth, induces apoptosis, and causes downregulation of Stat3 in human oral SCCa cells. Br J Cancer, *87:* 1396-1403, 2002.

129. Sinibaldi, D., Wharton, W., Turkson, J., Bowman, T., Pledger, W. J., and Jove, R. Induction of p21WAF1/CIP1 and cyclin D1 expression by the Src oncoprotein in mouse fibroblasts: role of activated STAT3 signaling. Oncogene, *19:* 5419-5427, 2000.

130. Karin, M. Nuclear factor-kappaB in cancer development and progression. Nature, *441:* 431-436, 2006.

131. Dolcet, X., Llobet, D., Pallares, J., and Matias-Guiu, X. NF-kB in development and progression of human cancer. Virchows Arch, *446:* 475-482, 2005.

132. Pikarsky, E. and Ben-Neriah, Y. NF-kappaB inhibition: a double-edged sword in cancer? Eur J Cancer, *42:* 779-784, 2006.

133. Ondrey, F. G., Dong, G., Sunwoo, J., Chen, Z., Wolf, J. S., Crowl-Bancroft, C. V., Mukaida, N., and Van Waes, C. Constitutive activation of transcription factors NF-(kappa)B, AP-1, and NF-IL6 in human head and neck squamous cell carcinoma cell lines

that express pro-inflammatory and pro-angiogenic cytokines. Mol Carcinog, *26:* 119-129, 1999.

134. Dong, G., Chen, Z., Kato, T., and Van Waes, C. The host environment promotes the constitutive activation of nuclear factor-kappaB and proinflammatory cytokine expression during metastatic tumor progression of murine squamous cell carcinoma. Cancer Res, *59:* 3495-3504, 1999.

135. Loercher, A., Lee, T. L., Ricker, J. L., Howard, A., Geoghegen, J., Chen, Z., Sunwoo, J. B., Sitcheran, R., Chuang, E. Y., Mitchell, J. B., Baldwin, A. S., Jr., and Van Waes, C. Nuclear factor-kappaB is an important modulator of the altered gene expression profile and malignant phenotype in squamous cell carcinoma. Cancer Res, *64:* 6511-6523, 2004.

136. Chang, A. A. and Van Waes, C. Nuclear factor-KappaB as a common target and activator of oncogenes in head and neck squamous cell carcinoma. Adv Otorhinolaryngol, *62:* 92-102, 2005.

137. Yu, M., Yeh, J., and Van Waes, C. Protein kinase casein kinase 2 mediates inhibitor-kappaB kinase and aberrant nuclear factor-kappaB activation by serum factor(s) in head and neck squamous carcinoma cells. Cancer Res, *66:* 6722-6731, 2006.

138. Leeman, R. J., Lui, V. W., and Grandis, J. R. STAT3 as a therapeutic target in head and neck cancer. Expert Opin Biol Ther, *6:* 231-241, 2006.

139. Van Waes, C., Chang, A. A., Lebowitz, P. F., Druzgal, C. H., Chen, Z., Elsayed, Y. A., Sunwoo, J. B., Rudy, S. F., Morris, J. C., Mitchell, J. B., Camphausen, K., Gius, D., Adams, J., Sausville, E. A., and Conley, B. A. Inhibition of nuclear factor-kappaB and target genes during combined therapy with proteosome inhibitor bortezomib and

reirradiation in patients with recurrent head-and-neck squamous cell carcinoma. Int J Radiat Oncol Biol Phys, *63:* 1400-1412, 2005.

140. Quon, H., Liu, F. F., and Cummings, B. J. Potential molecular prognostic markers in head and neck squamous cell carcinomas. Head Neck, *23:* 147-159, 2001.

141. Squarize, C. H., Castilho, R. M., Sriuranpong, V., Pinto, D. S., Jr., and Gutkind, J. S. Molecular cross-talk between the NFkappaB and STAT3 signaling pathways in head and neck squamous cell carcinoma. Neoplasia, *8:* 733-746, 2006.

142. Yoshida, Y., Kumar, A., Koyama, Y., Peng, H., Arman, A., Boch, J. A., and Auron, P. E. Interleukin 1 activates STAT3/nuclear factor-kappaB cross-talk via a unique TRAF6- and p65-dependent mechanism. J Biol Chem, *279:* 1768-1776, 2004.

143. Hoentjen, F., Sartor, R. B., Ozaki, M., and Jobin, C. STAT3 regulates NF-kappaB recruitment to the IL-12p40 promoter in dendritic cells. Blood, *105:* 689-696, 2005.

144. Yu, Z., Zhang, W., and Kone, B. C. Signal transducers and activators of transcription 3 (STAT3) inhibits transcription of the inducible nitric oxide synthase gene by interacting with nuclear factor kappaB. Biochem J, *367:* 97-105, 2002.

145. Yu, Z. and Kone, B. C. The STAT3 DNA-binding domain mediates interaction with NF-kappaB p65 and iuducible nitric oxide synthase transrepression in mesangial cells. J Am Soc Nephrol, *15:* 585-591, 2004.

146. Hagihara, K., Nishikawa, T., Sugamata, Y., Song, J., Isobe, T., Taga, T., and Yoshizaki, K. Essential role of STAT3 in cytokine-driven NF-kappaB-mediated serum amyloid A gene expression. Genes Cells, *10:* 1051-1063, 2005.

147. Pavia, M., Pileggi, C., Nobile, C. G., and Angelillo, I. F. Association between fruit and vegetable consumption and oral cancer: a meta-analysis of observational studies. Am J Clin Nutr, *83:* 1126-1134, 2006.

148. Helzlsouer, K. J., Block, G., Blumberg, J., Diplock, A. T., Levine, M., Marnett, L. J., Schulplein, R. J., Spence, J. T., and Simic, M. G. Summary of the round table discussion on strategies for cancer prevention: diet, food, additives, supplements, and drugs. Cancer Res, *54:* 2044s-2051s, 1994.

149. Talalay, P. and Fahey, J. W. Phytochemicals from cruciferous plants protect against cancer by modulating carcinogen metabolism. J Nutr, *131:* 3027S-3033S, 2001.

150. Dorai, T. and Aggarwal, B. B. Role of chemopreventive agents in cancer therapy. Cancer Lett, *215:* 129-140, 2004.

151. Aggarwal, B. B. and Shishodia, S. Molecular targets of dietary agents for prevention and therapy of cancer. Biochem Pharmacol, *71:* 1397-1421, 2006.

152. Matsumura, I., Kitamura, T., Wakao, H., Tanaka, H., Hashimoto, K., Albanese, C., Downward, J., Pestell, R. G., and Kanakura, Y. Transcriptional regulation of the cyclin D1 promoter by STAT5: its involvement in cytokine-dependent growth of hematopoietic cells. Embo J, *18:* 1367-1377, 1999.

153. Amin, H. M., McDonnell, T. J., Ma, Y., Lin, Q., Fujio, Y., Kunisada, K., Leventaki, V., Das, P., Rassidakis, G. Z., Cutler, C., Medeiros, L. J., and Lai, R. Selective inhibition of STAT3 induces apoptosis and G(1) cell cycle arrest in ALK-positive anaplastic large cell lymphoma. Oncogene, *23:* 5426-5434, 2004.

154. Kiuchi, N., Nakajima, K., Ichiba, M., Fukada, T., Narimatsu, M., Mizuno, K., Hibi, M., and Hirano, T. STAT3 is required for the gp130-mediated full activation of the c-myc gene. J Exp Med, *189:* 63-73, 1999.

155. Lord, J. D., McIntosh, B. C., Greenberg, P. D., and Nelson, B. H. The IL-2 receptor promotes lymphocyte proliferation and induction of the c-myc, bcl-2, and bcl-x genes through the trans-activation domain of Stat5. J Immunol, *164:* 2533-2541, 2000.

156. Narimatsu, M., Nakajima, K., Ichiba, M., and Hirano, T. Association of Stat3-dependent transcriptional activation of p19INK4D with IL-6-induced growth arrest. Biochem Biophys Res Commun, *238:* 764-768, 1997.

157. Bellido, T., O'Brien, C. A., Roberson, P. K., and Manolagas, S. C. Transcriptional activation of the p21(WAF1,CIP1,SDI1) gene by interleukin-6 type cytokines. A prerequisite for their pro-differentiating and anti-apoptotic effects on human osteoblastic cells. J Biol Chem, *273:* 21137-21144, 1998.

158. Takahashi, S., Harigae, H., Kaku, M., Sasaki, T., and Licht, J. D. Flt3 mutation activates p21WAF1/CIP1 gene expression through the action of STAT5. Biochem Biophys Res Commun, *316:* 85-92, 2004.

159. Shirogane, T., Fukada, T., Muller, J. M., Shima, D. T., Hibi, M., and Hirano, T. Synergistic roles for Pim-1 and c-Myc in STAT3-mediated cell cycle progression and antiapoptosis. Immunity, *11:* 709-719, 1999.

160. Mui, A. L., Wakao, H., Kinoshita, T., Kitamura, T., and Miyajima, A. Suppression of interleukin-3-induced gene expression by a C-terminal truncated Stat5: role of Stat5 in proliferation. Embo J, *15:* 2425-2433, 1996.

161. de Koning, J. P., Soede-Bobok, A. A., Ward, A. C., Schelen, A. M., Antonissen, C., van Leeuwen, D., Lowenberg, B., and Touw, I. P. STAT3-mediated differentiation and survival and of myeloid cells in response to granulocyte colony-stimulating factor: role for the cyclin-dependent kinase inhibitor p27(Kip1). Oncogene, *19:* 3290-3298, 2000.

162. Klausen, P., Pedersen, L., Jurlander, J., and Baumann, H. Oncostatin M and interleukin 6 inhibit cell cycle progression by prevention of p27kip1 degradation in HepG2 cells. Oncogene, *19:* 3675-3683, 2000.

163. Aoki, Y., Feldman, G. M., and Tosato, G. Inhibition of STAT3 signaling induces apoptosis and decreases survivin expression in primary effusion lymphoma. Blood, *101:* 1535-1542, 2003.

164. Epling-Burnette, P. K., Liu, J. H., Catlett-Falcone, R., Turkson, J., Oshiro, M., Kothapalli, R., Li, Y., Wang, J. M., Yang-Yen, H. F., Karras, J., Jove, R., and Loughran, T. P., Jr. Inhibition of STAT3 signaling leads to apoptosis of leukemic large granular lymphocytes and decreased Mcl-1 expression. J Clin Invest, *107:* 351-362, 2001.

165. Oritani, K., Tomiyama, Y., Kincade, P. W., Aoyama, K., Yokota, T., Matsumura, I., Kanakura, Y., Nakajima, K., Hirano, T., and Matsuzawa, Y. Both Stat3-activation and Stat3-independent BCL2 downregulation are important for interleukin-6-induced apoptosis of 1A9-M cells. Blood, *93:* 1346-1354, 1999.

166. Moucadel, V. and Constantinescu, S. N. Differential STAT5 signaling by ligand-dependent and constitutively active cytokine receptors. J Biol Chem, *280:* 13364-13373, 2005.

167. Niu, G., Wright, K. L., Huang, M., Song, L., Haura, E., Turkson, J., Zhang, S., Wang, T., Sinibaldi, D., Coppola, D., Heller, R., Ellis, L. M., Karras, J., Bromberg, J., Pardoll, D.,

Jove, R., and Yu, H. Constitutive Stat3 activity up-regulates VEGF expression and tumor angiogenesis. Oncogene, *21:* 2000-2008, 2002.

168. Niu, G., Briggs, J., Deng, J., Ma, Y., Lee, H., Kortylewski, M., Kujawski, M., Kay, H., Cress, W. D., Jove, R., and Yu, H. Signal transducer and activator of transcription 3 is required for hypoxia-inducible factor-1alpha RNA expression in both tumor cells and tumor-associated myeloid cells. Mol Cancer Res, *6:* 1099-1105, 2008.

169. Xie, T. X., Wei, D., Liu, M., Gao, A. C., Ali-Osman, F., Sawaya, R., and Huang, S. Stat3 activation regulates the expression of matrix metalloproteinase-2 and tumor invasion and metastasis. Oncogene, *23:* 3550-3560, 2004.

170. Dechow, T. N., Pedranzini, L., Leitch, A., Leslie, K., Gerald, W. L., Linkov, I., and Bromberg, J. F. Requirement of matrix metalloproteinase-9 for the transformation of human mammary epithelial cells by Stat3-C. Proc Natl Acad Sci U S A, *101:* 10602-10607, 2004.

171. Brender, C., Nielsen, M., Kaltoft, K., Mikkelsen, G., Zhang, Q., Wasik, M., Billestrup, N., and Odum, N. STAT3-mediated constitutive expression of SOCS-3 in cutaneous T-cell lymphoma. Blood, *97:* 1056-1062, 2001.

172. Schick, N., Oakeley, E. J., Hynes, N. E., and Badache, A. TEL/ETV6 is a signal transducer and activator of transcription 3 (Stat3)-induced repressor of Stat3 activity. J Biol Chem, *279:* 38787-38796, 2004.

173. Zhang, X. and Darnell, J. E., Jr. Functional importance of Stat3 tetramerization in activation of the alpha 2-macroglobulin gene. J Biol Chem, *276:* 33576-33581, 2001.

174. Wang, Y., Ripperger, J., Fey, G. H., Samols, D., Kordula, T., Wetzler, M., Van Etten, R. A., and Baumann, H. Modulation of hepatic acute phase gene expression by epidermal

growth factor and Src protein tyrosine kinases in murine and human hepatic cells. Hepatology, *30:* 682-697, 1999.

175. Kojima, H., Nakajima, K., and Hirano, T. IL-6-inducible complexes on an IL-6 response element of the junB promoter contain Stat3 and 36 kDa CRE-like site binding protein(s). Oncogene, *12:* 547-554, 1996.

176. Lai, R., Rassidakis, G. Z., Medeiros, L. J., Ramdas, L., Goy, A. H., Cutler, C., Fujio, Y., Kunisada, K., Amin, H. M., and Gilles, F. Signal transducer and activator of transcription-3 activation contributes to high tissue inhibitor of metalloproteinase-1 expression in anaplastic lymphoma kinase-positive anaplastic large cell lymphoma. Am J Pathol, *164:* 2251-2258, 2004.

177. Yun, T. K. Panax ginseng--a non-organ-specific cancer preventive? Lancet Oncol, *2:* 49-55, 2001.

178. Helms, S. Cancer prevention and therapeutics: Panax ginseng. Altern Med Rev, *9:* 259-274, 2004.

179. Hecht, S. S. Inhibition of carcinogenesis by isothiocyanates. Drug Metab Rev, *32:* 395-411, 2000.

180. Fahey, J. W., Zalcmann, A. T., and Talalay, P. The chemical diversity and distribution of glucosinolates and isothiocyanates among plants. Phytochemistry, *56:* 5-51, 2001.

181. Conaway, C. C., Yang, Y. M., and Chung, F. L. Isothiocyanates as cancer chemopreventive agents: their biological activities and metabolism in rodents and humans. Curr Drug Metab, *3:* 233-255, 2002.

182. Lui, V. W., Wentzel, A. L., Xiao, D., Lew, K. L., Singh, S. V., and Grandis, J. R. Requirement of a carbon spacer in benzyl isothiocyanate-mediated cytotoxicity and

MAPK activation in head and neck squamous cell carcinoma. Carcinogenesis, *24:* 1705-1712, 2003.

183. Urizar, N. L. and Moore, D. D. GUGULIPID: a natural cholesterol-lowering agent. Annu Rev Nutr, *23:* 303-313, 2003.

184. Morse, M. A., Eklind, K. I., Hecht, S. S., Jordan, K. G., Choi, C. I., Desai, D. H., Amin, S. G., and Chung, F. L. Structure-activity relationships for inhibition of 4-(methylnitrosamino)-1-(3-pyridyl)-1-butanone lung tumorigenesis by arylalkyl isothiocyanates in A/J mice. Cancer Res, *51:* 1846-1850, 1991.

185. Agarwal, R. C., Singh, S. P., Saran, R. K., Das, S. K., Sinha, N., Asthana, O. P., Gupta, P. P., Nityanand, S., Dhawan, B. N., and Agarwal, S. S. Clinical trial of gugulipid--a new hypolipidemic agent of plant origin in primary hyperlipidemia. Indian J Med Res, *84:* 626-634, 1986.

186. Meselhy, M. R. Inhibition of LPS-induced NO production by the oleogum resin of Commiphora wightii and its constituents. Phytochemistry, *62:* 213-218, 2003.

187. Shishodia, S. and Aggarwal, B. B. Guggulsterone inhibits NF-kappaB and IkappaBalpha kinase activation, suppresses expression of anti-apoptotic gene products, and enhances apoptosis. J Biol Chem, *279:* 47148-47158, 2004.

188. Singh, S. V., Zeng, Y., Xiao, D., Vogel, V. G., Nelson, J. B., Dhir, R., and Tripathi, Y. B. Caspase-dependent apoptosis induction by guggulsterone, a constituent of Ayurvedic medicinal plant Commiphora mukul, in PC-3 human prostate cancer cells is mediated by Bax and Bak. Mol Cancer Ther, *4:* 1747-1754, 2005.

189. Samudio, I., Konopleva, M., Safe, S., McQueen, T., and Andreeff, M. Guggulsterones induce apoptosis and differentiation in acute myeloid leukemia: identification of isomer-

specific antileukemic activities of the pregnadienedione structure. Mol Cancer Ther, *4:* 1982-1992, 2005.

190. Shishodia, S., Sethi, G., Ahn, K. S., and Aggarwal, B. B. Guggulsterone inhibits tumor cell proliferation, induces S-phase arrest, and promotes apoptosis through activation of c-Jun N-terminal kinase, suppression of Akt pathway, and downregulation of antiapoptotic gene products. Biochem Pharmacol, *74:* 118-130, 2007.

191. Singh, S. V., Choi, S., Zeng, Y., Hahm, E. R., and Xiao, D. Guggulsterone-induced apoptosis in human prostate cancer cells is caused by reactive oxygen intermediate dependent activation of c-Jun NH2-terminal kinase. Cancer Res, *67:* 7439-7449, 2007.

192. Xiao, D. and Singh, S. V. z-Guggulsterone, a constituent of Ayurvedic medicinal plant Commiphora mukul, inhibits angiogenesis in vitro and in vivo. Mol Cancer Ther, *7:* 171-180, 2008.

193. Sarfaraz, S., Siddiqui, I. A., Syed, D. N., Afaq, F., and Mukhtar, H. Guggulsterone modulates MAPK and NF-kappaB pathways and inhibits skin tumorigenesis in SENCAR mice. Carcinogenesis, *29:* 2011-2018, 2008.

194. Ahn, K. S., Sethi, G., Sung, B., Goel, A., Ralhan, R., and Aggarwal, B. B. Guggulsterone, a farnesoid X receptor antagonist, inhibits constitutive and inducible STAT3 activation through induction of a protein tyrosine phosphatase SHP-1. Cancer Res, *68:* 4406-4415, 2008.

195. Lin, C. J., Grandis, J. R., Carey, T. E., Gollin, S. M., Whiteside, T. L., Koch, W. M., Ferris, R. L., and Lai, S. Y. Head and neck squamous cell carcinoma cell lines: established models and rationale for selection. Head Neck, *29:* 163-188, 2007.

196. Heo, D. S., Snyderman, C., Gollin, S. M., Pan, S., Walker, E., Deka, R., Barnes, E. L., Johnson, J. T., Herberman, R. B., and Whiteside, T. L. Biology, cytogenetics, and sensitivity to immunological effector cells of new head and neck squamous cell carcinoma lines. Cancer Res, *49:* 5167-5175, 1989.

197. Sacks, P. G., Parnes, S. M., Gallick, G. E., Mansouri, Z., Lichtner, R., Satya-Prakash, K. L., Pathak, S., and Parsons, D. F. Establishment and characterization of two new squamous cell carcinoma cell lines derived from tumors of the head and neck. Cancer Res, *48:* 2858-2866, 1988.

198. Riser, B. L., Mitra, R., Perry, D., Dixit, V., and Varani, J. Monocyte killing of human squamous epithelial cells: role for thrombospondin. Cancer Res, *49:* 6123-6129, 1989.

199. Koppikar, P., Choi, S. H., Egloff, A. M., Cai, Q., Suzuki, S., Freilino, M., Nozawa, H., Thomas, S. M., Gooding, W. E., Siegfried, J. M., and Grandis, J. R. Combined inhibition of c-Src and epidermal growth factor receptor abrogates growth and invasion of head and neck squamous cell carcinoma. Clin Cancer Res, *14:* 4284-4291, 2008.

200. Kirken, R. A., Malabarba, M. G., Xu, J., Liu, X., Farrar, W. L., Hennighausen, L., Larner, A. C., Grimley, P. M., and Rui, H. Prolactin stimulates serine/tyrosine phosphorylation and formation of heterocomplexes of multiple Stat5 isoforms in Nb2 lymphocytes. J Biol Chem, *272:* 14098-14103, 1997.

201. Verma, N., Singh, SK, Gupta, RC Pharmacokinetics of Guggulsterone after Intravenous and Oral Administration in Rats. Pharmacy and Pharmacology Communications, *5:* 349-354, 1999.

202. Joyce, D., Albanese, C., Steer, J., Fu, M., Bouzahzah, B., and Pestell, R. G. NF-kappaB and cell-cycle regulation: the cyclin connection. Cytokine Growth Factor Rev, *12:* 73-90, 2001.

203. Nabekura, T., Yamaki, T., Ueno, K., and Kitagawa, S. Effects of plant sterols on human multidrug transporters ABCB1 and ABCC1. Biochem Biophys Res Commun, *369:* 363-368, 2008.

204. Muller, S., Su, L., Tighiouart, M., Saba, N., Zhang, H., Shin, D. M., and Chen, Z. G. Distinctive E-cadherin and epidermal growth factor receptor expression in metastatic and nonmetastatic head and neck squamous cell carcinoma: predictive and prognostic correlation. Cancer, *113:* 97-107, 2008.

205. Silva, P., Homer, J. J., Slevin, N. J., Musgrove, B. T., Sloan, P., Price, P., and West, C. M. Clinical and biological factors affecting response to radiotherapy in patients with head and neck cancer: a review. Clin Otolaryngol, *32:* 337-345, 2007.

206. Chi, J. T., Wang, Z., Nuyten, D. S., Rodriguez, E. H., Schaner, M. E., Salim, A., Wang, Y., Kristensen, G. B., Helland, A., Borresen-Dale, A. L., Giaccia, A., Longaker, M. T., Hastie, T., Yang, G. P., van de Vijver, M. J., and Brown, P. O. Gene expression programs in response to hypoxia: cell type specificity and prognostic significance in human cancers. PLoS Med, *3:* e47, 2006.

207. Cohen, N. A., Lai, S. Y., Ziober, A. F., and Ziober, B. L. Dysregulation of hypoxia inducible factor-1alpha in head and neck squamous cell carcinoma cell lines correlates with invasive potential. Laryngoscope, *114:* 418-423, 2004.

208. Aebersold, D. M., Burri, P., Beer, K. T., Laissue, J., Djonov, V., Greiner, R. H., and Semenza, G. L. Expression of hypoxia-inducible factor-1alpha: a novel predictive and

prognostic parameter in the radiotherapy of oropharyngeal cancer. Cancer Res, *61:* 2911-2916, 2001.

209. Zhong, H., De Marzo, A. M., Laughner, E., Lim, M., Hilton, D. A., Zagzag, D., Buechler, P., Isaacs, W. B., Semenza, G. L., and Simons, J. W. Overexpression of hypoxia-inducible factor 1alpha in common human cancers and their metastases. Cancer Res, *59:* 5830-5835, 1999.

210. Jung, Y. J., Isaacs, J. S., Lee, S., Trepel, J., and Neckers, L. IL-1beta-mediated up-regulation of HIF-1alpha via an NFkappaB/COX-2 pathway identifies HIF-1 as a critical link between inflammation and oncogenesis. Faseb J, *17:* 2115-2117, 2003.

211. Rius, J., Guma, M., Schachtrup, C., Akassoglou, K., Zinkernagel, A. S., Nizet, V., Johnson, R. S., Haddad, G. G., and Karin, M. NF-kappaB links innate immunity to the hypoxic response through transcriptional regulation of HIF-1alpha. Nature, *453:* 807-811, 2008.

212. Shemirani, B. and Crowe, D. L. Hypoxic induction of HIF-1alpha and VEGF expression in head and neck squamous cell carcinoma lines is mediated by stress activated protein kinases. Oral Oncol, *38:* 251-257, 2002.

213. Darnowski, J. W., Goulette, F. A., Guan, Y. J., Chatterjee, D., Yang, Z. F., Cousens, L. P., and Chin, Y. E. Stat3 cleavage by caspases: impact on full-length Stat3 expression, fragment formation, and transcriptional activity. J Biol Chem, *281:* 17707-17717, 2006.

214. Oda, A., Wakao, H., and Fujita, H. Calpain is a signal transducer and activator of transcription (STAT) 3 and STAT5 protease. Blood, *99:* 1850-1852, 2002.

215. Lornejad-Schafer, M., Albrecht, U., Poppek, D., Gehrmann, T., Grune, T., Bode, J. G., Haussinger, D., and Schliess, F. Osmotic regulation of STAT3 stability in H4IIE rat hepatoma cells. FEBS Lett, *579:* 5791-5797, 2005.

216. Malek, R. L. and Halvorsen, S. W. Ciliary neurotrophic factor and phorbol ester each decrease selected STAT3 pools in neuroblastoma cells by proteasome-dependent mechanisms. Cytokine, *11:* 192-199, 1999.

217. Perry, E., Tsruya, R., Levitsky, P., Pomp, O., Taller, M., Weisberg, S., Parris, W., Kulkarni, S., Malovani, H., Pawson, T., Shpungin, S., and Nir, U. TMF/ARA160 is a BC-box-containing protein that mediates the degradation of Stat3. Oncogene, *23:* 8908-8919, 2004.

218. Kato, T., Sakamoto, E., Kutsuna, H., Kimura-Eto, A., Hato, F., and Kitagawa, S. Proteolytic conversion of STAT3alpha to STAT3gamma in human neutrophils: role of granule-derived serine proteases. J Biol Chem, *279:* 31076-31080, 2004.

219. Nakajima, H., Suzuki, K., and Iwamoto, I. Lineage-specific negative regulation of STAT-mediated signaling by proteolytic processing. Cytokine Growth Factor Rev, *14:* 375-380, 2003.

220. Silva, J., Dasgupta, S., Wang, G., Krishnamurthy, K., Ritter, E., and Bieberich, E. Lipids isolated from bone induce the migration of human breast cancer cells. J Lipid Res, *47:* 724-733, 2006.

221. De Gottardi, A., Dumonceau, J. M., Bruttin, F., Vonlaufen, A., Morard, I., Spahr, L., Rubbia-Brandt, L., Frossard, J. L., Dinjens, W. N., Rabinovitch, P. S., and Hadengue, A. Expression of the bile acid receptor FXR in Barrett's esophagus and enhancement of apoptosis by guggulsterone in vitro. Mol Cancer, *5:* 48, 2006.

222. Sinal, C. J. and Gonzalez, F. J. Guggulsterone: an old approach to a new problem. Trends Endocrinol Metab, *13:* 275-276, 2002.

223. Urizar, N. L., Liverman, A. B., Dodds, D. T., Silva, F. V., Ordentlich, P., Yan, Y., Gonzalez, F. J., Heyman, R. A., Mangelsdorf, D. J., and Moore, D. D. A natural product that lowers cholesterol as an antagonist ligand for FXR. Science, *296:* 1703-1706, 2002.

224. Liby, K., Royce, D. B., Williams, C. R., Risingsong, R., Yore, M. M., Honda, T., Gribble, G. W., Dmitrovsky, E., Sporn, T. A., and Sporn, M. B. The synthetic triterpenoids CDDO-methyl ester and CDDO-ethyl amide prevent lung cancer induced by vinyl carbamate in A/J mice. Cancer Res, *67:* 2414-2419, 2007.

225. Burris, T. P., Montrose, C., Houck, K. A., Osborne, H. E., Bocchinfuso, W. P., Yaden, B. C., Cheng, C. C., Zink, R. W., Barr, R. J., Hepler, C. D., Krishnan, V., Bullock, H. A., Burris, L. L., Galvin, R. J., Bramlett, K., and Stayrook, K. R. The hypolipidemic natural product guggulsterone is a promiscuous steroid receptor ligand. Mol Pharmacol, *67:* 948-954, 2005.

226. Ali, S., El-Rayes, B. F., Heilbrun, L. K., Sarkar, F. H., Ensley, J. F., Kucuk, O., and Philip, P. A. Cytochrome p450 and glutathione transferase expression in squamous cell cancer. Clin Cancer Res, *10:* 4412-4416, 2004.

227. Li, Y., Du, H., Qin, Y., Roberts, J., Cummings, O. W., and Yan, C. Activation of the signal transducers and activators of the transcription 3 pathway in alveolar epithelial cells induces inflammation and adenocarcinomas in mouse lung. Cancer Res, *67:* 8494-8503, 2007.

228. Allen, C. T., Ricker, J. L., Chen, Z., and Van Waes, C. Role of activated nuclear factor-kappaB in the pathogenesis and therapy of squamous cell carcinoma of the head and neck. Head Neck, *29:* 959-971, 2007.

229. Wolf, J. S., Chen, Z., Dong, G., Sunwoo, J. B., Bancroft, C. C., Capo, D. E., Yeh, N. T., Mukaida, N., and Van Waes, C. IL (interleukin)-1alpha promotes nuclear factor-kappaB and AP-1-induced IL-8 expression, cell survival, and proliferation in head and neck squamous cell carcinomas. Clin Cancer Res, *7:* 1812-1820, 2001.

230. Chen, Z., Malhotra, P. S., Thomas, G. R., Ondrey, F. G., Duffey, D. C., Smith, C. W., Enamorado, I., Yeh, N. T., Kroog, G. S., Rudy, S., McCullagh, L., Mousa, S., Quezado, M., Herscher, L. L., and Van Waes, C. Expression of proinflammatory and proangiogenic cytokines in patients with head and neck cancer. Clin Cancer Res, *5:* 1369-1379, 1999.

231. Cheon, J. H., Kim, J. S., Kim, J. M., Kim, N., Jung, H. C., and Song, I. S. Plant sterol guggulsterone inhibits nuclear factor-kappaB signaling in intestinal epithelial cells by blocking IkappaB kinase and ameliorates acute murine colitis. Inflamm Bowel Dis, *12:* 1152-1161, 2006.

232. Bradburn, J. E., Pei, P., Kresty, L. A., Lang, J. C., Yates, A. J., McCormick, A. P., and Mallery, S. R. The effects of reactive species on the tumorigenic phenotype of human head and neck squamous cell carcinoma (HNSCC) cells. Anticancer Res, *27:* 3819-3827, 2007.

233. Wang, X., Greilberger, J., Ledinski, G., Kager, G., Paigen, B., and Jurgens, G. The hypolipidemic natural product Commiphora mukul and its component guggulsterone inhibit oxidative modification of LDL. Atherosclerosis, *172:* 239-246, 2004.

234. Saxena, G., Singh, S. P., Pal, R., Singh, S., Pratap, R., and Nath, C. Gugulipid, an extract of Commiphora whighitii with lipid-lowering properties, has protective effects against streptozotocin-induced memory deficits in mice. Pharmacol Biochem Behav, *86:* 797-805, 2007.

235. Semenza, G. L. Targeting HIF-1 for cancer therapy. Nat Rev Cancer, *3:* 721-732, 2003.

236. Harikumar, K. B. and Aggarwal, B. B. Resveratrol: a multitargeted agent for age-associated chronic diseases. Cell Cycle, *7:* 1020-1035, 2008.

237. Yao, H., Wang, H., Zhang, Z., Jiang, B. H., Luo, J., and Shi, X. Sulforaphane inhibited expression of hypoxia-inducible factor-1alpha in human tongue squamous cancer cells and prostate cancer cells. Int J Cancer, *123:* 1255-1261, 2008.

238. Opitz, O. G., Harada, H., Suliman, Y., Rhoades, B., Sharpless, N. E., Kent, R., Kopelovich, L., Nakagawa, H., and Rustgi, A. K. A mouse model of human oral-esophageal cancer. J Clin Invest, *110:* 761-769, 2002.

239. Lu, S. L., Herrington, H., and Wang, X. J. Mouse models for human head and neck squamous cell carcinomas. Head Neck, 2006.

240. Lu, S. L., Herrington, H., Reh, D., Weber, S., Bornstein, S., Wang, D., Li, A. G., Tang, C. F., Siddiqui, Y., Nord, J., Andersen, P., Corless, C. L., and Wang, X. J. Loss of transforming growth factor-beta type II receptor promotes metastatic head-and-neck squamous cell carcinoma. Genes Dev, *20:* 1331-1342, 2006.

241. Hoa, M., Davis, S. L., Ames, S. J., and Spanjaard, R. A. Amplification of wild-type K-ras promotes growth of head and neck squamous cell carcinoma. Cancer Res, *62:* 7154-7156, 2002.

242. Caulin, C., Nguyen, T., Longley, M. A., Zhou, Z., Wang, X. J., and Roop, D. R. Inducible activation of oncogenic K-ras results in tumor formation in the oral cavity. Cancer Res, *64:* 5054-5058, 2004.

243. Prime, S. S., Davies, M., Pring, M., and Paterson, I. C. The role of TGF-beta in epithelial malignancy and its relevance to the pathogenesis of oral cancer (part II). Crit Rev Oral Biol Med, *15:* 337-347, 2004.

244. Zhou, Z., Wang, D., Wang, X. J., and Roop, D. R. In utero activation of K5.CrePR1 induces gene deletion. Genesis, *32:* 191-192, 2002.

245. Hawkins, B. L., Heniford, B. W., Ackermann, D. M., Leonberger, M., Martinez, S. A., and Hendler, F. J. 4NQO carcinogenesis: a mouse model of oral cavity squamous cell carcinoma. Head Neck, *16:* 424-432, 1994.

246. Tang, X. H., Knudsen, B., Bemis, D., Tickoo, S., and Gudas, L. J. Oral cavity and esophageal carcinogenesis modeled in carcinogen-treated mice. Clin Cancer Res, *10:* 301-313, 2004.

247. Grandis, J. R. and Tweardy, D. J. Elevated levels of transforming growth factor alpha and epidermal growth factor receptor messenger RNA are early markers of carcinogenesis in head and neck cancer. Cancer Res, *53:* 3579-3584, 1993.

248. Watanabe, K., Watanabe, H. Y., Goto, Y., Yamamoto, N., and Yoshizaki, M. Studies on the active principles of magnolia bark. Centrally acting muscle relaxant activity of magnolol and honokiol. Jpn J Pharmacol, *25:* 605-607, 1975.

249. Kim, B. H. and Cho, J. Y. Anti-inflammatory effect of honokiol is mediated by PI3K/Akt pathway suppression. Acta Pharmacol Sin, *29:* 113-122, 2008.

250. Lee, J., Jung, E., Park, J., Jung, K., Lee, S., Hong, S., Park, E., Kim, J., Park, S., and Park, D. Anti-inflammatory effects of magnolol and honokiol are mediated through inhibition of the downstream pathway of MEKK-1 in NF-kappaB activation signaling. Planta Med, *71:* 338-343, 2005.

251. Son, H. J., Lee, H. J., Yun-Choi, H. S., and Ryu, J. H. Inhibitors of nitric oxide synthesis and TNF-alpha expression from Magnolia obovata in activated macrophages. Planta Med, *66:* 469-471, 2000.

252. Ho, K. Y., Tsai, C. C., Chen, C. P., Huang, J. S., and Lin, C. C. Antimicrobial activity of honokiol and magnolol isolated from Magnolia officinalis. Phytother Res, *15:* 139-141, 2001.

253. Liou, K. T., Shen, Y. C., Chen, C. F., Tsao, C. M., and Tsai, S. K. The anti-inflammatory effect of honokiol on neutrophils: mechanisms in the inhibition of reactive oxygen species production. Eur J Pharmacol, *475:* 19-27, 2003.

254. Park, E. J., Kim, S. Y., Zhao, Y. Z., and Sohn, D. H. Honokiol reduces oxidative stress, c-jun-NH2-terminal kinase phosphorylation and protects against glycochenodeoxycholic acid-induced apoptosis in primary cultured rat hepatocytes. Planta Med, *72:* 661-664, 2006.

255. Lin, Y. R., Chen, H. H., Ko, C. H., and Chan, M. H. Neuroprotective activity of honokiol and magnolol in cerebellar granule cell damage. Eur J Pharmacol, *537:* 64-69, 2006.

256. Hu, H., Zhang, X. X., Wang, Y. Y., and Chen, S. Z. Honokiol inhibits arterial thrombosis through endothelial cell protection and stimulation of prostacyclin. Acta Pharmacol Sin, *26:* 1063-1068, 2005.

257. Sheu, M. L., Chiang, C. K., Tsai, K. S., Ho, F. M., Weng, T. I., Wu, H. Y., and Liu, S. H. Inhibition of NADPH oxidase-related oxidative stress-triggered signaling by honokiol suppresses high glucose-induced human endothelial cell apoptosis. Free Radic Biol Med, *44:* 2043-2050, 2008.

258. Konoshima, T., Kozuka, M., Tokuda, H., Nishino, H., Iwashima, A., Haruna, M., Ito, K., and Tanabe, M. Studies on inhibitors of skin tumor promotion, IX. Neolignans from Magnolia officinalis. J Nat Prod, *54:* 816-822, 1991.

259. Bai, X., Cerimele, F., Ushio-Fukai, M., Waqas, M., Campbell, P. M., Govindarajan, B., Der, C. J., Battle, T., Frank, D. A., Ye, K., Murad, E., Dubiel, W., Soff, G., and Arbiser, J. L. Honokiol, a small molecular weight natural product, inhibits angiogenesis in vitro and tumor growth in vivo. J Biol Chem, *278:* 35501-35507, 2003.

260. Battle, T. E., Arbiser, J., and Frank, D. A. The natural product honokiol induces caspase-dependent apoptosis in B-cell chronic lymphocytic leukemia (B-CLL) cells. Blood, *106:* 690-697, 2005.

261. Chen, F., Wang, T., Wu, Y. F., Gu, Y., Xu, X. L., Zheng, S., and Hu, X. Honokiol: a potent chemotherapy candidate for human colorectal carcinoma. World J Gastroenterol, *10:* 3459-3463, 2004.

262. Deng, J., Qian, Y., Geng, L., Chen, J., Wang, X., Xie, H., Yan, S., Jiang, G., Zhou, L., and Zheng, S. Involvement of p38 mitogen-activated protein kinase pathway in honokiol-induced apoptosis in a human hepatoma cell line (hepG2). Liver Int, 2008.

263. Hahm, E. R., Arlotti, J. A., Marynowski, S. W., and Singh, S. V. Honokiol, a constituent of oriental medicinal herb magnolia officinalis, inhibits growth of PC-3 xenografts in vivo in association with apoptosis induction. Clin Cancer Res, *14:* 1248-1257, 2008.

264. Ishitsuka, K., Hideshima, T., Hamasaki, M., Raje, N., Kumar, S., Hideshima, H., Shiraishi, N., Yasui, H., Roccaro, A. M., Richardson, P., Podar, K., Le Gouill, S., Chauhan, D., Tamura, K., Arbiser, J., and Anderson, K. C. Honokiol overcomes conventional drug resistance in human multiple myeloma by induction of caspase-dependent and -independent apoptosis. Blood, *106:* 1794-1800, 2005.

265. Li, Z., Liu, Y., Zhao, X., Pan, X., Yin, R., Huang, C., Chen, L., and Wei, Y. Honokiol, a natural therapeutic candidate, induces apoptosis and inhibits angiogenesis of ovarian tumor cells. Eur J Obstet Gynecol Reprod Biol, *140:* 95-102, 2008.

266. Sheu, M. L., Liu, S. H., and Lan, K. H. Honokiol induces calpain-mediated glucose-regulated protein-94 cleavage and apoptosis in human gastric cancer cells and reduces tumor growth. PLoS ONE, *2:* e1096, 2007.

267. Shigemura, K., Arbiser, J. L., Sun, S. Y., Zayzafoon, M., Johnstone, P. A., Fujisawa, M., Gotoh, A., Weksler, B., Zhau, H. E., and Chung, L. W. Honokiol, a natural plant product, inhibits the bone metastatic growth of human prostate cancer cells. Cancer, *109:* 1279-1289, 2007.

268. Tse, A. K., Wan, C. K., Shen, X. L., Yang, M., and Fong, W. F. Honokiol inhibits TNF-alpha-stimulated NF-kappaB activation and NF-kappaB-regulated gene expression through suppression of IKK activation. Biochem Pharmacol, *70:* 1443-1457, 2005.

269. Yang, S. E., Hsieh, M. T., Tsai, T. H., and Hsu, S. L. Down-modulation of Bcl-XL, release of cytochrome c and sequential activation of caspases during honokiol-induced apoptosis in human squamous lung cancer CH27 cells. Biochem Pharmacol, *63:* 1641-1651, 2002.

270. Jiang, Q. Q., Fan, L. Y., Yang, G. L., Guo, W. H., Hou, W. L., Chen, L. J., and Wei, Y. Q. Improved therapeutic effectiveness by combining liposomal honokiol with cisplatin in lung cancer model. BMC Cancer, *8:* 242, 2008.

271. Luo, H., Zhong, Q., Chen, L. J., Qi, X. R., Fu, A. F., Yang, H. S., Yang, F., Lin, H. G., Wei, Y. Q., and Zhao, X. Liposomal honokiol, a promising agent for treatment of cisplatin-resistant human ovarian cancer. J Cancer Res Clin Oncol, *134:* 937-945, 2008.

272. Wolf, I., O'Kelly, J., Wakimoto, N., Nguyen, A., Amblard, F., Karlan, B. Y., Arbiser, J. L., and Koeffler, H. P. Honokiol, a natural biphenyl, inhibits in vitro and in vivo growth of breast cancer through induction of apoptosis and cell cycle arrest. Int J Oncol, *30:* 1529-1537, 2007.

273. Ahn, K. S., Sethi, G., Shishodia, S., Sung, B., Arbiser, J. L., and Aggarwal, B. B. Honokiol potentiates apoptosis, suppresses osteoclastogenesis, and inhibits invasion through modulation of nuclear factor-kappaB activation pathway. Mol Cancer Res, *4:* 621-633, 2006.

274. Hahm, E. R. and Singh, S. V. Honokiol causes G0-G1 phase cell cycle arrest in human prostate cancer cells in association with suppression of retinoblastoma protein level/phosphorylation and inhibition of E2F1 transcriptional activity. Mol Cancer Ther, *6:* 2686-2695, 2007.

275. Lee, B., Kim, C. H., and Moon, S. K. Honokiol causes the p21WAF1-mediated G(1)-phase arrest of the cell cycle through inducing p38 mitogen activated protein kinase in vascular smooth muscle cells. FEBS Lett, *580:* 5177-5184, 2006.

276. Liu, H., Zang, C., Emde, A., Planas-Silva, M. D., Rosche, M., Kuhnl, A., Schulz, C. O., Elstner, E., Possinger, K., and Eucker, J. Anti-tumor effect of honokiol alone and in

combination with other anti-cancer agents in breast cancer. Eur J Pharmacol, *591:* 43-51, 2008.

277. Fong, W. F., Tse, A. K., Poon, K. H., and Wang, C. Magnolol and honokiol enhance HL-60 human leukemia cell differentiation induced by 1,25-dihydroxyvitamin D3 and retinoic acid. Int J Biochem Cell Biol, *37:* 427-441, 2005.

278. Gioanni, J., Fischel, J. L., Lambert, J. C., Demard, F., Mazeau, C., Zanghellini, E., Ettore, F., Formento, P., Chauvel, P., Lalanne, C. M., and et al. Two new human tumor cell lines derived from squamous cell carcinomas of the tongue: establishment, characterization and response to cytotoxic treatment. Eur J Cancer Clin Oncol, *24:* 1445-1455, 1988.

279. Kimmel, K. A. and Carey, T. E. Altered expression in squamous carcinoma cells of an orientation restricted epithelial antigen detected by monoclonal antibody A9. Cancer Res, *46:* 3614-3623, 1986.

280. Raja, S. M., Chen, S., Yue, P., Acker, T. M., Lefkove, B., Arbiser, J. L., Khuri, F. R., and Sun, S. Y. The natural product honokiol preferentially inhibits cellular FLICE-inhibitory protein and augments death receptor-induced apoptosis. Mol Cancer Ther, *7:* 2212-2223, 2008.

281. Xu, D., Lu, Q., and Hu, X. Down-regulation of P-glycoprotein expression in MDR breast cancer cell MCF-7/ADR by honokiol. Cancer Lett, *243:* 274-280, 2006.

282. Hou, W., Chen, L., Yang, G., Zhou, H., Jiang, Q., Zhong, Z., Hu, J., Chen, X., Wang, X., Yuan, Y., Tang, M., Wen, J., and Wei, Y. Synergistic antitumor effects of liposomal honokiol combined with adriamycin in breast cancer models. Phytother Res, *22:* 1125-1132, 2008.

283. Nagase, H., Ikeda, K., and Sakai, Y. Inhibitory effect of magnolol and honokiol from Magnolia obovata on human fibrosarcoma HT-1080. Invasiveness in vitro. Planta Med, *67:* 705-708, 2001.

284. Brobst, D. E., Ding, X., Creech, K. L., Goodwin, B., Kelley, B., and Staudinger, J. L. Guggulsterone activates multiple nuclear receptors and induces CYP3A gene expression through the pregnane X receptor. J Pharmacol Exp Ther, *310:* 528-535, 2004.

285. Wang, Y. D., Chen, W. D., Wang, M., Yu, D., Forman, B. M., and Huang, W. Farnesoid X receptor antagonizes nuclear factor kappaB in hepatic inflammatory response. Hepatology, *48:* 1632-1643, 2008.

286. Dikalov, S., Losik, T., and Arbiser, J. L. Honokiol is a potent scavenger of superoxide and peroxyl radicals. Biochem Pharmacol, *76:* 589-596, 2008.

287. Fan, Z., Masui, H., Altas, I., and Mendelsohn, J. Blockade of epidermal growth factor receptor function by bivalent and monovalent fragments of 225 anti-epidermal growth factor receptor monoclonal antibodies. Cancer Res, 53: 4322-4328, 1993.

288. Azemar, M., Schmidt, M., Arlt, F., Kennel, P., Brandt, B., Papadimitriou, A., Groner, B., and Wels, W. Recombinant antibody toxins specific for ErbB2 and EGF receptor inhibit the in vitro growth of human head and neck cancer cells and cause rapid tumor regression in vivo. Int J Cancer, *86:* 269-275, 2000.

289. Phillips, P. C., Levow, C., Catterall, M., Colvin, O. M., Pastan, I., and Brem, H. Transforming growth factor-alpha-Pseudomonas exotoxin fusion protein (TGF-alpha-PE38) treatment of subcutaneous and intracranial human glioma and medulloblastoma xenografts in athymic mice. Cancer Res, *54:* 1008-1015, 1994.

290. Rubin Grandis, J., Chakraborty, A., Melhem, M. F., Zeng, Q., and Tweardy, D. J. Inhibition of epidermal growth factor receptor gene expression and function decreases proliferation of head and neck squamous carcinoma but not normal mucosal epithelial cells. Oncogene, *15:* 409-416, 1997.

291. Endo, S., Zeng, Q., Burke, N. A., He, Y., Melhem, M. F., Watkins, S. F., Lango, M. N., Drenning, S. D., Huang, L., and Rubin Grandis, J. TGF-alpha antisense gene therapy inhibits head and neck squamous cell carcinoma growth in vivo. Gene Ther, *7:* 1906-1914, 2000.

292. Turkson, J., Bowman, T., Adnane, J., Zhang, Y., Djeu, J. Y., Sekharam, M., Frank, D. A., Holzman, L. B., Wu, J., Sebti, S., and Jove, R. Requirement for Ras/Rac1-mediated p38 and c-Jun N-terminal kinase signaling in Stat3 transcriptional activity induced by the Src oncoprotein. Mol Cell Biol, *19:* 7519-7528, 1999.

293. Nikitakis, N. G., Hamburger, A. W., and Sauk, J. J. The nonsteroidal anti-inflammatory drug sulindac causes down-regulation of signal transducer and activator of transcription 3 in human oral squamous cell carcinoma cells. Cancer Res, *62:* 1004-1007, 2002.